การแยกอิแนนทิโอเมอร์ของแอมีนด้วยแก๊สโครมาโทกราฟี
ที่ใช้อนุพันธ์ไซโคลเดกซ์ทรินเป็นเฟสคงที่

นายณัฏฐพล อิสรเสรีรักษ์

จุฬาลงกรณ์มหาวิทยาลัย
Chulalongkorn University

วิทยานิพนธ์นี้เป็นส่วนหนึ่งของการศึกษาตามหลักสูตรปริญญาวิทยาศาสตรดุษฎีบัณฑิต
สาขาวิชาเคมี ภาควิชาเคมี
คณะวิทยาศาสตร์ จุฬาลงกรณ์มหาวิทยาลัย
ปีการศึกษา 2556

ลิขสิทธิ์ของจุฬาลงกรณ์มหาวิทยาลัย

บทคัดย่อและแฟ้มข้อมูลฉบับเต็มของวิทยานิพนธ์ตั้งแต่ปีการศึกษา 2554 ที่ให้บริการในคลังปัญญาจุฬาฯ (CUIR)
เป็นแฟ้มข้อมูลของนิสิตเจ้าของวิทยานิพนธ์ ที่ส่งผ่านทางบัณฑิตวิทยาลัย
The abstract and full text of theses from the academic year 2011 in Chulalongkorn University Intellectual Repository (CUIR)
are the thesis authors' files submitted through the University Graduate School.

ENANTIOMERIC SEPARATION OF AMINES BY GAS CHROMATOGRAPHY USING DERIVATIZED CYCLODEXTRINS AS STATIONARY PHASES

Mr. Natthapol Issaraseriruk

จุฬาลงกรณ์มหาวิทยาลัย
Chulalongkorn University

A Dissertation Submitted in Partial Fulfillment of the Requirements
for the Degree of Doctor of Philosophy Program in Chemistry
Department of Chemistry
Faculty of Science
Chulalongkorn University
Academic Year 2013

Copyright of Chulalongkorn University

Thesis Title	ENANTIOMERIC SEPARATION OF AMINES BY GAS CHROMATOGRAPHY USING DERIVATIZED CYCLODEXTRINS AS STATIONARY PHASES
By	Mr. Natthapol Issaraseriruk
Field of Study	Chemistry
Thesis Advisor	Assistant Professor Aroonsiri Shitangkoon, Ph.D.
Thesis Co-Advisor	Assistant Professor Yongsak Sritana-anant, Ph.D.

Accepted by the Faculty of Science, Chulalongkorn University in Partial Fulfillment of the Requirements for the Doctoral Degree

.....Dean of the Faculty of Science

(Professor Supot Hannongbua, Dr.rer.nat.)

THESIS COMMITTEE

.....Chairman

(Assistant Professor Warinthorn Chavasiri, Ph.D.)

.....Thesis Advisor

(Assistant Professor Aroonsiri Shitangkoon, Ph.D.)

.....Thesis Co-Advisor

(Assistant Professor Yongsak Sritana-anant, Ph.D.)

.....Examiner

(Assistant Professor Pakorn Varanusupakul, Ph.D.)

.....Examiner

(Assistant Professor Sumrit Wacharasindhu, Ph.D.)

.....External Examiner

(Assistant Professor Atitaya Siripinyanond, Ph.D.)

ณัฏฐพล อิสรเสรีรักษ์ : การแยกอิแนนทิโอเมอร์ของแอมีนด้วยแก๊สโครมาโทกราฟีที่ใช้อนุพันธ์ไซโคลเดกซ์ทรินเป็นเฟสคงที่. (ENANTIOMERIC SEPARATION OF AMINES BY GAS CHROMATOGRAPHY USING DERIVATIZED CYCLODEXTRINS AS STATIONARY PHASES) อ.ที่ปรึกษาวิทยานิพนธ์หลัก: ผศ. ดร.อรุณศิริ ชิตางกูร, อ.ที่ปรึกษาวิทยานิพนธ์ร่วม: ผศ. ดร.ยงศักดิ์ ศรีธนาอนันต์, 116 หน้า.

สังเคราะห์แอมีน 32 ชนิด ได้แก่ กลุ่มของ 1-ฟีนิลเอทิลลามีน, 1-ฟีนิลโพรพิลลามีน, และ 1-แอมิโนอินเดน ที่มีชนิดและตำแหน่งของหมู่แทนที่ที่แตกต่างกันด้วยวิธีรีดักทีฟแอมิเนชัน จากนั้น ทำการแยกอิแนนทิโอเมอร์ของแอมีนในรูปของอนุพันธ์ไตรฟลูออโรแอซีทิลด้วยแคปิลารีแก๊สโครมาโทกราฟีที่ใช้อนุพันธ์ 2,3-ได-โอ-เมทิล-6-โอ-เทอร์ต-บิวทิลไดเมทิลไซลิลของแอลฟา, บีตา, และแกมมาไซโคลเดกซ์ทริน (ASiMe, BSiMe, และ GSiMe) เป็นเฟสคงที่ชนิดไครัล โดยศึกษาผลของอุณหภูมิ, ขนาดของวงไซโคลเดกซ์ทริน, และโครงสร้างของแอมีนที่มีต่อค่ารีเทนชันและค่าการเลือกจำเพาะของอิแนนทิโอเมอร์ พบว่า ทั้งชนิดและตำแหน่งของหมู่แทนที่บนโครงสร้างของแอมีนมีผลอย่างมากต่อการแยกของอิแนนทิโอเมอร์ในคอลัมน์ทั้งสามชนิด นอกจากนี้ ขนาดของวงไซโคลเดกซ์ทรินก็ส่งผลต่อการแยกของอิแนนทิโอเมอร์เช่นเดียวกัน สำหรับคอลัมน์ ASiMe สามารถแยกอิแนนทิโอเมอร์ของแอมีนที่นำมาศึกษาได้จำนวน 24 ชนิด สามารถแยกอิแนนทิโอเมอร์ของแอมีนที่มีหมู่แทนที่ที่ตำแหน่งเมตาได้ดี ยกเว้นหมู่แทนที่ชนิดไตรฟลูออโรเมทิล และแยกอิแนนทิโอเมอร์ของแอมีนที่มีหมู่แทนที่ที่ตำแหน่งออร์โธได้ทั้งหมด ในขณะที่แยกแนนทิโอเมอร์ของแอมีนที่มีหมู่แทนที่ที่ตำแหน่งพาราได้แย่หรือไม่สามารถแยกได้ สำหรับคอลัมน์ BSiMe สามารถแยกอิแนนทิโอเมอร์ของแอมีนที่นำมาศึกษาได้จำนวน 24 ชนิด พบว่าสามารถแยกอิแนนทิโอเมอร์ของแอมีนที่มีหมู่แทนที่เป็นหมู่ฮาโลเจนที่ตำแหน่งออร์โธและเมตาได้ดี และสามารถแยกสารในกลุ่ม 1-แอมิโนอินเดนได้ทั้งหมด ยกเว้น 5ClA ในขณะที่คอลัมน์ GSiMe สามารถแยกอิแนนทิโอเมอร์ของแอมีนที่นำมาศึกษาได้จำนวน 13 ชนิด โดยแยกอิแนนทิโอเมอร์ของสารส่วนใหญ่ได้แย่กว่าคอลัมน์ ASiMe และ BSiMe ยกเว้น 4Me, 4MeP, 4CFP นอกจากนี้ อิแนนทิโอเมอร์ของแอมีนทุกตัวสามารถแยกได้ด้วยเฟสคงที่ชนิดใดชนิดหนึ่ง ยกเว้น 4OMeP

ภาควิชา เคมี	ลายมือชื่อนิสิต .....
สาขาวิชา เคมี	ลายมือชื่อ อ.ที่ปรึกษาวิทยานิพนธ์หลัก .....
ปีการศึกษา 2556	ลายมือชื่อ อ.ที่ปรึกษาวิทยานิพนธ์ร่วม .....

5173812823 : MAJOR CHEMISTRY
KEYWORDS: GAS CHROMATOGRAPHY / ENANTIOMER / AMINE

NATTHAPOL ISSARASERIRUK: ENANTIOMERIC SEPARATION OF AMINES BY GAS CHROMATOGRAPHY USING DERIVATIZED CYCLODEXTRINS AS STATIONARY PHASES. ADVISOR: ASST. PROF. AROONSIRI SHITANGKOON, Ph.D., CO-ADVISOR: ASST. PROF. YONGSAK SRITANA-ANANT, Ph.D., 116 pp.

Thirty-two amines with different types and positions of substitution including 1-phenylethylamines, 1-phenylpropyamines, and 1-aminoindanes were synthesized by reductive amination. All synthesized amines were derivatized to trifluoroacetyl (TFA) derivatives. Enantioseparation of all TFA amine derivatives were studied by capillary gas chromatography using 2,3-di-O-methyl-6-O-tert-butyldimethylsilyl derivative of alpha, beta, and gamma cyclodextrins (ASiMe, BSiMe, and GSiMe, respectively) as chiral stationary phases. The influence of temperature, cyclodextrin ring size, and structure of amines on retention and enantioselectivity were studied. Both type and position of substituents on amine structures strongly influence enantioseparation on three chiral columns. In addition, cyclodextrin ring size also affects the enantioseparation as well. ASiMe column could separate twenty-four enantiomers of TFA amine derivatives. Meta-substituted TFA amine derivatives show good enantioseparation, except for trifluoromethyl group. All ortho-substituted TFA amine derivatives could be separated. Unfortunately, para-substituted TFA amine derivatives show poor enantioseparation or could not be separated. BSiMe column could also separate twenty-four enantiomers of TFA amine derivatives. Ortho- and meta-substitution of halogenated TFA amine derivatives seemed to promote the enantioseparation. All TFA 1-aminoindanes could be separated, except for 5ClA. GSiMe column could separate only thirteen TFA amine derivatives. Most of TFA amine derivatives show poorer enantioseparation than both ASiMe and BSiMe columns, except for 4Me, 4MeP, 4CFP. Moreover, all TFA amine derivatives could be successfully enantioseparated with at least one column, except for 4OMeP.

Department:	Chemistry	Student's Signature	.....
Field of Study:	Chemistry	Advisor's Signature	.....
Academic Year:	2013	Co-Advisor's Signature	.....

ACKNOWLEDGEMENTS

First of all, I would like to express my sincere gratitude and deep appreciation to my research advisor, Assistant Professor Dr. Aroonsiri Shitangkoon, for her professional suggestion, valuable guidance, continuous support, encouragement and critical proofreading of this research.

I would also like to express my sincere appreciation to my research co-advisor, Assistant Professor Dr. Yongsak Sritana-anant who provides me with his extensive scientific knowledge, valuable guidance and suggestions during synthesis works, encouragement and careful proofreading of this research.

I would like to thank my thesis committee members, Assistant Professor Dr. Warinthorn Chavasiri, Assistant Professor Dr. Pakorn Varanusupakul, Assistant Professor Dr. Sumrit Wacharasindhu, and Assistant Professor Dr. Atitaya Siripinyanond, for their valuable suggestions and comments.

My special thanks go to Professor Gyula Vigh (Texas A&M University, USA) for his kind provision of cyclodextrin derivatives used in this research.

I would also like to thank the Department of Chemistry, Faculty of Science, Chulalongkorn University for providing research facilities and financial support. I also thank all the staffs in the Department of Chemistry for their helpfulness. Financial support from the 90th Anniversary of Chulalongkorn University Fund (Ratchadaphiseksomphot Endowment) is gratefully acknowledged.

Many thanks to all members of the chiral separation group and all my friends for their help, cheerfulness during my study.

CHULALONGKORN UNIVERSITY

CONTENTS

Page

จุฬาลงกรณ์มหาวิทยาลัย
CHULALONGKORN UNIVERSITY

LIST OF TABLES

Table Page

จุฬาลงกรณ์มหาวิทยาลัย
CHULALONGKORN UNIVERSITY

LIST OF FIGURES

Figure Page

จุฬาลงกรณ์มหาวิทยาลัย
CHULALONGKORN UNIVERSITY

LIST OF ABBREVIATIONS AND SIGNS

ASiMe	=	hexakis(2,3-di-*O*-methyl-6-*O*-*tert*-butyldimethylsilyl)cyclomaltohexaose
BSiMe	=	heptakis(2,3-di-*O*-methyl-6-*O*-*tert*-butyldimethylsilyl)cyclomaltoheptaose
CD	=	cyclodextrin
CSP	=	chiral stationary phase
GSiMe	=	octakis(2,3-di-*O*-methyl-6-*O*-*tert*-butyldimethylsilyl) cyclomaltooctaose
GC	=	gas chromatography
i.d.	=	internal diameter
K	=	distribution coefficient
k′	=	retention factor or capacity factor
m	=	meter
min	=	minute
mm	=	millimeter
mL	=	milliliter
OV-	=	7% phenyl, 7% cyanopropyl, 86% dimethyl polysiloxane
R	=	universal gas constant (1.987 cal/mol·K)
R^2	=	correlation coefficient
SD	=	standard deviation
T	=	absolute temperature (K)
TFA	=	trifluoroacetyl
α	=	selectivity factor
β	=	phase ratio
ΔG	=	Gibbs free energy
$\Delta\Delta G$	=	difference in Gibbs free energy for an enantiomeric pair
ΔH	=	enthalpy change of each enantiomer
$\Delta\Delta H$	=	difference in enthalpy change for an enantiomeric pair
ΔS	=	entropy change of each enantiomer
$\Delta\Delta S$	=	difference in entropy change for an enantiomeric pair

จุฬาลงกรณ์มหาวิทยาลัย
Chulalongkorn University

μm	=	micrometer, 10^{-6} m
^{o}C	=	degree celsius
$\bar{x}$	=	mean value

จุฬาลงกรณ์มหาวิทยาลัย
CHULALONGKORN UNIVERSITY

CHAPTER I

INTRODUCTION

Many chiral organic compounds are used in pharmaceutical and agrochemical industries. Chiral compounds have two non-superimposable mirror image forms called enantiomers. In an achiral environment, enantiomers have identical physical and chemical properties (melting point, boiling point, solubility, etc). But in a chiral environment, one enantiomer may display different chemical and pharmacologic behavior than the other enantiomer. Because living systems are themselves chiral, one of the enantiomer of a chiral drug is often more active for given desired effect, while the other, may either inactive or cause serious and undesirable side effects [1]. For example, both enantiomers of citalopram are used in the treatment of depression but (*S*)-citalopram is 30-fold more potent than (*R*)-citalopram [1]. An unfortunate example was the case of thalidomide. In the 1960s, thalidomide was used to relieve anxiety and promote sleep in pregnant woman as a racemic mixture. While the (*R*)-enantiomer was an effective form, (*S*)-enantiomer was teratogenic, which caused serious defects in the embryos [2].

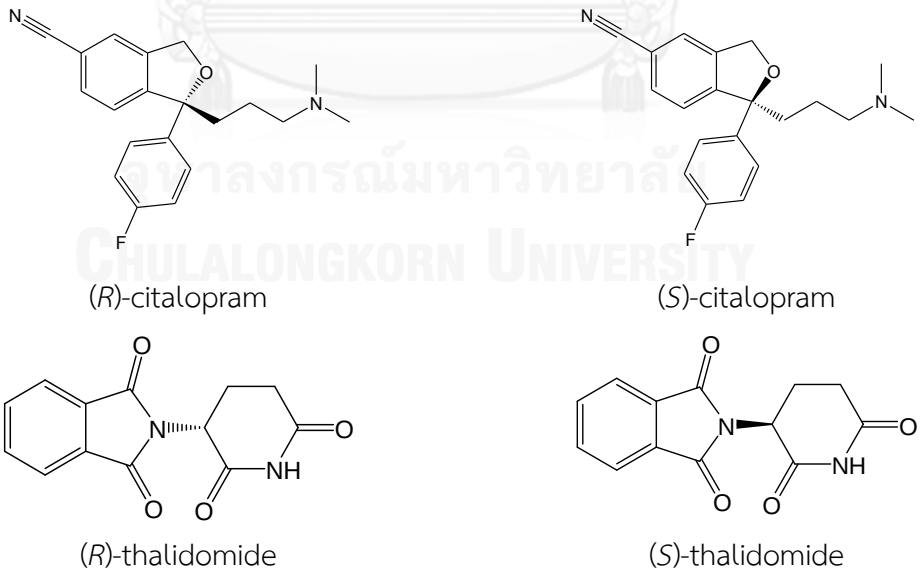

Figure 1.1 Structures of *(R)*- and *(S)*-enantiomers of citalopram and thalidomide

In 1992, the US Food and Drug Administration (FDA) issued a guideline that for chiral drugs only its therapeutically active isomer was brought to market and that each enantiomer of the drug has to be studied pharmacological and toxicological evaluation separately. However, the manufacture of purely single enantiomers can potentially lead to simpler and more selective pharmacologic profiles, improved therapeutic abilities. Survey of worldwide pharmaceutical data through the last decades indicates that approximately 50% of marketed drugs are chiral, and approximately 40% of these chiral drugs are pure single enantiomers [3].

Consequently, separations of enantiomers were required to obtain the purity of synthesized compounds. The common techniques used for enantiomeric separation are capillary electrophoresis (CE), high performance liquid chromatography (HPLC) and gas chromatography (GC). Among these techniques, GC is an accurate and reliable technique for the determination of enantiomeric purity of volatile and thermally stable organic compounds [4]. Enantiomeric separation by GC is achieved with two methods. The first is indirect method, which based on the formation of diastereomers through use of chiral derivatizing agents. The diastereomers formed can be separated on achiral stationary phases. The other way to achieve enantioseparation is direct method, which requires chiral selector as chiral stationary phase (CSP).

Cyclodextrins (CDs) and their derivatives are frequently used as chiral stationary phases in GC [5] because they can form inclusion complexes with many substances. Generally, the enantioseparation occurs through interaction between CD and the analytes resulting in transient diastereomeric complexes between each enantiomer and CD molecule. Nevertheless, the mechanism of chiral recognition of enantiomers by CDs is still not understood. Because of the differing inclusion of enantiomers is not the only mechanism by which chiral recognition can occur. In general, analyte molecules may not interact with the CD by only one mechanism but through a simultaneous combination of interaction, such as, π–π interactions, dipole-dipole interactions, van der Waals and hydrophobic interactions [6]. There are various parameters that affect enantiomeric separations using CD derivatives such as size, shape of CD derivatives, and analyte structure [4].

Chiral amines were selected as the analytes in this study because of their importance as chiral catalyst in asymmetric synthesis [7], chiral auxiliaries [8], chiral resolving agents [9], chiral building blocks in pharmaceuticals and other important bioactive molecules, such as $GABA_B$ receptor which use for Parkinson's disease treatment [10].

The aim of this work was to systematically investigate the influence of amine structures with different types, positions of substitutions on aromatic ring, different types of side chain towards the enantioseparation with three different sizes of CD derivatives: 2,3-di-*O*-methyl-6-*O*-*tert*-butyldimethylsilyl-α-, β-, and γ-CDs. These studies were determined through retention factors (k'), selectivity factor (α) obtained from chromatogram and thermodynamic parameters (ΔH, ΔS, ΔΔH, ΔΔS).

Hopefully, the results obtained from this study would enable us to explain the influence of size of CD derivatives and analyte structure on the enantioselectivity. This will aid in the selection of appropriate chiral stationary phases for the enantioseparation of these analytes, including other compounds having similar structures to the analytes.

จุฬาลงกรณ์มหาวิทยาลัย
CHULALONGKORN UNIVERSITY

CHAPTER II

THEORY & LITERATURE REVIEWS

2.1 Chiral amines

Chiral amines play an importance role in organic synthesis because of their importance as chiral catalyst in asymmetric synthesis [7], chiral auxiliaries [8], chiral resolving agents [9], chiral building blocks in pharmaceuticals and other important bioactive molecules [10]. For example, (*R*)-1-phenylethylamine was used to synthesize etomidate [11] which is anaesthetic agent used for the induction of general anaesthesia. Another example is using (*S*)-1-(3-methoxyphenyl)ethylamine to synthesize rivastigmine [12] which is a drug used for treatment of Alzheimer's disease.

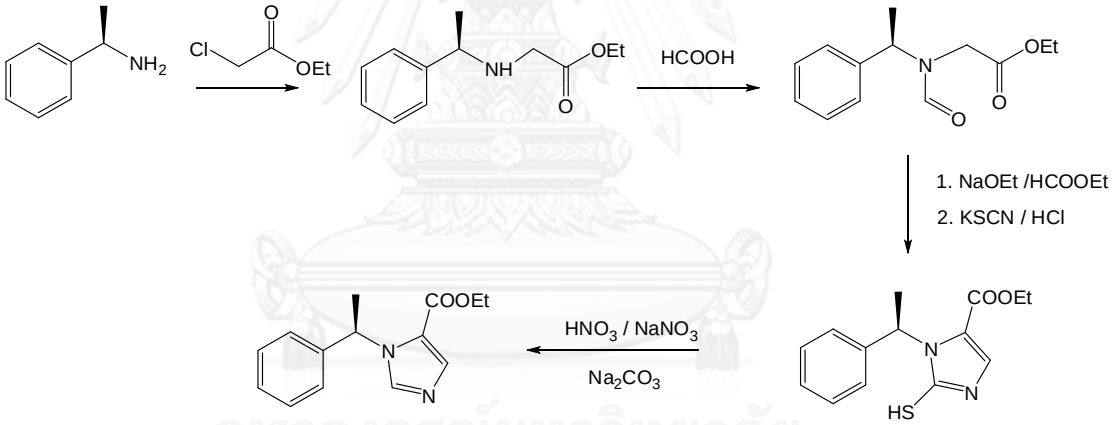

Figure 2.1 Synthesis of etomidate [11].

One of the most common methods to prepare amines is the reductive amination of carbonyl compounds [13]. The reductive amination of aldehydes or ketones proceeds in several consecutive steps. Firstly, condensation of the carbonyl compound forms a carbinol-amine, which eliminates H_2O to give an imine. Subsequently, the imine intermediate was reduced to the amine. A carbonyl compound/amine mixture can often be reduced using metal hydrides [14].

2.2 Gas chromatographic separation of amines

Gas chromatography (GC) is usually considered as an accurate and reliable technique for the separation of volatile and thermally stable organic compounds. Its advantages include simple, relatively inexpensive, and high reproducibility [15]. But amines can be difficult to detect using GC because there is significant adsorption of the basic amines on the acidic column as well as decomposition of the analyte.

Nevertheless, it is possible to analyze them by derivatizing them before injection. There are several advantages of derivatizing amines in that it enables them to become volatile enough for GC analysis, improves peak shape by reducing tailing, increases sensitivity and selectivity. The commonly used derivatization reactions for GC analysis are acylation and silylation [16].

Acylation is one of the most popular derivatization reactions for primary and secondary amines. Acid anhydrides such as acetic anhydride or trifluoroacetic anhydride (TFAA) have been used as acylating reagents. These reagents easily react with amino groups under mild reaction conditions. In the reaction of amines with acid anhydrides and acyl chlorides, it is usually necessary to remove excess reagent and by-product acid by solvent extraction or purge with nitrogen gas, because these compounds damage the GC column [17].

Silylation is another derivatization reaction to convert amino group to silyl group. However, amino group is less reactive to silylating reagents compared to hydroxyl or carboxyl group. For silylation, *N*,*O*-bis(trimethylsilyl)acetamide (BSA) and *N*,*O*-bis(trimethylsilyl)trifluoroacetamide (BSTFA) can be used as silylating reagents. Trimethylchlorosilane (TMCS) is usually an effective catalyst which added to reactions to ensure the effective derivatization. However, the *N*-trimethylsilyl (TMS) derivatives produced by the reaction with these reagents are unstable to moisture. On the other hand, the *N*-*tert*-butyldimethylsilyl (TBDMS) derivatives can also be produced by the reaction with *N*-methyl-*N*-(*tert*-butyldimethylsilyl)trifluoroacetamide (MTBSTFA). The TBDMS derivatives are generally less reactive but give more stable to hydrolysis than the corresponding TMS derivatives [17].

2.3 Gas chromatographic separation of enantiomers

For chiral separation using GC, two approaches can be performed: direct and indirect approaches [18]. The indirect approach involves the coupling of the enantiomers with an enantiomerically pure chiral auxiliary to convert them into diastereomers. The diastereomers can then be separated by any achiral stationary phases. Many disadvantages of this approach include the requirement of purely chiral reagent, inconvenience, and possible biased results for enantiomeric composition due to partial racemization during derivatization. In the direct approach, enantiomers are separated via chiral stationary phase (CSP) which form transient diastereomeric intermediates with the chiral analyte. This method was preferred because it offers some advantages over indirect methods. There is no need to chemically manipulate the analytes, interference with sample matrix, chiral purity of the chiral stationary phase (CSP) does not need be known.

Among several chiral selectors, CDs and their derivatives are frequently used in GC because of their ability to form inclusion complexes with various types of substances. Moreover, the wide operating temperature of CDs and their derivatives makes them one of the most versatile stationary phases for GC [4, 19].

2.4 Cyclodextrins and their derivatives

Cyclodextrins (CDs) are cyclic oligosaccharides which consist of α-(1,4) linked D-glucose units. They are produced by the digestion of starch by cyclodextrin glycosyltransferases (CGTases) of bacteria such as Bacillus strains. The three most common CDs are composed of six, seven, and eight D-glucose units; referred to α-, β- and γ-CDs, respectively [20]. Molecular dimension and some physical properties of the three native CDs are summarized in Table 2.1

Table 2.1 Molecular dimensions and physical properties of native CDs [20].

	α-CD	β-CD	γ-CD
Number of glucopyranose units	6	7	8
Chemical formula	$(C_6H_{10}O_5)_6$	$(C_6H_{10}O_5)_7$	$(C_6H_{10}O_5)_8$
Number of chiral centers	30	35	40
Internal diameter (Å)	4.7–5.3	6.0–6.5	7.5–8.3
Cavity volume ($Å^3$)	174	262	427

CDs are *shaped like* a *hollow torus* with a lipophilic cavity and a hydrophobic outside. The narrower rim is formed by the primary C6-hydroxyl groups, while the wider rim contained the secondary C2- and C3-hydroxyl groups of the glucose unit (Figure 2.2) [4, 19, 20].

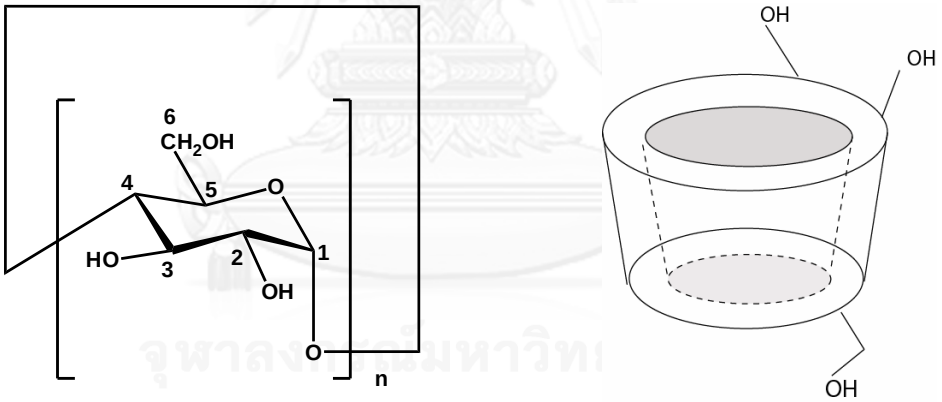

Figure 2.2 Structure of CD molecule with n glucose units (left) resembling a truncated cone (right) with secondary C2- and C3-hydroxyl groups on the wider side and primary C6-hydroxyl groups on the narrower side

2.5 Gas chromatographic separation of enantiomers using cyclodextrin derivatives

CDs can be chemically modified to improve their physical and chemical properties, such as decomposition temperature and solubility, by substituting various

functional groups at the primary and/or secondary hydroxyl groups. In general, the secondary hydroxyl groups at C2 and C3 positions of each glucose unit are modified with small alkyl or acyl groups to change the enantioselectivity, whereas the primary C6 hydroxyl groups are replaced with longer alkyl or bulky groups to change polarity, viscosity, or solubility in polysiloxane [4].

As described above, the enantiomeric separation occurs by generating a transient diastereomeric intermediate between the chiral analyte and CSP. The chiral recognition process involves various forces between the chiral analyte and CSP such as dispersion force, dipole-dipole interaction, and hydrogen bonding [4-6]. Derivatization of the free CD hydroxyls changes the type of interactions between the analyte and CSP. Thus, the chiral discriminations are generally different for each enantiomeric pair.

Previous researches have been demonstrated that enantioseparation by GC using CD derivatives as chiral selectors is governed by the size and shape of CDs, the concentration of CDs in polysiloxane, the separation temperature, and the structures of chiral analytes [4, 21-26]. Important results obtained from previous studies can be summarized as follows:

Armstrong and co-workers [21] separated alcohols, esters, ketones ethers, lactones, furan derivatives including 9 different structure of trifluoroacetyl amine derivatives on three chiral columns coated with permethyl-*O*-(*S*)-2-hydroxypropyl (PMHP) α-, β- and γ-CDs. The results showed that all analytes were resolved on one or more columns. Overall, it was found that the PMHP β-CD column can resolve a larger number of analytes followed by the α-CD and γ-CD analogs. However, there were several compounds that were resolved on the PMHP α-CD column only. All of the compounds that separated on γ-CD could be resolved on either α- or β-CDs.

Armstrong and co-workers [22] separated more than 150 chiral compounds such as alcohols, esters, halohydrocarbons, epoxides, lactones, ketones, furan and pyran derivatives including 10 different structure of trifluoroacetyl amine derivatives on three chiral columns coated with 2,6-di-*O*-pentyl-3-*O*-trifluoroacetyl α-, β- and γ-CDs. The results showed that all analytes were resolved on one or more columns.

The α- and β-CD column were useful for the enantioseparation of the aliphatic amines with different alkyl chain length. It was found that longer carbon chain affect the retention but not the selectivity and the orientation of the molecule can be affected by the substituent group and the size of the CD cavity. For the other amines, it was found that only β-CD column could resolve 1-cyclohexylamine and 1-phenylethylamine. Whereas α- and γ-CD columns could separate 1,2,3,4 tetrahydro-1-naphthylamine which could not be resolved on β-CD column. Overall results showed that the functionality of analyte structure may also play an important role on the enantioseparation.

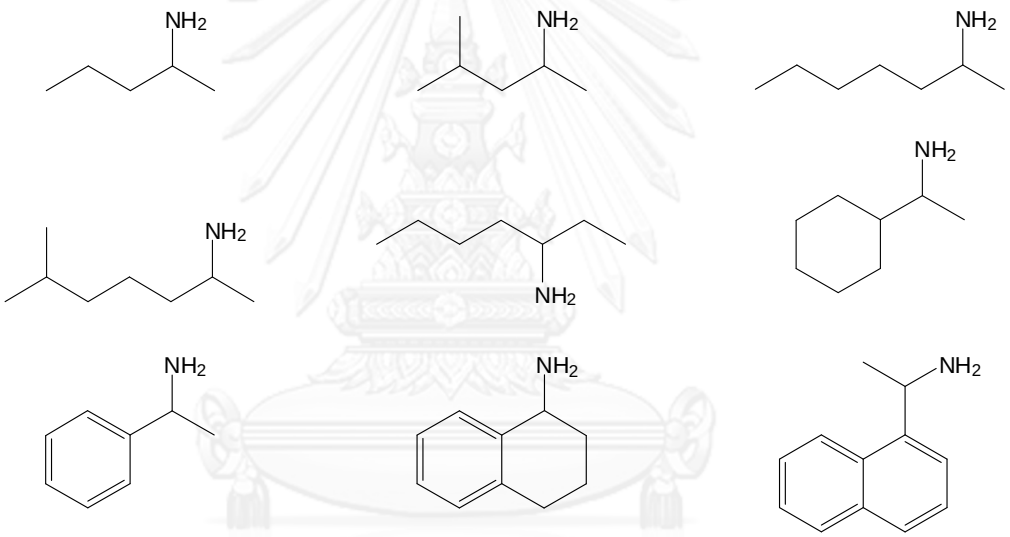

Figure 2.3 Structures of amines studied by Armstrong and co-workers [21, 22]

Nie and co-workers [23] separated the enantiomers of alcohols, diols carboxylic acids, amino acids, epoxides, alkylhalides, ketones including amines by GC using three derivatized β-CDs as CSPs: heptakis-(2,6-di-*O*-nonyl-3-*O*-trifluoroacetyl)-β-CD (DNTBCD); heptakis-(2,6-di-*O*-dodecyl-3-*O*-trifluoroacetyl)-β-CD (DDTBCD); and heptakis-(2,6-di-*O*-pentyl-3-*O*-trifluoroacetyl)-β-CD (DPTBCD). The results showed that DNTBCD exhibited the best chiral selectivity among the three stationary phases. Moreover, they studied the thermodynamic of enantioseparation of methyl- and methoxy-substituted 1-phenylethylamines at *ortho*-, *meta*- and *para*- positions on

the aromatic ring which were separated on DNTBCD and DPTBCD columns. They found that the $-\Delta\Delta H$ and $-\Delta\Delta S$ values of all analytes on DNTBCD column were higher than the corresponding ones on DPTBCD column, indicating that DNTBCD column has better enantioseparation than DPTBCD column. In addition, position of substituents on the aromatic ring also affects on enantioseparation. *Ortho*-derivatives give better enantioseparation than *meta*- and *para*-derivatives.

Anderson and co-workers [24] separated the 17 chiral sulfoxides and 8 chiral sulfinate esters by GC using four types of CD derivatives: 2,6-di-*O*-pentyl-3-trifluoroacetyl-γ-CD (G-TA); 2,6-di-*O*-pentyl-3-propionyl-γ-CD (G-PN); 2,6-di-*O*-pentyl-3-butyryl-γ-CD (G-BP); and 2,6-di-*O*-methyl-β-CD (B-DM). For chiral sulfoxides, the results indicated that G-PN and G-BP columns possessed similar retention factor and selectivity factor for most of the analytes. However, G-PN exhibited slightly higher resolution compared to the G-BP column. For chiral sulfinate esters, B-DM column showed the best enantioseparation. Among the three γ-CD derivatives, G-TA column exhibited greater enantioselectivity for most sulfoxides and sulfinate esters. The size and polarity of sulfoxide substituents affect their enantioselectivities on all CSPs in this study.

Shi and co-workers [25] also separated the enantiomers of 7 chiral epoxides by GC using four derivatized β-CDs: 2,6-di-*O*-benzyl-3-*O*-heptanonyl-β-CD (column 1); 2,6-di-*O*-benzyl-3-*O*-octanonyl-β-CD (column 2); 2,3-di-*O*-benzyl-6-*O*-heptanonyl-β-CD (column 3); and 2,3-di-*O*-benzyl-6-*O*-octanonyl-β-CD (column 4). The results suggested that column 1 was more favorable for enantioseparation of the epoxides than column 2. Therefore, heptanonyl substituted on 3-position of CD is more favorable for enantioseparation of the epoxides than octanonyl substituted on the same position. Whereas octanonyl substituted on 6-positon on column 4 is more favorable for enantioseparation of the epoxides than heptanonyl substituted in column 3. These results indicate that both the substitution type and position on CD ring have much influence on the enantioseparation of epoxides.

Shi and co-workers [26] examined the influence of substitution type and position on CD ring on the enantiomeric separation of alcohols, esters, and epoxides by GC using four derivatized-β-CDs as CSPs: 2,6-di-*O*-pentyl-3-*O*-allyl-β-CD (column 1); 2,3-di-*O*-pentyl-6-*O*-allyl-β-CD (column 2); 2,6-di-*O*-pentyl-3-*O*-propyl-β-CD (column 3); and 2,3-di-*O*-pentyl-6-*O*-propyl-β-CD (column 4). The results indicated that although the substitute positions of allyl groups in column 1 and 2 were different, it was found that the enantioseparation abilities of column 1 and 2 were similar. Therefore, the substitute position of allyl groups on 3-position or 6-position did not affect the enantioseparation greatly. Similar results were also obtained on column 3 and 4. However, they were found that the enantioseparation was related to both of the structures of CDs and analytes.

The 6-*O*-*tert*-butyldimethylsilyl derivatives of CDs have been proven to be valuable chiral selectors and are widely used for enantiomer separation by GC. The enantioselectivities as well as some selected applications of these CSPs are summarized as follows:

Kobor and Schomburg [27] studied the influence of CD ring size on the enantioseparation of homologous series of 1-phenylalkanols using 6-*tert*-butyl dimethylsilyl-2,3-dimethyl derivatives of α-, β-, and γ-CDs (TB-α-CD, TB-β-CD, and TB-γ-CD, respectively) as CSPs. The results indicated that 1-phenylalkanols with short side chains, such as 1-phenylethanol and 1-phenyl-1-propanol, exhibit greater enantioselectivity on TB-α-CD as CSP, whereas the larger ring β-CD is more enantioselective for 1-phenyl-1-butanol and 1-phenyl-1-pentanol, which have longer side chains. Nonetheless, no enantiomeric separation of any homologous 1-phenylalkanols could be resolved on the TB-γ-CD CSP. These results indicated that the enantioseparation of 1-phenylalkanols was affected by size of CD cavity and structure of analyte.

Shitangkoon and Vigh [28] studied the enantioseparation of several compounds such as hydrocarbon, alkylhalides, ethers, epoxides, lactones, ketones, aldehydes, alcohols, diols, amine, *etc.* on 2,3-di-*O*-methyl β-CD with different substitution on 6-position of CD such as methyl- (BMe), deoxyfluoro- (BFMe), *n*-pentyl

(BPMe), *n*-propyldimethylsilyl (BSiPMe), *tert*-butyldimethylsilyl (BSiMe), triisopropylsilyl (BTIPSMe). Each solid CD derivative was dissolved at identical molal concentration in OV-1701 polysiloxane. It was found that the silyl substituted CD derivatives can be used at lower temperature than alkyl substituted CD derivatives. For the enantioseparation, it was found that the substituents on 6-position of CD molecule had an influence on enantioselectivities of all analytes. Among six CD derivatives, BSiMe showed the most widely enantioseparated for studied analytes.

Takahisa and Engel [29] studied the enantioseparation of several compounds such as alcohols, aldehydes, ketones, carboxylic acids, esters, lactone, *etc.* using octakis(2,3-di-*O*-methoxymethyl-6-*O*-*tert*-butyldimethylsilyl)-γ-CD (2,3-MOM-6-TBDMS-γ-CD) diluted in OV-1701 polysiloxane as CSP. The results showed that 2,3-MOM-6-TBDMS-γ-CD is a versatile CSP for enantioseparation of volatile compounds containing various functional groups (alcohol, aldehyde, ketone, carboxylic acid, ester). In addition, the enantioseparation of these chiral compounds were also compared to the corresponding one with heptakis(2,3-di-*O*-methoxymethyl-6-*O*-*tert*-butyldimethylsilyl)-β-CD (2,3-MOM-6-TBDMS-β-CD). The results showed that the range of compounds for which enantiomers could be separated with 2,3-MOM-6-TBDMS-β-CD was more limited and the enantioselectivity was lower than 2,3-MOM-6-TBDMS-γ-CD [30].

2.6 Thermodynamic investigation of enantiomeric separation by gas chromatography

Although the mechanism of chiral recognition in chromatographic method is not well understood, some mechanistic aspects can be derived from the thermodynamic investigation of the reliable experimental parameters. In general, it is accepted that the direct enantiomeric separation is based on the formation of transient diastereomic complexes between enantiomers and a chiral selector by intermolecular interactions. For the complex formation, temperature is an important factor influencing the retention factor, enantioselectivity, and resolution. The chemical equilibrium between individual enantiomer and CSP can be described by thermodynamic data using the Gibbs–Helmholtz equation [4, 31].

Due to the simplicity of the van't Hoff approach, it is used to determine the thermodynamic parameters from retention factor (k′) and separation factor (α) obtained at different temperatures on a single chiral column.

In van't Hoff approach, the difference in Gibbs free energy, $\Delta\Delta G$, is calculated from the separation factor (α) obtained from enantiomeric separation on a chiral column at a given temperature according to equation (1):

$$\Delta\Delta G = RT \cdot \ln \alpha \qquad (1)$$

$$\Delta\Delta G = RT \cdot \ln \left(\frac{k'_2}{k'_1}\right) \qquad (2)$$

where α is the separation factor or selectivity obtained from the ratio of k′ of two enantiomers

k′ is the retention factor or capacity factor of each enantiomer calculated from solute retention time according to

$$k' = \frac{t_R - t_m}{t_m}$$

R is the universal gas constant (1.987 cal/mol·K)

T is the absolute temperature (K)

$_{1,2}$ refer to the less and the more retained enantiomers, respectively

t_R is the retention time of an enantiomer or analyte

t_M is the time for unretained compound to travel at the same distance as analyte

Combining equation (2) with the Gibbs-Helmholtz relationship, equation (3), leads to equation (4):

$$-\Delta\Delta G = -\Delta\Delta H + T \cdot \Delta\Delta S \qquad (3)$$

$$RT \cdot \ln \alpha = -\Delta\Delta H + T \cdot \Delta\Delta S \qquad (4)$$

Equation (4) can be rewritten as

$$\ln \alpha = -\frac{\Delta\Delta H}{RT} + \frac{\Delta\Delta S}{R} \quad (5)$$

where $\Delta\Delta H$ is the difference in enthalpy for an enantiomeric pair

$\Delta\Delta S$ is the difference in entropy for an enantiomeric pair

According to equation (5), $\Delta\Delta H$ and $\Delta\Delta S$ could be evaluated from the slope and y-intercept of the ln α versus 1/T plot. However, the calculations of thermodynamic parameters from these plots are not possible, as a result of curvatures observed in many cases. This is due to the nonlinear dependence of selectivity on the concentration in diluted stationary phase. Therefore, this method is only valid for undiluted chiral selectors [19].

Alternatively, thermodynamic parameters can be calculated from retention factors (k′) instead of separation factors (α). The linear relationship between ln k′ and 1/T can be derived from the combination of equations (6) and (8) resulted in equation (12). Thermodynamic parameters of individual enantiomers including the differences in enthalpy and entropy of an enantiomeric pair can be obtained from the plot of ln k′ against 1/T.

$$\Delta G = -RT \cdot \ln K \quad (6)$$

The relationship between k′and K is:

$$k' = \frac{K}{\beta} \text{ and } \beta = \frac{V_m}{V_s} \quad (7)$$

where K is the distribution coefficient of an analyte between gas phase and liquid phase

β is a constant called phase ratio (the ratio of mobile phase volume to stationary phase volume)

With the previous equation (6) is modified as

$$\Delta G = -RT \ln k' \cdot \beta \quad (8)$$

$$\Delta G = \Delta H - T\Delta S \quad (9)$$

$$-RT \ln k' \cdot \beta = \Delta H - T\Delta S \quad (10)$$

Equation (9) can be rewritten as

$$\ln k' + \ln \beta = -\frac{\Delta H}{RT} + \frac{\Delta S}{R} \quad (11)$$

$$\ln k' = -\frac{\Delta H}{RT} + \frac{\Delta S}{R} - \ln \beta \quad (12)$$

where ΔH is enthalpy change resulting from the interaction of the enantiomer with the stationary phase. ΔH value describes the degree of the interaction strength. The more negative ΔH value indicates stronger interaction between analyte and stationary phase.

ΔS is entropy change resulting from the interaction of the enantiomer with the stationary phase. ΔS describes the degree of which the solute structure influences the interaction.

จุฬาลงกรณ์มหาวิทยาลัย
CHULALONGKORN UNIVERSITY

CHAPTER III

EXPERIMENTAL

3.1 Synthesis of amines

3.1.1 Chemical and reagents

Most of chemicals and solvents were purchased from various commercial sources and used without further purifications. Amines were prepared from their corresponding ketone substrates. All chemicals are listed below:

Starting materials:

- 2′-bromoacetophenone, [2142-69-0] 99% (Aldrich)
- 3′-bromoacetophenone, [2142-63-4] 99% (Aldrich)
- 4′-bromoacetophenone, [99-90-1] 98% (Aldrich)
- 5-bromo-1-indanone, [34598-49-7] 97% (Aldrich)
- 4′-bromopropiophenone, [10342-83-3] 99% (Aldrich)
- 2′-chloroacetophenone, [2142-68-9] 97% (Aldrich)
- 3′-chloroacetophenone, [99-02-5] 97% (Fluka)
- 4′-chloroacetophenone, [99-91-2] 97% (Aldrich)
- 5-chloro-1-indanone, [42348-86-7] 99% (Aldrich)
- 4′-chloropropiophenone, [6285-05-8] 98% (Aldrich)
- 2′-fluoroacetophenone, [445-27-2] 97% (Aldrich)
- 3′-fluoroacetophenone, [455-36-7] 99% (Aldrich)
- 4′-fluoroacetophenone, [403-42-9] 99% (Aldrich)
- 5-fluoro-1-indanone, [700-84-5] 99% (Aldrich)
- 4′-fluoropropiophenone, [456-03-1] 98% (Aldrich)
- 1-indanone, [83-33-0] 99% (Aldrich)

- 2′-methoxyacetophenone, [579-74-8] 99% (Fluka)
- 3′-methoxyacetophenone, [586-37-8] 97% (Fluka)
- 4′-methoxyacetophenone, [100-06-1] 99% (Fluka)
- 5-methoxy-1-indanone, [5111-70-6] 98% (Aldrich)
- 4′-methoxypropiophenone, [121-97-1] 99% (Aldrich)
- 2′-methylacetophenone, [577-16-2] 98% (Fluka)
- 3′-methylacetophenone, [585-74-0] 97% (Fluka)
- 4′-methylacetophenone, [122-00-9] 95% (Fluka)
- α-methylbenzylamine, [618-36-0] 99% (Fluka)
- 5-methyl-1-indanone, [4593-38-8] 97% (Aldrich)
- 4′-methylpropiophenone, [5337-93-9] 90% (Aldrich)
- propiophenone, [93-55-0] 99% (Fluka)
- 2′-(trifluoromethyl)acetophenone, [17408-14-9] 99% (Aldrich)
- 3′-(trifluoromethyl)acetophenone, [349-76-8] 99% (Aldrich)
- 4′-(trifluoromethyl)acetophenone, [709-63-7] 98% (Aldrich)
- 4′-(trifluoromethyl)propiophenone, [711-33-1] 99% (Aldrich)

Organic solvents :

- acetone (J.T. Baker)
- dichloromethane (J.T. Baker)
- isopropanol (Fluka)

Other chemicals :

- ammonium hydroxide (Merck)
- anhydrous ammonia (Unigue gas and petrochemical)
- anhydrous sodium sulphate (Fluka)
- hydrochloric acid (Merck)

- sodium borohydride (Fluka)
- sodium chloride (Fluka)
- sodium hydroxide (Merck)
- titanium(IV) isopropoxide (Aldrich)
- trifluoroacetic anhydride (Aldrich)

3.1.2 General procedure [32]

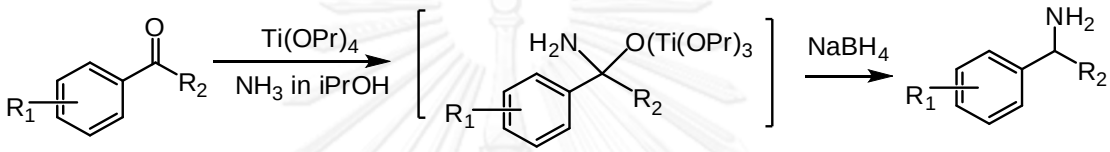

R_1 = F, Cl, Br, Me, OMe, CF_3 and R_2 = CH_3, C_2H_5

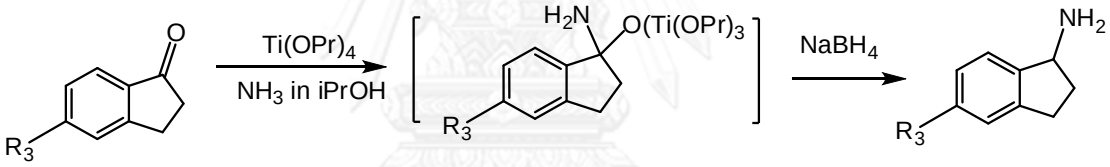

R_3 =H, F, Cl, Br, Me, OMe

The ketone (~0.7 g, 5 mmol) and titanium(IV) isopropoxide (3 mL, 2 equiv) were dissolved and stirred in isopropanol (25 mL) under purging ammonia gas 5–7 h at ambient temperature. Then, sodium borohydride (0.4 g, 1.5 equiv) was added and the reaction was stirred at room temperature for 2 h.

The reaction was then quenched by adding 25 mL of 2 M ammonium hydroxide, the resulting precipitate was filtered off. The filtrate was extracted with dichloromethane (2×25 mL). The combined organic layer was extracted with 2 M hydrochloric acid (30 mL). The acidic aqueous extract was treated with 1 M sodium hydroxide to pH 10-12, and extracted again with dichloromethane (2×25mL). The combined organic extract was washed with brine and dried with anhydrous sodium sulfate. The solvent was evaporated to obtain the corresponding pure amine

derivatives. The identities of the synthesized products were confirmed by ^{1}H and ^{13}C-NMR techniques.

The compound names, their abbreviations, and chemical structures of all relevant amine derivatives are given in Table 3.1

Table 3.1 Chemical structures and abbreviations of amine derivatives

compound	abbreviation	chemical structure
1-phenylethylamine	**PEA**	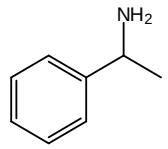
1-phenylpropylamine	**PPA**	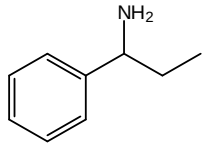
1-aminoindane	**AI**	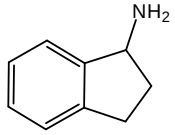
Group 1: 1-phenylethylamine with mono-substitution on aromatic ring		
1-(2´-fluorophenyl)ethylamine	**2F**	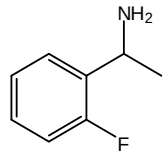
1-(3´-fluorophenyl)ethylamine	**3F**	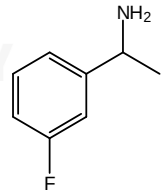
1-(4´-fluorophenyl)ethylamine	**4F**	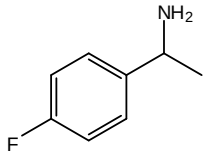

Table 3.1 (continued)

compound	abbreviation	chemical structure
1-(2´-chlorophenyl)ethylamine	**2Cl**	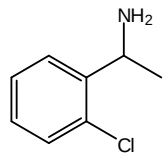
1-(3´-chlorophenyl)ethylamine	**3Cl**	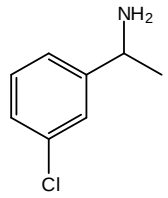
1-(4´-chlorophenyl)ethylamine	**4Cl**	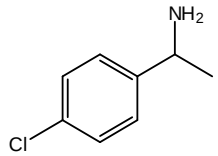
1-(2´-bromophenyl)ethylamine	**2Br**	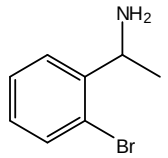
1-(3´-bromophenyl)ethylamine	**3Br**	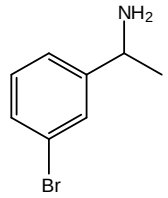
1-(4´-bromophenyl)ethylamine	**4Br**	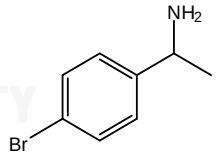
1-(2´-methylphenyl)ethylamine	**2Me**	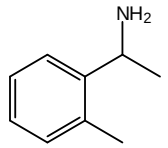
1-(3´-methylphenyl)ethylamine	**3Me**	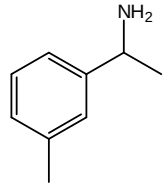

Table 3.1 (continued)

compound	abbreviation	chemical structure
1-(4´-methylphenyl)ethylamine	**4Me**	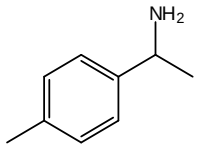
1-(2´-methoxyphenyl)ethylamine	**2OMe**	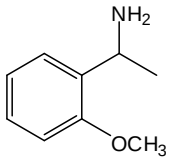
1-(3´-methoxyphenyl)ethylamine	**3OMe**	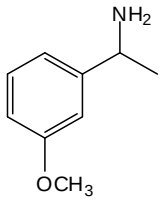
1-(4´-methoxyphenyl)ethylamine	**4OMe**	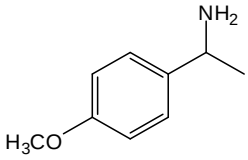
1-(2´-trifluoromethylphenyl)ethylamine	**2CF**	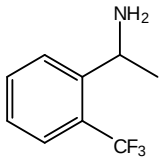
1-(3´-trifluoromethylphenyl)ethylamine	**3CF**	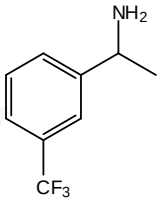
1-(4´-trifluoromethylphenyl)ethylamine	**4CF**	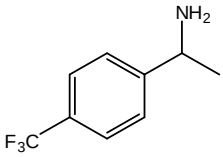

Table 3.1 (continued)

Group 2: 1-phenylpropylamine with mono-substitution on aromatic ring		
compound	abbreviation	chemical structure
1-(4´-fluorophenyl)propylamine	**4FP**	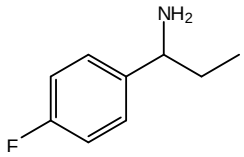
1-(4´-chlorophenyl)propylamine	**4ClP**	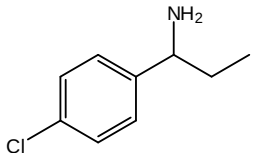
1-(4´-bromophenyl)propylamine	**4BrP**	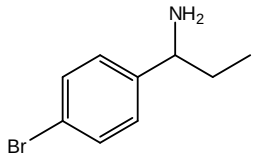
1-(4´-methylphenyl)propylamine	**4MeP**	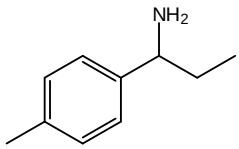
1-(4´-methoxyphenyl)propylamine	**4OMeP**	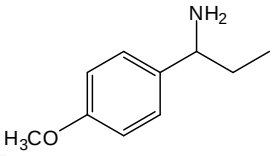
1-(4´-trifluoromethylphenyl)propylamine	**4CFP**	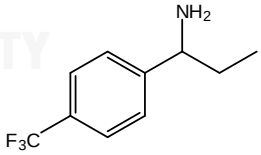
Group 3: 1-aminoindane with mono-substitution on aromatic ring		
5´-fluoro-1-aminoindane	**5FA**	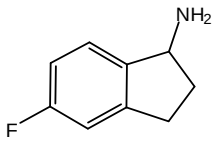

Table 3.1 (continued)

compound	abbreviation	chemical structure
5´-chloro-1-aminoindane	**5ClA**	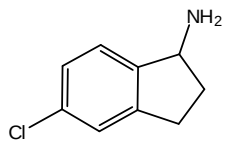
5´-bromo-1-aminoindane	**5BrA**	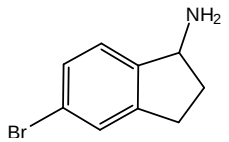
5´-methyl-1-aminoindane	**5MeA**	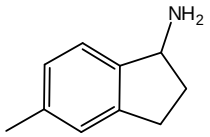
5´-methoxy-1-aminoindane	**5OMeA**	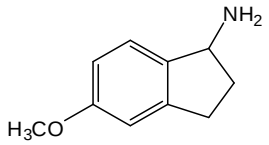

3.2 Derivatization of amines [17]

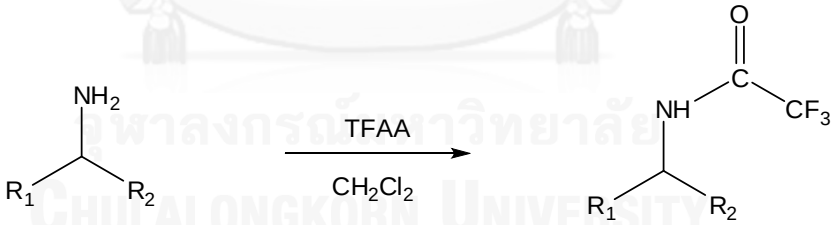

R_1, R_2 = alkyl, aryl or cycloalkyl

Amine (20 μL) was dissolved in dichloromethane (1 mL) and added trifluoroacetic anhydride (TFAA, 50 μL). The reaction was performed at room temperature for 30 min. The solvent and the excess reagent were removed by a stream of purging nitrogen for 10 min. The residue was re-dissolved in dichloromethane at a concentration of 10–20 mg/mL. Each 0.4 μL of this solution was injected into GC.

3.3 Gas chromatographic analysis

3.3.1 GC experiment

All chromatographic analyses were performed on an Agilent 6890 series gas chromatograph equipped with a split/splitless injector and a flame ionization detector (FID). The temperature of injector and detector were maintained at 250 °C. Hydrogen was used as carrier gas with an average linear velocity of 50 cm/s. The separation was carried out on the 15 m×0.25 mm i.d. capillary column coated with a 0.25 μm thick film of stationary phase. Four types of stationary phase were used in this research:

achiral reference column:

- polysiloxane OV-1701 (7% cyanopropyl, 7% phenyl, 86 % dimethyl polysiloxane, Supelco) as a reference stationary phase and diluent for solid cyclodextrin derivatives in three chiral columns

chiral columns:

- 26.7 % hexakis(2,3-di-*O*-methyl-6-*O*-*tert*-butyldimethylsilyl)cyclomalto hexaose (or ASiMe) in OV-1701
- 30.0 % heptakis(2,3-di-*O*-methyl-6-*O*-*tert*-butyldimethylsilyl)cyclomalto heptaose (or BSiMe) in OV-1701
- 32.8 % octakis(2,3-di-*O*-methyl-6-*O*-*tert*-butyldimethylsilyl)cyclomalto octaose (or GSiMe) in OV-1701

Three chiral columns were prepared to contain identical molality of cyclodextrin derivatives. All columns were conditioned at 220 °C until a stable baseline was observed. Column efficiency was checked at each working temperature with *n*-alkane which had plate number (N) above 3,500 plates/m for all columns.

3.3.2 Determination of thermodynamic parameters

Each analyte solution was injected at least in duplicate on four columns, a reference column and three chiral stationary phases. All thermodynamic studies were carried out isothermally over the temperature range 80–220 °C (in 10 °C increments). From the chromatograms obtained from OV-1701 column, retention

factors (k′) of all analytes were calculated, and the thermodynamic parameters (ΔH, ΔS) were determined by means of van't Hoff plots. For three chiral stationary phase columns, both retention factors (k') and enantioselectivities (α) of all analytes were calculated, and used to determine thermodynamic parameters (ΔH, ΔS, $\Delta\Delta H$, $\Delta\Delta S$) by means of van't Hoff plots.

Thermodynamic data of each column were compared and used to explain the strength of interactions between analyte and stationary phase. Their enantioselectivities of all analytes on three CSP columns were also compared to discuss the differences and/or similarities in terms of type and position of substituents includes the main structure of analyte.

จุฬาลงกรณ์มหาวิทยาลัย
CHULALONGKORN UNIVERSITY

CHAPTER IV

RESULTS AND DISCUSSION

4.1 Synthesis of amines

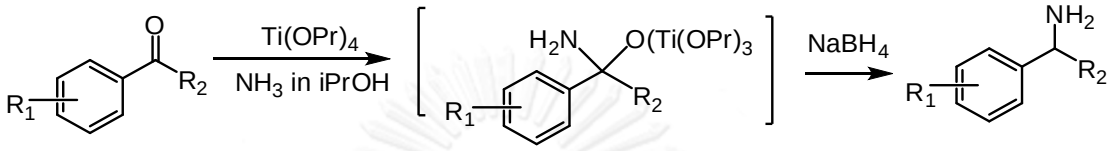

R_1 = F, Cl, Br, Me, OMe, CF_3 and R_2 = CH_3, C_2H_5

Amine derivatives were synthesized via reductive amination reaction between the corresponding ketone precursors and ammonia gas in the presence of titanium(IV) isopropoxide as a catalyst, followed by sodium borohydride reduction. The reaction begins with titanium chelating of ketone, followed by nucleophilic addition of ammonia to the carbonyl group of ketone. The intermediate titanium(IV) complex was formed by stirring a mixture of the carbonyl compound, ammonia and titanium(IV) isopropoxide at ambient temperature for 5–7 h. Sodium borohydride was then added and the resulting mixture was further stirred for 2–3 h. The reaction may occur through the titanium(IV) complex which is either reduced directly or via a transient imine species [33]. Finally, the reaction mixture was quenched with 2 M ammonium hydroxide and the resulting precipitate was filtered. The filtrate was extracted with dichloromethane. The primary amines were isolated in their pure forms by simple acid-base extraction. The proposed mechanism of reductive amination via titanium(IV) complex was shown in Figure 4.1.

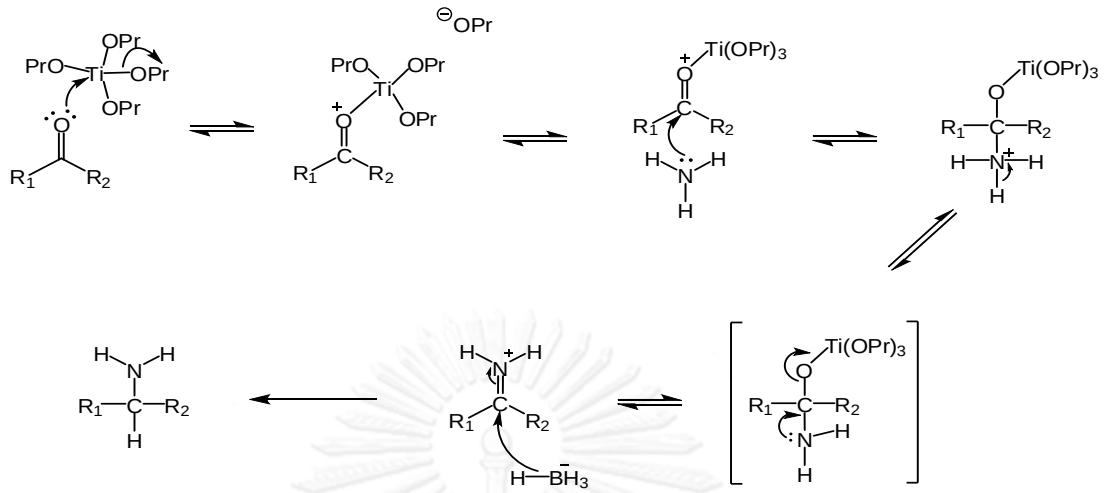

Figure 4.1 Proposed mechanism of reductive amination via titanium(IV) complex

All ketones led to the formation of the desired primary amines in varying yields of 40 to 85%, depending on the structures of ketones (Table 4.1). According to Table 4.1, all *ortho*-substituents showed similar % yield in the range of 50-65 % (entries 1-5). While only **3F** and **3Cl** (entries 7-8) showed higher % yield than **2F** and **2Cl**, respectively. Only **4Cl** and **4Me** (entries 14 and 16) showed higher % yield than *ortho- and meta*-substituents. These results indicated that size and position of substituents on the aromatic ring of ketones somewhat affected the % yield of the desired products from the reaction.

All *para*-phenylpropylamines (entries 20-25) were obtained in lower % yield than their corresponding *para*-phenylethylamine analogs (entries 13-18), except for **4OMeP** (entry 24). The results may be implied that the yields of amines in the reactions decreased with increasing steric hindrance from the longer aliphatic chain around the carbonyl functional group.

Table 4.1 % yields of the amine products

Entry	R_1	R_2	Product	%yield
1	2-F	CH_3	**2F**	65
2	2-Cl	CH_3	**2Cl**	50
3	2-Br	CH_3	**2Br**	55
4	2-CH_3	CH_3	**2Me**	55
5	2-OCH_3	CH_3	**2OMe**	57
6	2-CF_3	CH_3	**2CF**	53
7	3-F	CH_3	**3F**	85
8	3-Cl	CH_3	**3Cl**	63
9	3-Br	CH_3	**3Br**	55
10	3-CH_3	CH_3	**3Me**	47
11	3-OCH_3	CH_3	**3OMe**	54
12	3-CF_3	CH_3	**3CF**	46
13	4-F	CH_3	**4F**	62
14	4-Cl	CH_3	**4Cl**	85
15	4-Br	CH_3	**4Br**	60
16	4-CH_3	CH_3	**4Me**	86
17	4-OCH_3	CH_3	**4OMe**	40
18	4-CF_3	CH_3	**4CF**	52
19	H	C_2H_5	**PPA**	52
20	4-F	C_2H_5	**4FP**	60
21	4-Cl	C_2H_5	**4ClP**	52
22	4-Br	C_2H_5	**4BrP**	40
23	4-CH_3	C_2H_5	**4MeP**	53
24	4-OCH_3	C_2H_5	**4OMeP**	66
25	4-CF_3	C_2H_5	**4CFP**	40

The same synthetic procedure can be adapted for 1-indanone to synthesize 1-aminoindane derivatives as show below.

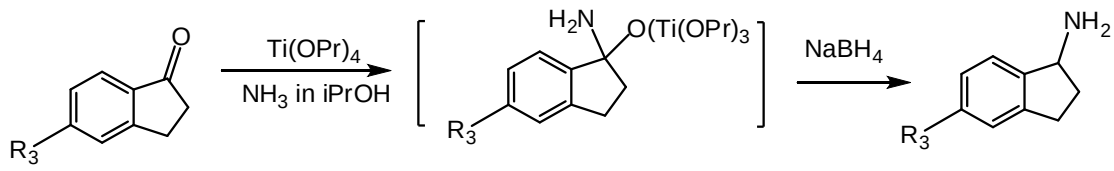

R_3 =H, F, Cl, Br, Me, OMe

All 1-aminoindanes (Table 4.2) were obtained in lower % yield than their corresponding phenylpropylamine analogs (Table 4.1, entries 19-24), except for **5BrA** (Table 4.2, entry 4)**.** These results may come from lower activity of the carbonyl group of the cyclic ketones and the transient imine species towards nucleophiles. The advantages of this method are mild reaction conditions, simple work-up procedure, and no chromatographic purification needed.

Table 4.2 % yields of the 1-aminoindane products

Entry	R_3	Product	%yield
1	H	**AI**	40
2	F	**5FA**	45
3	Cl	**5ClA**	42
4	Br	**5BrA**	59
5	CH_3	**5MeA**	49
6	OCH_3	**5OMeA**	52

4.2 Derivatization of amines

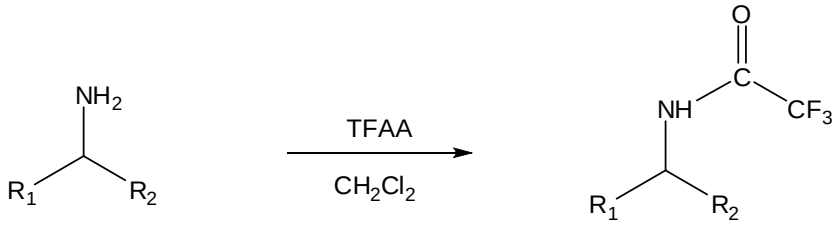

R_1, R_2 = alkyl, aryl or cycloalkyl

The derivatizations of amines with trifluoroacetic anhydride were performed at room temperature for 30 min. The solvent and the excess reagent could be easily removed by a stream of nitrogen. The structures of trifluoroacetyl (TFA) amine derivatives of these acylation reactions had been confirmed by others using gas chromatography-mass spectrometry (GC-MS) [16, 34-36]. In this work, the presence of trifluoroacetyl group of TFA 1-phenylethylamine was confirmed by ^{13}C NMR as shown in Figure 4.2

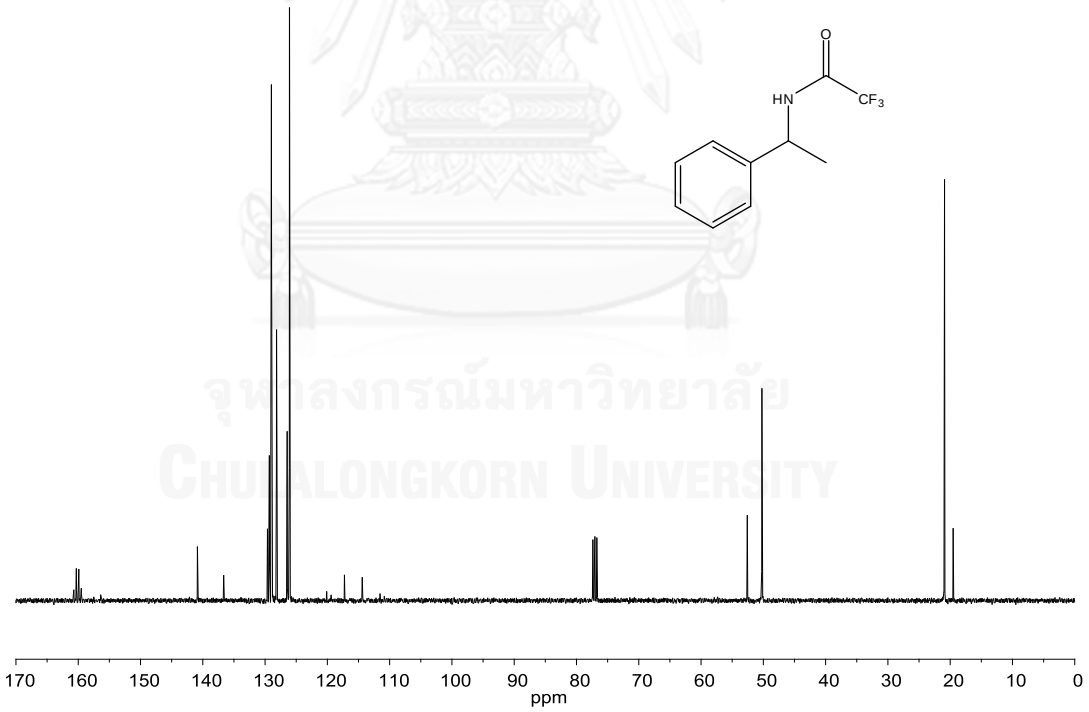

Figure 4.2 ^{13}C NMR spectrum of trifluoroacetyl-1-phenylethylamine (100 MHz, $CDCl_3$) δ (ppm): 160.1 (q, J_{CF} = 40.3 Hz), 138.8 (d, J_{CF}= 424.0 Hz), 129.5 (d, J_{CF} = 30.5 Hz), 128.6 (d, J_{CF} = 82.9 Hz), 126.3 (d, J_{CF} = 36.8 Hz), 115.8 (q, J_{CF} = 287.4 Hz), 51.4 (d, J_{CF} = 235.8 Hz), 20.2 (d, J_{CF} = 139.6 Hz)

4.3 Gas chromatographic separation of amine derivatives

Enantioseparations of all TFA amine derivatives were analyzed on four columns: OV-1701, ASiMe, BSiMe, and GSiMe. They were performed at isothermal conditions in the temperature range of 80–220 °C with 10 °C increments. Each analytes was injected at least in duplicate. From the chromatographic results, the retention factor (k′) and enantioselectivity (α) of analytes at each operating temperature could be obtained, but could not be directly compared due to highly varied physical properties of analytes such as boiling point and vapor. Therefore, thermodynamic parameters obtained over a temperature range were determined to provide better understanding of the interactions between analytes and stationary phases.

4.4 Thermodynamic investigation

Thermodynamic parameters associated with the interactions between chiral amines and stationary phase could be acquired through the van't Hoff plot (see equation (12) in section 2.5). All ln k′ versus 1/T plots showed linear relationship with correlation coefficient value (R^2) greater than 0.9980. From these plots, enthalpy (ΔH) and entropy (ΔS) values for each enantiomer could be calculated from slope and y-intercept, respectively. When enantiomeric pairs were separated, the enthalpy and entropy differences ($\Delta\Delta H$ and $\Delta\Delta S$) could be determined from the differences in ΔH and ΔS values of two enantiomers.

In order to understand the influence of size of CD ring, thermodynamic value of amines obtained from three CSP columns in this study (ASiMe, BSiMe, and GSiMe) were compared.

4.4.1 Enthalpy change (ΔH) and entropy change (ΔS)

The enthalpy change ($-\Delta H$) indicates the strength of interaction between the analyte and the stationary phase. The larger $-\Delta H$ (more negative value), the higher strength of interaction. While the entropy change ($-\Delta S$) indicates the loss of degree of freedom resulted from the interaction between the enantiomer and the stationary phase. The larger $-\Delta S$ (more negative value), fewer degree of freedom on the CSP.

The –ΔH and –ΔS values of all analytes on the OV-1701 reference column were shown in Figures 4.3 and 4.4, respectively. It was observed that each analyte show –ΔH values in parallel –ΔS values. All analytes exhibited average –ΔH values of 14.80 ± 0.69 kcal/mol. Among all studied analytes, **2F** exhibited the smallest, whereas analyte **5BrA** showed the largest –ΔH values. According to Figure 4.3, halogenated substitution at *meta*- or *para*-position on the aromatic ring seems to give higher strength of interaction.

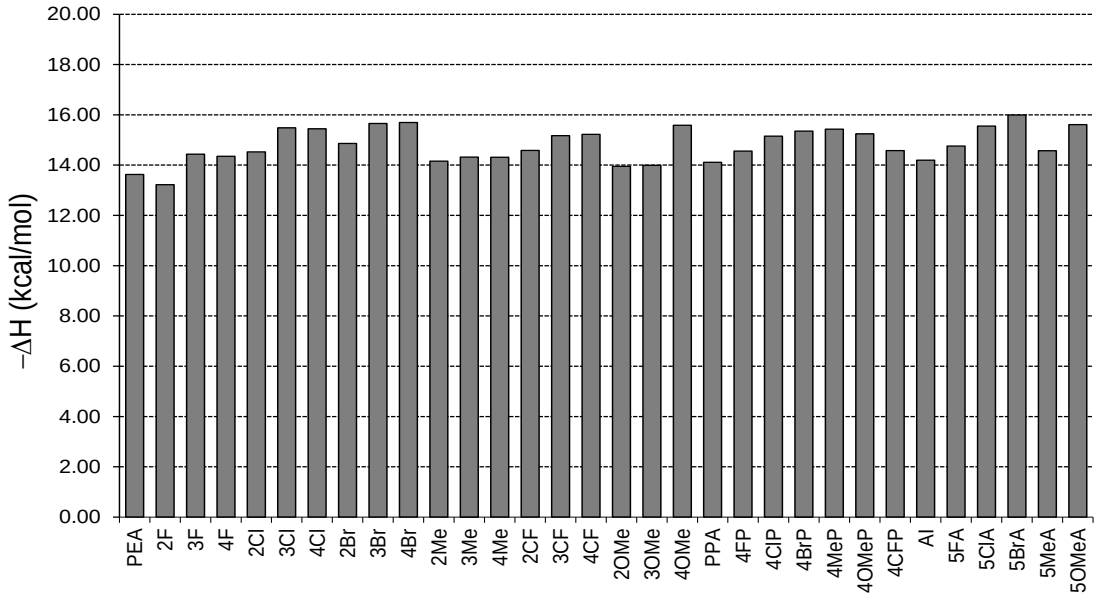

Figure 4.3 Enthalpy change (–ΔH, kcal/mol) of TFA amine derivatives on OV-1701 column ($\bar{x}$ = 14.80; SD = 0.69)

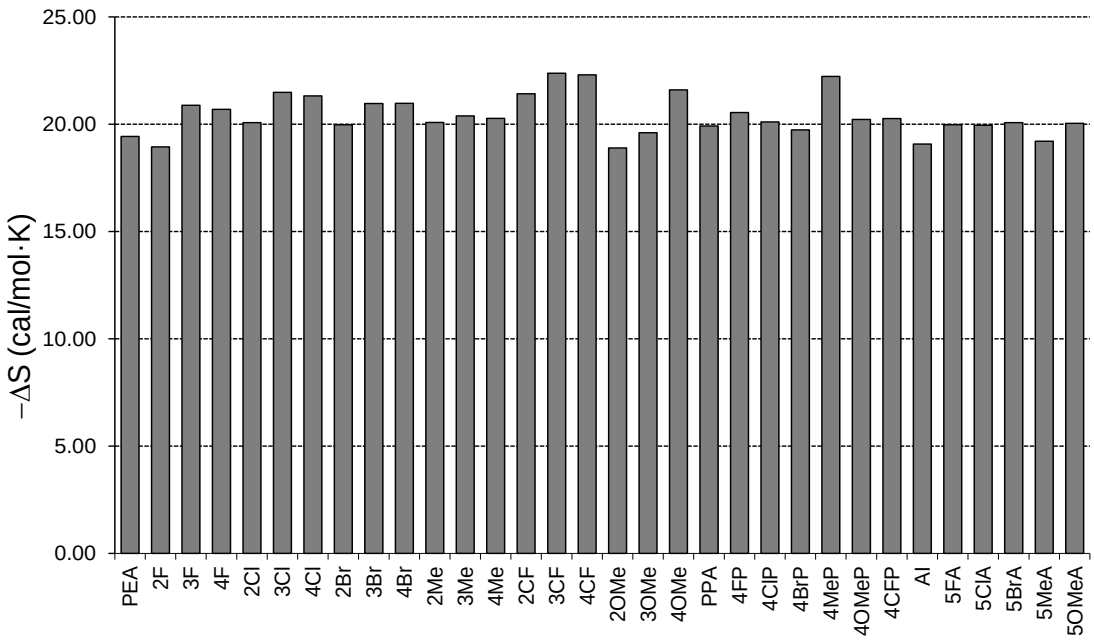

Figure 4.4 Entropy change (−ΔS, cal/mol·K) of TFA amine derivatives on OV-1701 column ($\bar{x}$ = 20.41; SD = 0.94)

Enthalpy and entropy values of the more retained enantiomers ($-\Delta H_2$ and $-\Delta S_2$) of all analytes on three CSP columns were shown in Figures 4.5 and 4.6, respectively. The $-\Delta H_2$ and $-\Delta S_2$ values on three CSP columns were higher than those on OV-1701 reference column. These results indicate the increase interaction between analytes and cyclodextrin derivatives**.** The $-\Delta H_2$ and $-\Delta S_2$ values on the same column showed similar trend. Therefore, we will discuss using enthalpy values as the model.

On ASiMe column, mono-substituted PEAs exhibited the $-\Delta H_2$ values in the descending order: *para- > meta- > ortho-*. The halogenated substitution at *meta-* and *para*-position on the aromatic ring tend to give higher $-\Delta H_2$ values. This similar trend was also observed for *para*-substituted PPAs and AIs. These results suggested that the influence toward the interaction between analyte and stationary phase depend on type and position of substitution of analyte.

On BSiMe column, most of analytes show $-\Delta H_2$ values slightly lower than ASiMe column**.** The steric hindrance of analyte may lead to poorer interaction of

analyte with the large cavity of β-CD than α-CD. For mono-substituted PEAs, similar trend in the descending order: *para-* > *meta-* > *ortho-* was also observed except for analytes **3F** and **3Me** which show slightly larger $-\Delta H_2$ values than **4F** and **4Me**, respectively. Nevertheless, the halogenated substitution at *meta-* and *para-* position on the aromatic ring also still give higher $-\Delta H_2$ values on this column.

On column GSiMe, most of analytes show similar $-\Delta H_2$ values and slightly lower than column ASiMe and BSiMe**.** On three CSPs, all analytes exhibited the average $-\Delta H_2$ value of 16.58 ± 1.29, 15.85 ± 1.04, and 15.53 ± 0.72 kcal/mol, respectively. It was generally noticed that the average strength of interaction between analyte and CSP slightly decreased from ASiMe > BSiMe > GSiMe, as the size of cavity of CD ring increased.

จุฬาลงกรณ์มหาวิทยาลัย
CHULALONGKORN UNIVERSITY

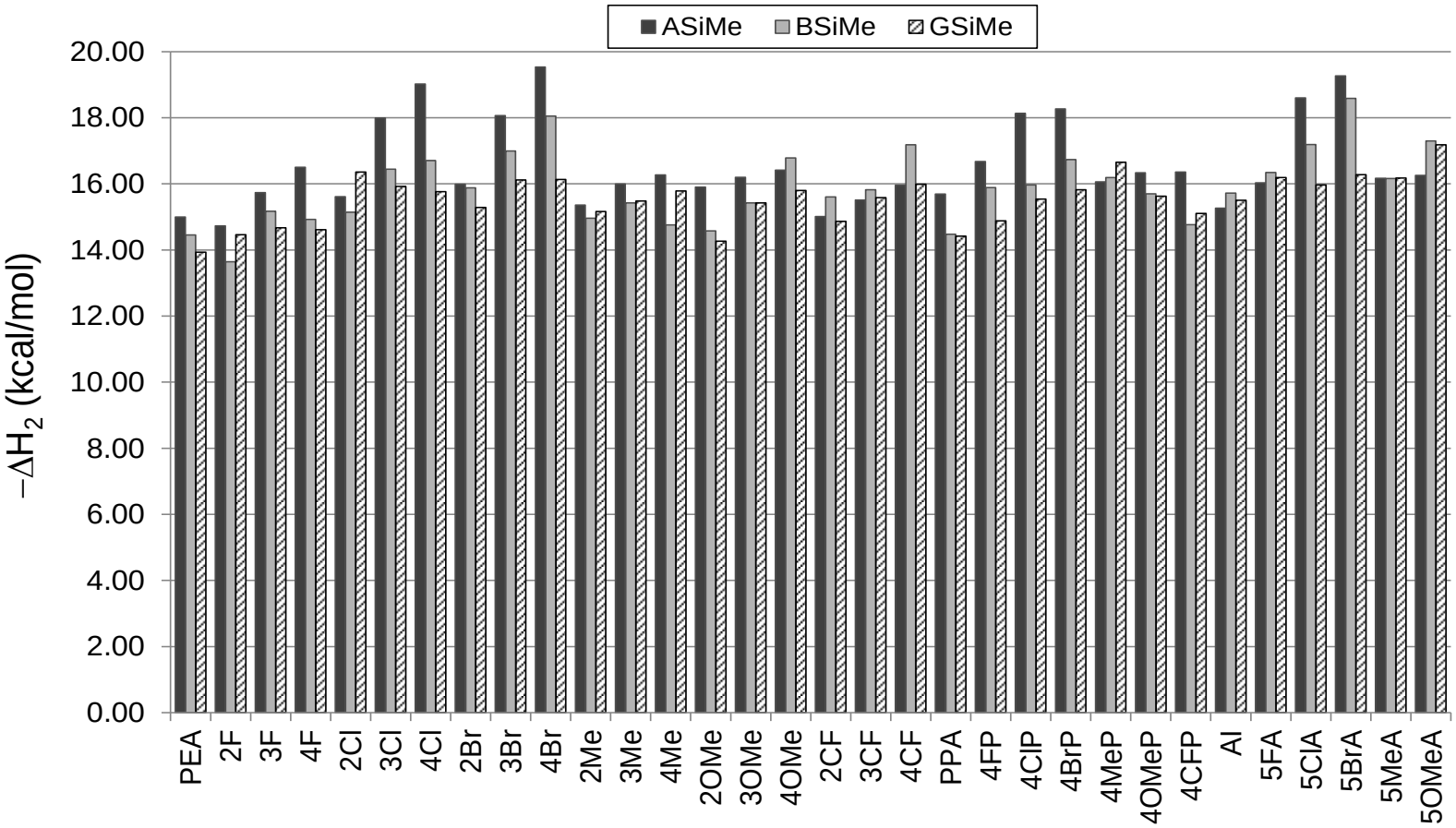

Figure 4.5 Enthalpy change ($-\Delta H_2$, kcal/mol) of the more retained enantiomers of TFA amine derivatives on three CSP columns

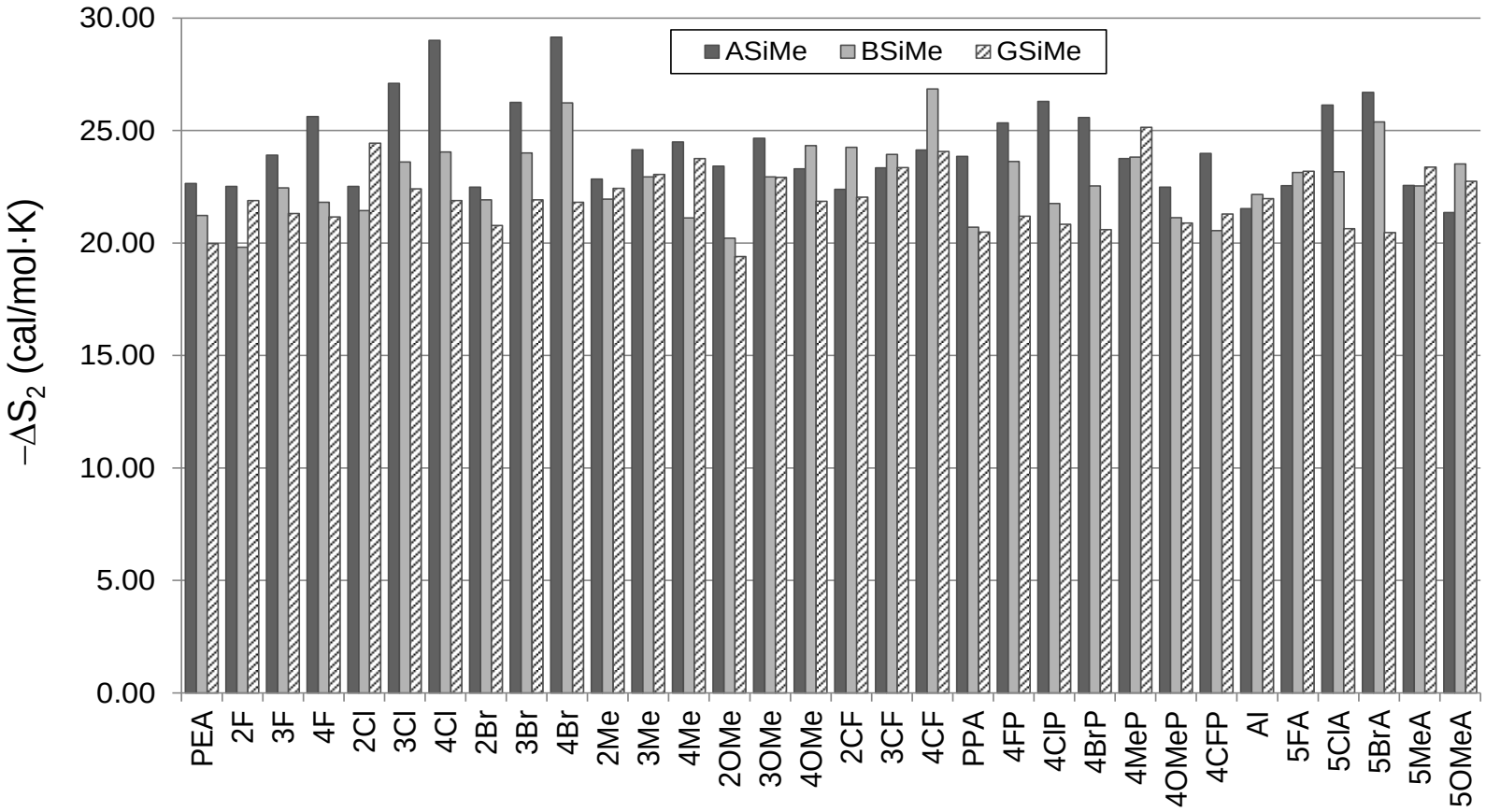

Figure 4.6 Entropy change ($-\Delta S_2$, cal/mol·K) of the more retained enantiomers of TFA amine derivatives on three CSP columns

4.4.2 Enthalpy difference ($\Delta\Delta H$) and entropy difference ($\Delta\Delta S$)

The $-\Delta\Delta H$ and $-\Delta\Delta S$ values were calculated from the difference in $-\Delta H$ and $-\Delta S$ values of each enantiomer obtained from van't Hoff plots. The $-\Delta\Delta H$ and $-\Delta\Delta S$ values of all amine derivatives on three CSP columns were shown in Figures 4.7 and 4.8, respectively. In this research, **PEA** was regarded as a reference analyte and the influence of analyte structure and substituents on enantioseparation were systematically examined and discussed through the thermodynamic values. The $-\Delta\Delta H$ and $-\Delta\Delta S$ values from the same column showed similar trend. Therefore, the discussion on enantioseparation will be mentioned through $-\Delta\Delta H$ values only. Due to the $-\Delta\Delta H$ values of all analytes were significantly different depending on analyte structure, i.e. type and position of substituents, and the main structure of analyte, the influence of analyte structure on enantioseparation will be discussed and classified into three groups according to the similarity of analyte structure.

จุฬาลงกรณ์มหาวิทยาลัย
CHULALONGKORN UNIVERSITY

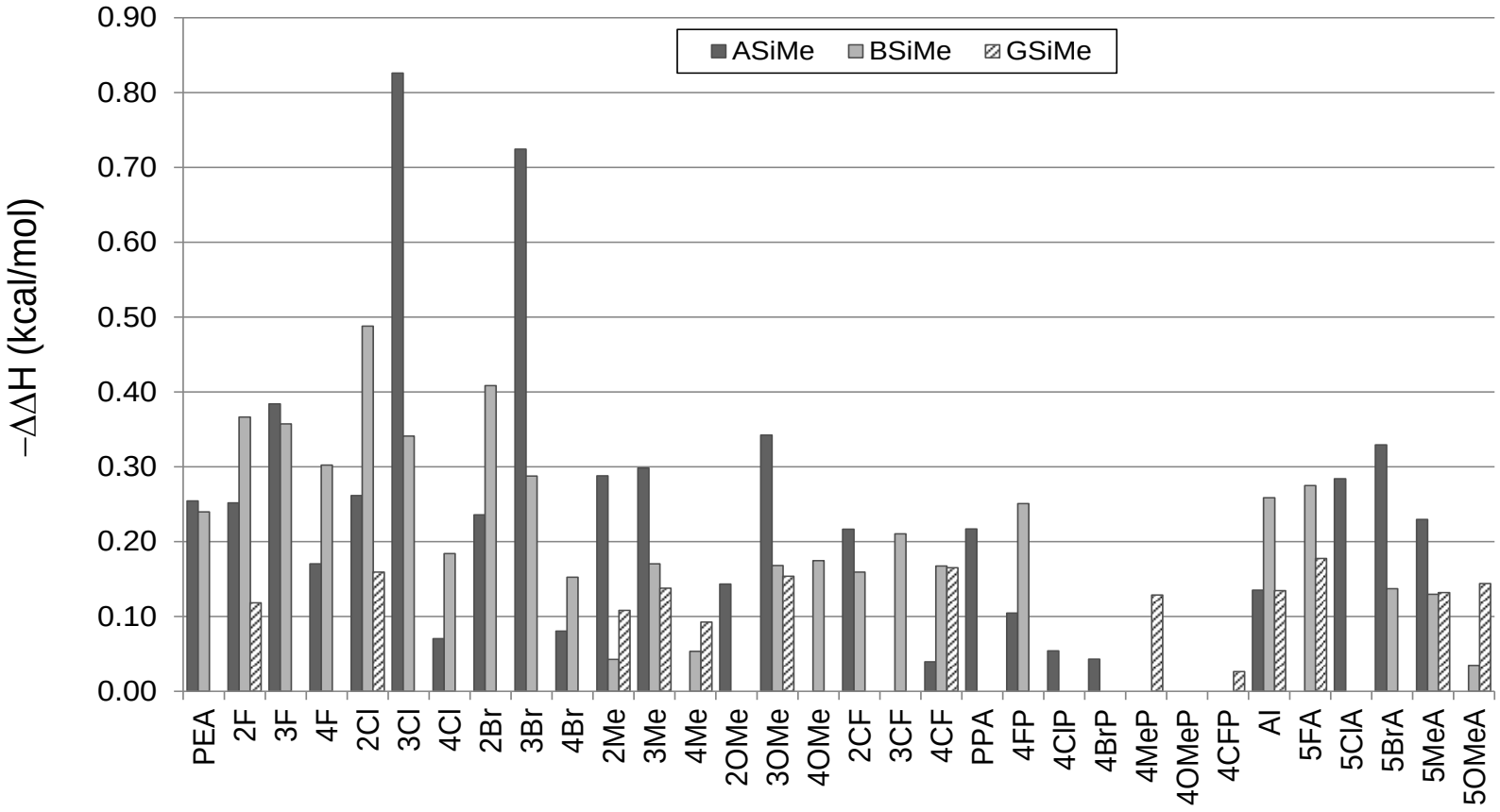

Figure 4.7 Enthalpy difference (−ΔΔH, kcal/mol) of TFA amine derivatives on three CSP columns

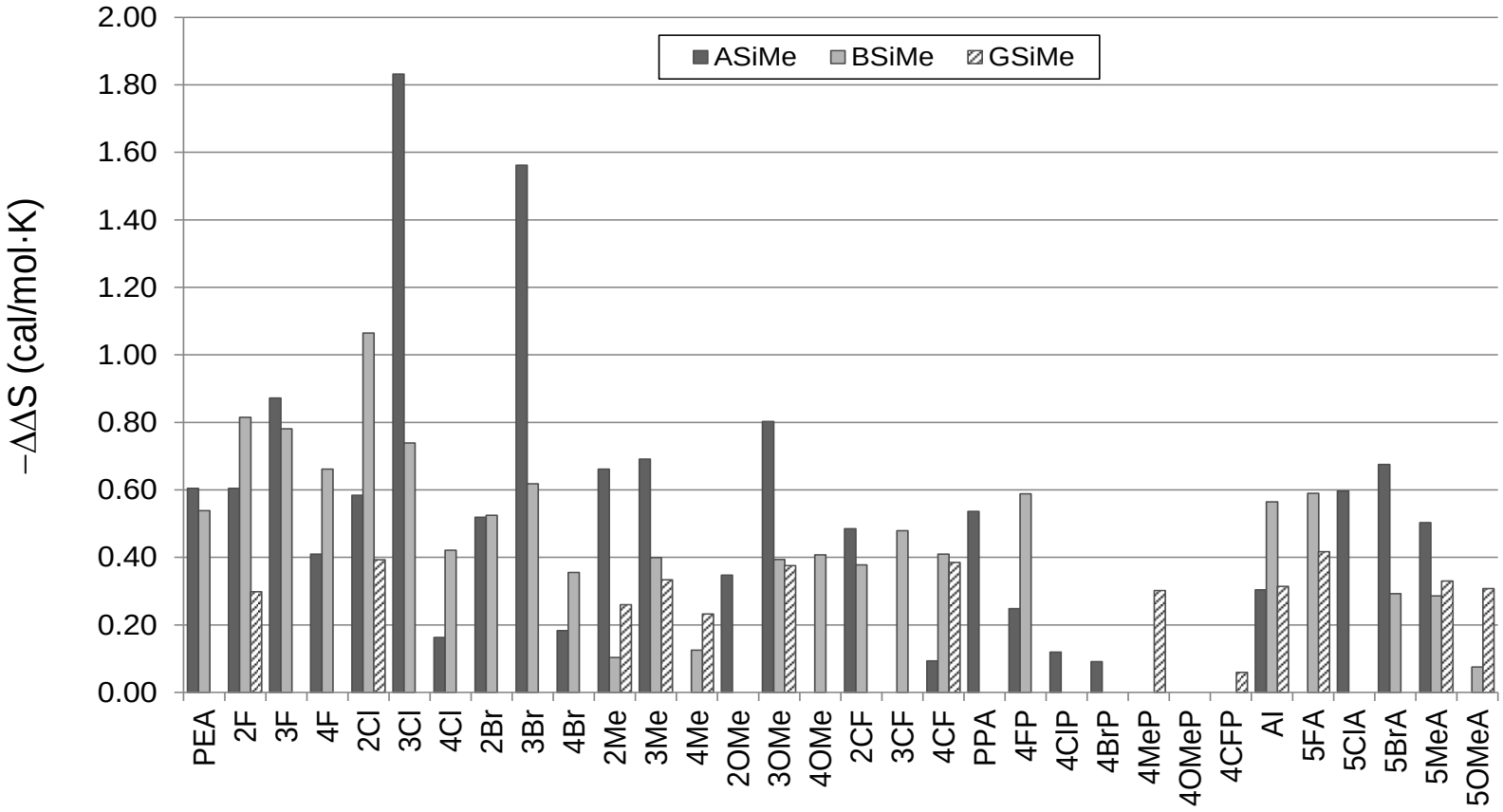

Figure 4.8 Entropy difference (−ΔΔS, cal/mol·K) of TFA amine derivatives on three CSP columns

Group 1: 1-Phenylethylamines (PEA) with mono-substitution on the aromatic ring

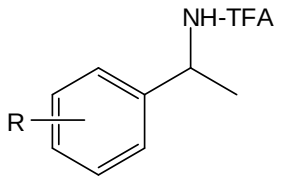

R = H, F, Cl, Br, Me, OMe, CF_3

Enantiomer of amines in group 1 were TFA derivatives of 1-phenylethylamines with mono-substitution on the aromatic ring as shown above. The substituent type includes fluoro, chloro, bromo, methyl, methoxy, and trifluoromethyl at *ortho-*, *meta-* and *para*-positions. The $-\Delta\Delta H$ values representing enantioseparation of TFA amine derivatives in group 1 on three chiral columns were displayed in Figure 4.9.

From Figure 4.9, it was clear that enantioseparation of TFA amine derivatives mainly depend on both type and position of substitution on three chiral columns. Using ASiMe column, fifteen enantiomers from eighteen enantiomers of mono-substituted PEAs were enantioseparated as seen from Figure 4.9(a).

According to Figure 4.9(a), it was clear that the position of substituent on the aromatic ring of mono-substituted analytes strongly influenced on the enantioseparation. Compared to **PEA** as a reference, it was found that *meta*-substituted analytes seemed to enhance enantioseparation as seen from high $-\Delta\Delta H$ values, except for **3CF**. Among six *meta*-substituted analytes, **3Cl** showed the highest $-\Delta\Delta H$ values. Moreover, most analytes exhibited the $-\Delta\Delta H$ values in the descending order of *meta-* > *ortho-* > *para-.* Exception was found for trifluoromethyl substituted analytes with $-\Delta\Delta H$ values in the descending order of *ortho-* > *para-*> *meta-.*

Considering *ortho*-substituted analytes, all *ortho*-substituted analytes were enantioseparated on this column. While *para*-substituted analytes show poor enantioseparation or could not be separated on this column. These results may implied that *para*-substitution on the aromatic ring seem to reduce the enantioseparation on this column due to the small cavity of α-CD.

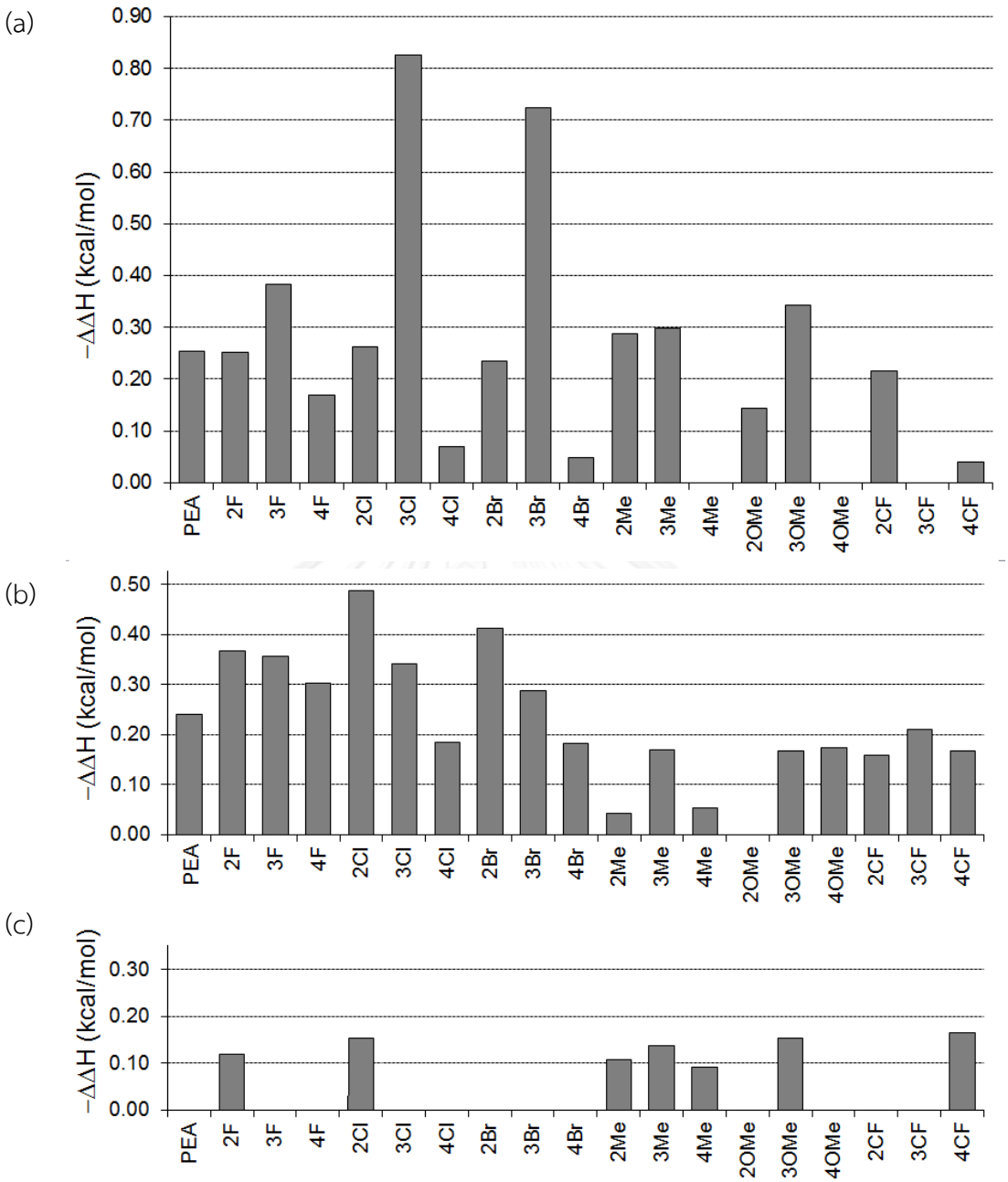

Figure 4.9 Enthalpy difference (−ΔΔH) of the enantiomers of TFA derivatives of PEAs on (a) ASiMe, (b) BSiMe, and (c) GSiMe columns

The influence of position of substituent towards retention and enantioselectivity was studied. Relationship between ln k'_2 versus 1/T and between ln α versus 1/T of three monofluoro-substituted analytes (**2F**, **3F**, and **4F**) on ASiMe column were shown in Figures 4.10-4.11.

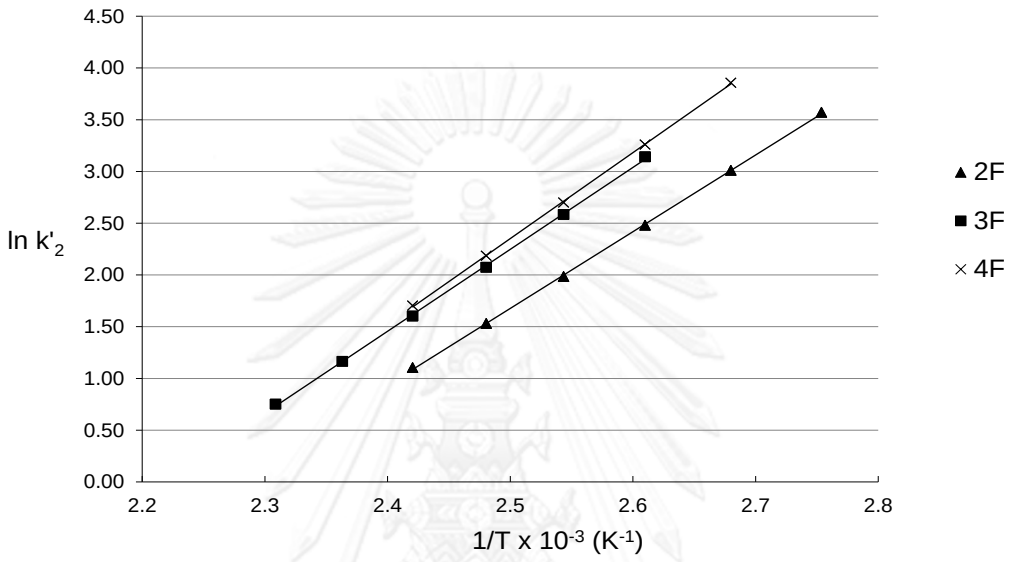

Figure 4.10 Plots of ln k'_2 versus 1/T of **2F**, **3F**, and **4F** on ASiMe column

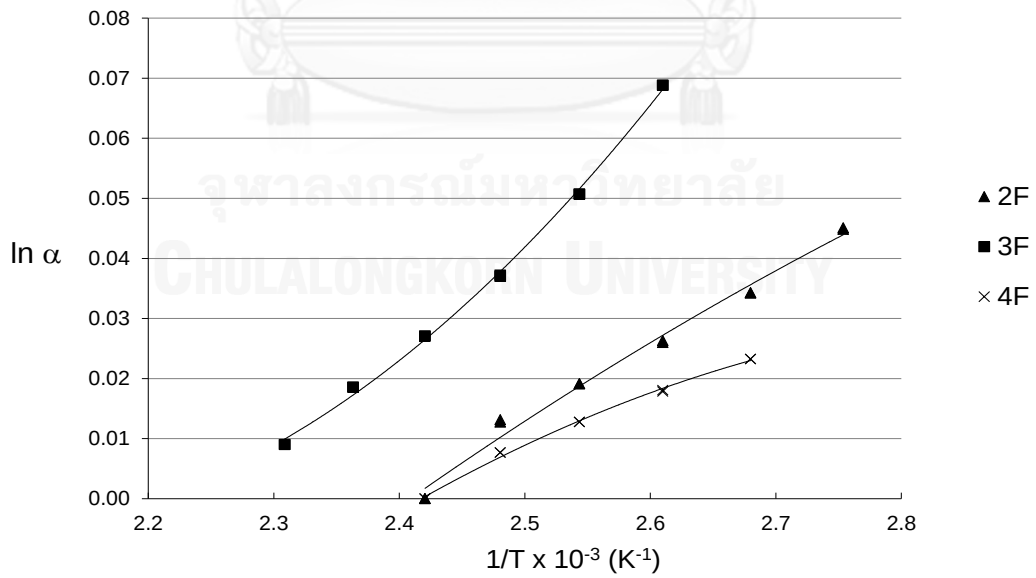

Figure 4.11 Plots of ln α versus 1/T of **2F**, **3F**, and **4F** on ASiMe column

As seen from Figure 4.10, the highest slope of **4F** from the plot of ln k′ versus 1/T indicating the largest increase in k′ value with a decrease in temperature. However, the strong retention factor of analytes did not necessarily correlate to their enantioselectivities. All analytes show slightly higher k′ with a decrease in temperature. At the same temperature, **4F** were more retained than **2F** and **3F**. Nevertheless, it was seen that **3F** had the highest enantioselectivities at every temperature studied (Figure 4.10). Among three monofluoro-substituted analytes, **3F** showed the highest $-\Delta\Delta H$ value and the highest slope of ln α versus 1/T (Figures 4.9(a) and 4.11), indicating that enantioseparation of **3F** could be easily improved by slight decrease in temperature. Chromatograms demonstrating the effects of temperature and position of substituent of **2F**, **3F**, and **4F** were compared in Figure 4.12. The decrease in temperature by 10 °C improved the enantioseparation of **3F** than for **2F** and **4F**.

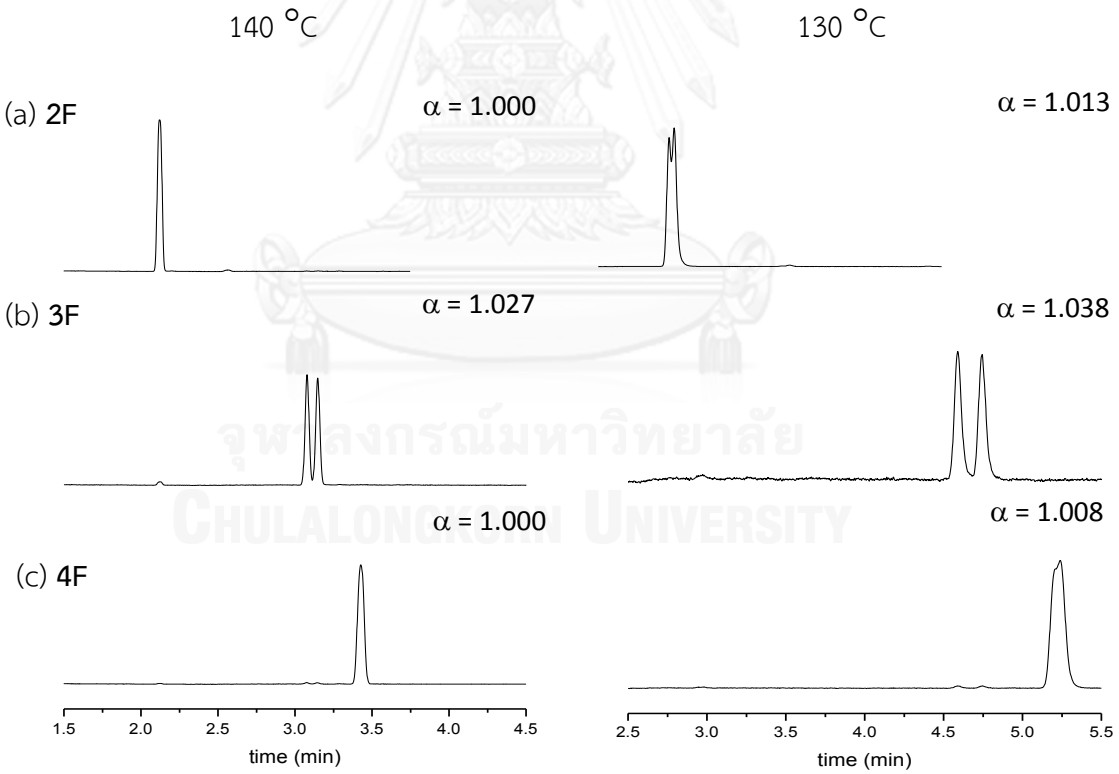

Figure 4.12 Chromatograms of (a) **2F**, (b) **3F**, and (c) **4F** at 140 °C (left) and 130 °C (right) on ASiMe column

The influence of type of substituent on the aromatic ring of analytes in group 1 on enantioseparation was also studied. Among all *meta*-substituted analytes, the $-\Delta\Delta H$ values decreased in descending order of **3Cl** > **3Br** >> **3F** > **3OMe** > **3Me >> 3CF**. It was clearly seen that *meta*-halogenated analytes showed good enantioseparation on ASiMe column. Considering three *meta*-halogenated analytes (**3F**, **3Cl** and **3Br**), **3Cl** showed the highest $-\Delta\Delta H$ values (Figure 4.9(a))**.** However, it was seen that enantioselectivity of **3Br** had the highest enantioselectivities at every temperature studied (Figure 4.13). The results suggest that several parameters must be considered simultaneously in selecting appropriate separation condition. The separation of **3F**, **3Cl** and **3Br** at 160 and 150°C were compared in Figure 4.14. The decrease in temperature by 10 °C improved the enantioseparation of **3Cl** than for **3Br** and **3F**.

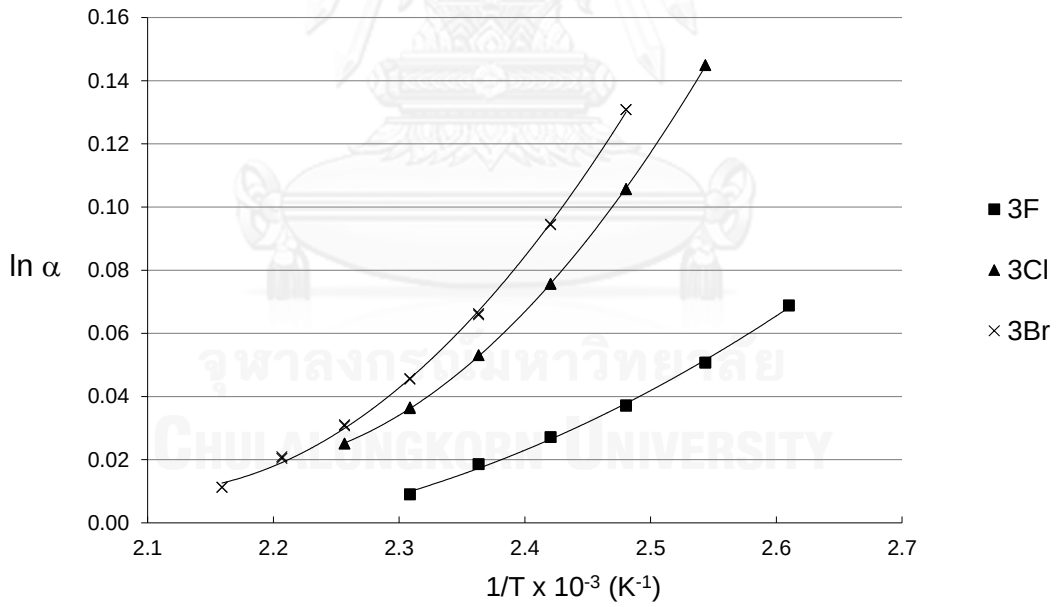

Figure 4.13 Plots of ln α versus 1/T of **3F**, **3Cl**, and **3Br** on ASiMe column

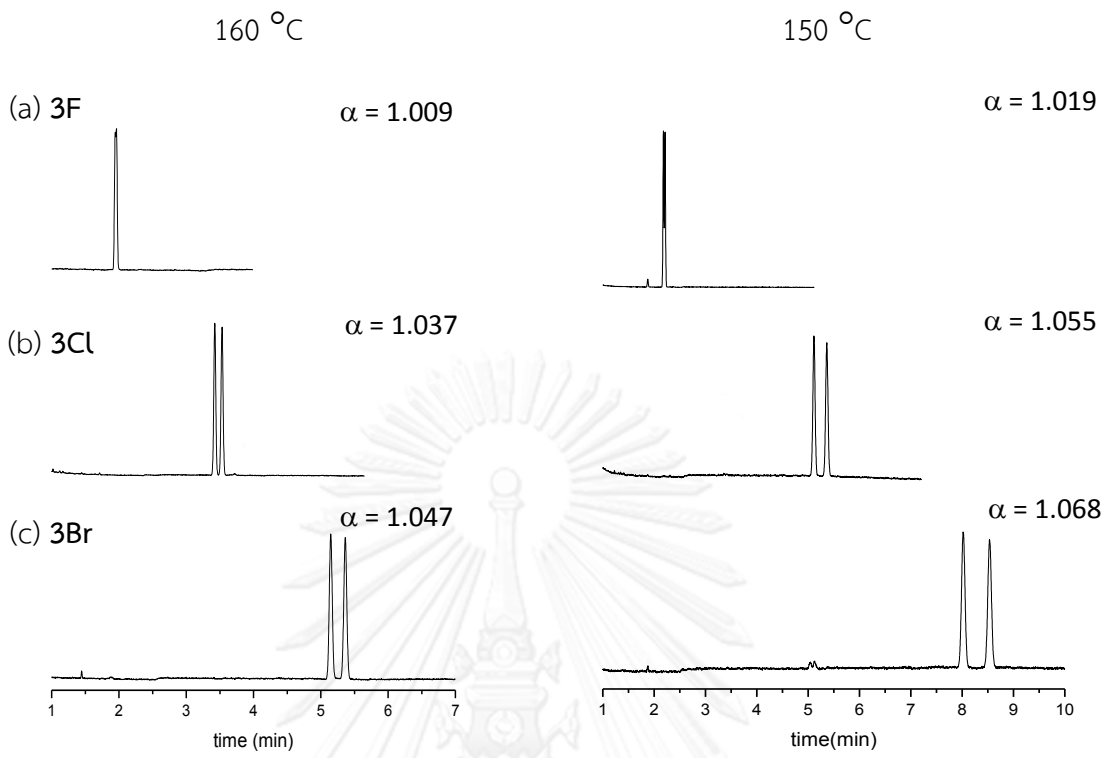

Figure 4.14 Chromatograms of (a) **3F**, (b) **3Cl**, and (c) **3Br** at 160 °C (left) and 150 °C (right) on ASiMe column

On BSiMe column, all mono-substituted analytes in group 1 could be separated, except for **2OMe** (Figure 4.9(b)). The influence of position of substituent on the aromatic ring of mono-substituted analytes on enantioseparation was studied. Using **PEA** as a reference, it was found that *ortho*-halogenated analytes seemed to promote the enantioseparation. Among all halogenated analytes, **2Cl** gives the best enantioseparation on this column with the highest $-\Delta\Delta H$ value of 0.49 kcal/mol. The $-\Delta\Delta H$ values of all halogenated analytes are in descending ordered of *ortho-* > *meta-* > *para-*. Plots of ln α versus 1/T of three monochloro-substituted analytes (**2Cl**, **3Cl,** and **4Cl**) on BSiMe column were compared in Figure 4.15. Among three monochloro-substituted analytes, **2Cl** showed the highest $-\Delta\Delta H$ value and the highest slope of ln α versus 1/T (Figures 4.9(b) and 4.15), indicating that enantioseparation of **2Cl** could be easily improved by slight decrease in temperature. Chromatograms demonstrating the effects of temperature and position of substituent of **2Cl**, **3Cl,** and **4Cl** were compared in Figure 4.16. Whereas large group substituted

analytes (Me, OMe, CF_3) showed the different trend. According to Figure 4.9(b), *meta*-substitution of large group analytes showed $-\Delta\Delta H$ values higher than *ortho- and para*-substituents.

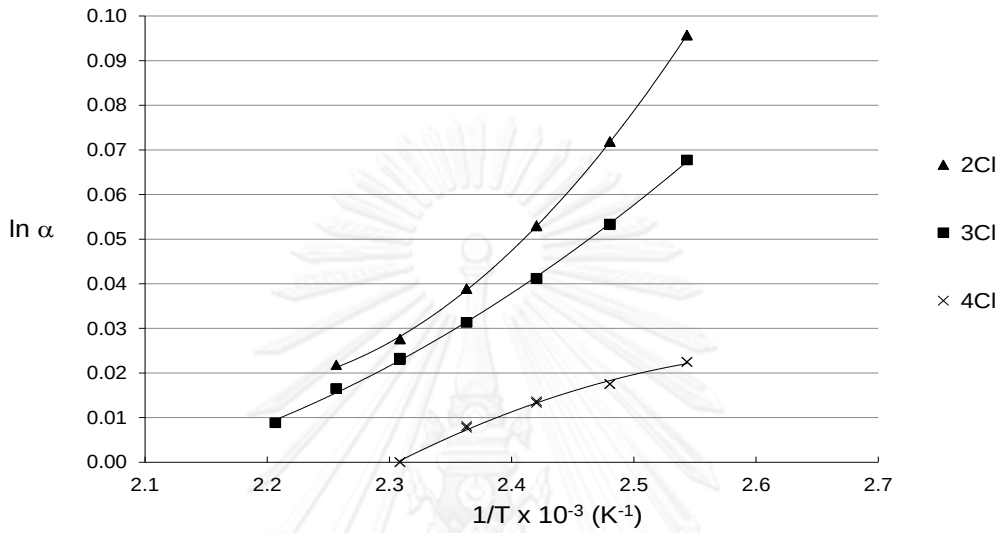

Figure 4.15 Plots of ln α versus 1/T of **2Cl**, **3Cl**, and **4Cl** on BSiMe column

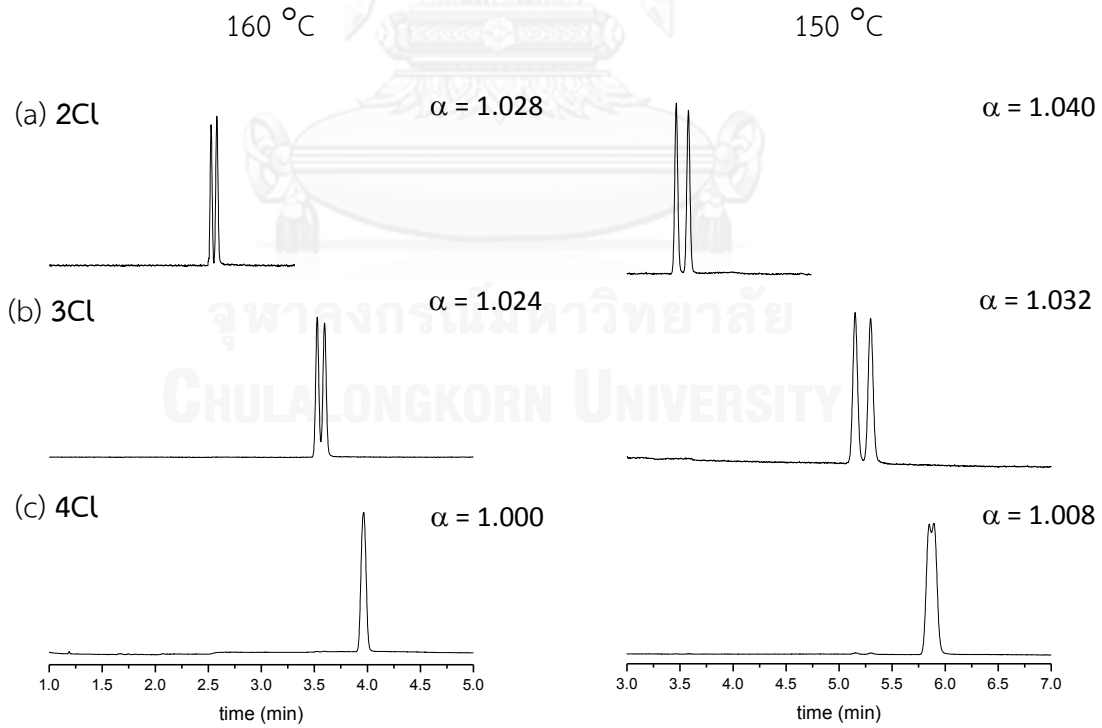

Figure 4.16 Chromatograms of (a) **2Cl**, (b) **3Cl**, and (c) **4Cl** at 160 °C (left) and 150 °C (right) on BSiMe column

Considering analytes with halogenated substitution at *ortho*-position, their $-\Delta\Delta H$ values decreased in descending order of **2Cl** > **2Br** > **2F** > **2CF** > **2Me** > **2OMe** (Figure 4.9(b)). Plots of ln α versus 1/T of three *ortho*-halogenated substituted PEAs (**2F**, **2Cl**, and **2Br**) on BSiMe column were shown in Figure 4.17. Chromatograms demonstrating the effects of temperature and type of substituent of **2F**, **2Cl**, and **2Br** were compared in Figure 4.18. The decrease in temperature by 10 °C improved the enantioseparation of **2Cl** than for **2F** and **2Br**. The effect of type of substituent on *meta*- and *para*-substituted analytes was different. For *meta*-substituted analytes, the $-\Delta\Delta H$ values decreased in descending order of **3F** > **3Cl** > **3Br** > **3CF** >**3Me** ≈ **3OMe**. Whereas *para*-substituted analytes, the $-\Delta\Delta H$ values decreased in descending order of **4F** > **4Cl** ≈ **4Br** > **4OMe** ≈ **4CF** > **4Me**. It was clearly seen that halogenated analytes showed better enantioseparation than large group substituted analytes in every substitution position. These results indicated that size of substitution was also the main influence on enantioseparation.

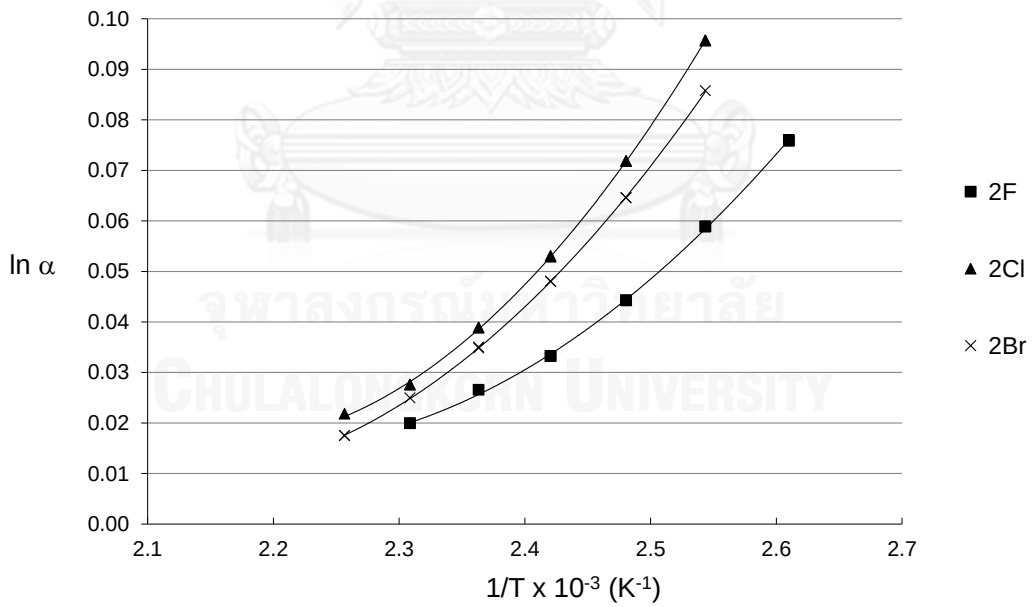

Figure 4.17 Plots of ln α versus 1/T of **2F**, **2Cl**, and **2Br** on BSiMe column

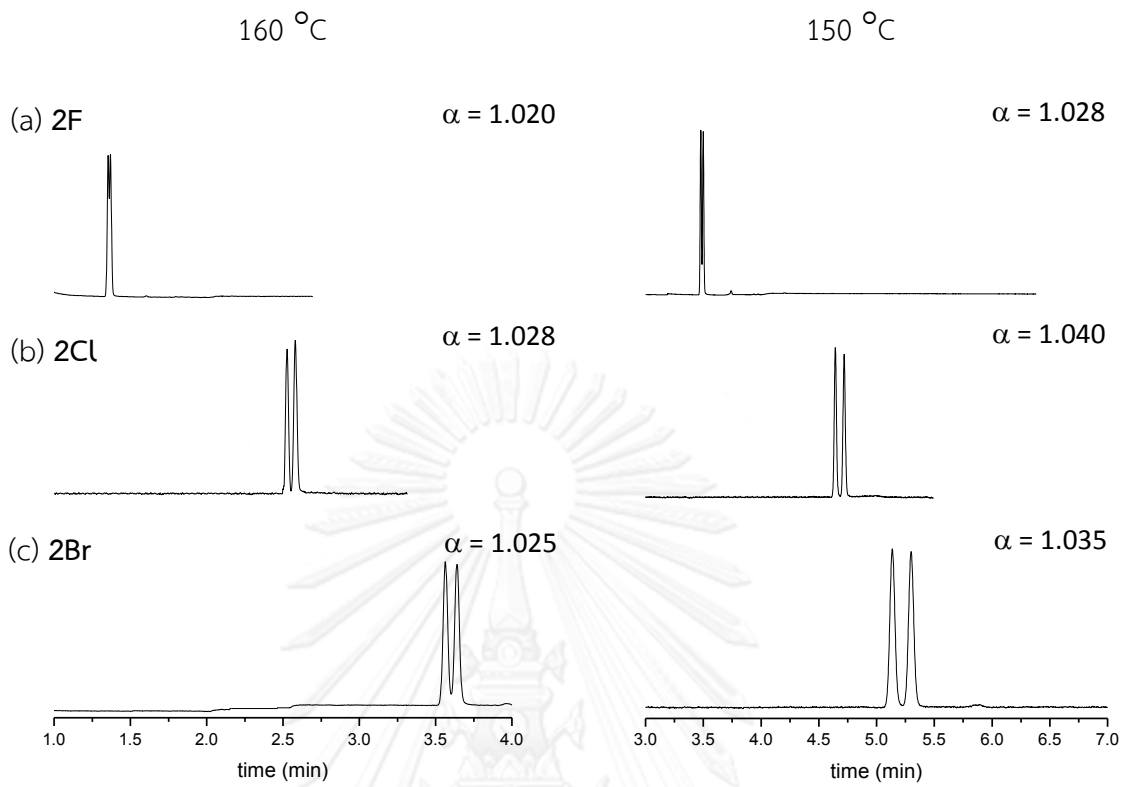

Figure 4.18 Chromatograms of (a) **2F**, (b) **2Cl**, and (c) **2Br** at 160 °C (left) and 150 °C (right) on BSiMe column

The −ΔΔH value of *para*-substituted analytes obtained from BSiMe column were compared to values obtained from ASiMe column. The enantioseparation of all *para*-substituted analytes on BSiMe was better than ASiMe column. These results indicated that the size of cavity of CDs also plays the important effect to enantioseparation. **4Me**, **4OMe**, and **3CF** which could not be separated on ASiMe column, could be separated on BSiMe column.

On GSiMe column, the −ΔΔH values of all analytes are rather small. Only seven mono-substituted PEAs (**2F**, **2Cl**, **2Me**, **3Me**, **4Me**, **3OMe**, **and 4CF**) could be enantioseparated in this column (Figure 4.9(c)). Interestingly, we found that **4Me** and **4CF** give better enantioseparation on GSiMe column than ASiMe and BSiMe columns. Nevertheless, this pointed to the bigger cavity of γ-CD may not suitable for enantioseparation of mono-substituted PEAs.

Group 2: 1-Phenylpropylamine with mono-substitution at *para*- position on the aromatic ring

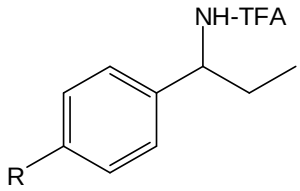

R = H, F, Cl, Br, Me, OMe, CF_3

Group 2 analytes contain seven TFA derivatives of 1-phenylpropylamines (PPAs) with mono-substitution on the aromatic ring at *para*-position as shown above. The substituent type includes fluoro, chloro, bromo, methyl, methoxy, and trifluoromethyl. The $-\Delta\Delta H$ values of all analytes in this group on three CSP columns were displayed and were compared to *para*-substituted of PEAs in Figure 4.19.

On ASiMe column, four enantiomers from seven enantiomers of mono-substituted PPAs could be separated. Their $-\Delta\Delta H$ values decreased in descending order of **PPA** > **4FP** > **4ClP** > **4BrP** (Figure 4.19(a)). Using **PPA** as a reference**,** all *para*-substituted TFA derivatives of PPAs show lower $-\Delta\Delta H$ values than **PPA** or could not be separated. These observations also agree with those obtained from *para*-substituted of PEAs where they also show lower $-\Delta\Delta H$ values than **PEA** or could not be separated on this column due to the small size of α-CD. These results may be implied that the small cavity of α-CD may not be suitable for separation of large group substituted PPAs at *para*-position.

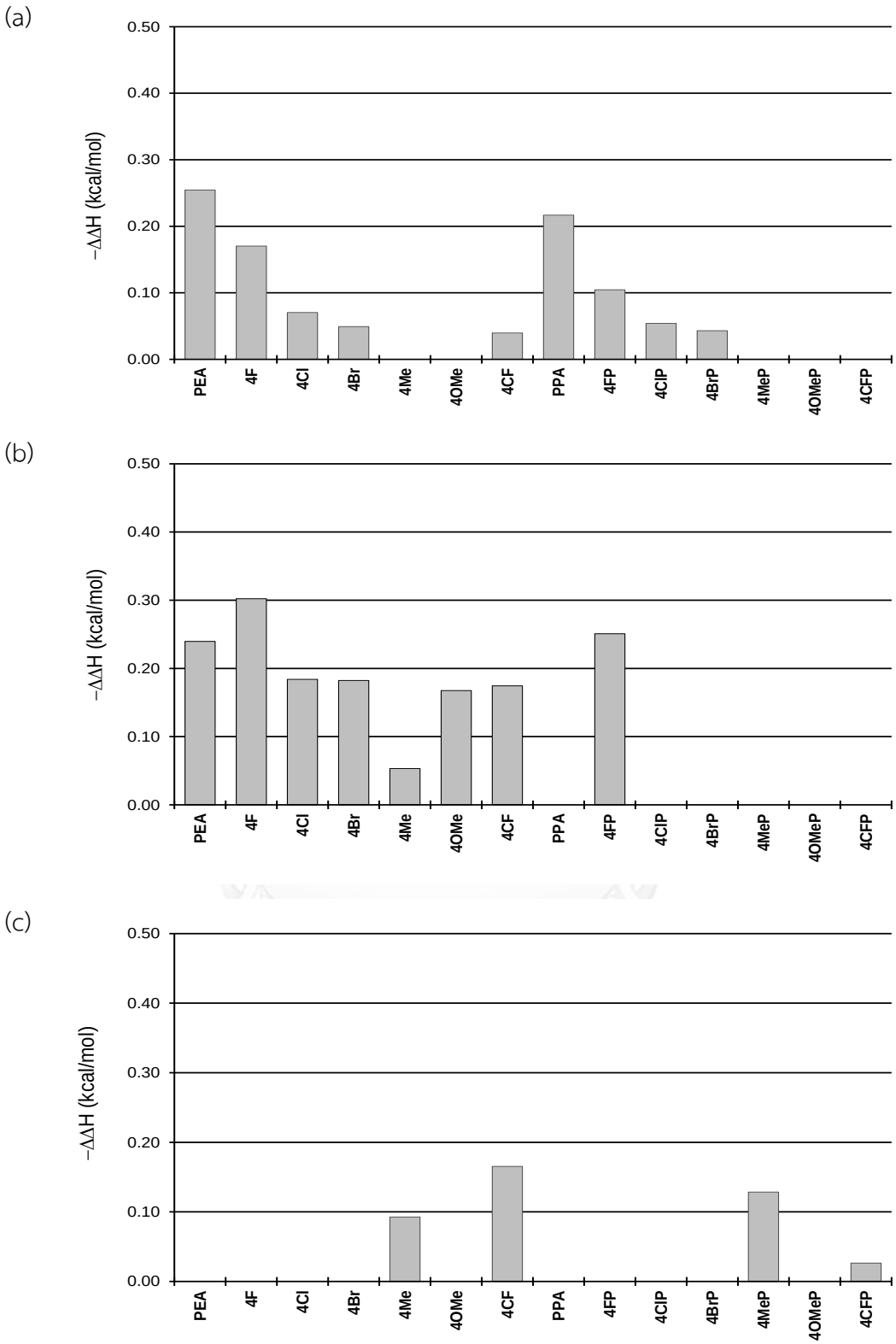

Figure 4.19 Enthalpy difference (–ΔΔH) of the enantiomers of *para*-substitution of TFA derivatives of PEAs and PPAs on (a) ASiMe, (b) BSiMe, and (c) GSiMe columns

The influence of longer aliphatic side chain of chiral center on enantioseparation was also studied. Plots of ln α versus 1/T of **PEA, PPA, 4F** and **4FP** on ASiMe column were shown in Figure 4.20. As seen from Figure 4.20, at the same temperature, **PEA** and **4F** had the higher enantioselectivities than **PPA** and **4FP** at every temperature studied, respectively. These results indicating that increase length of side chain on the chiral center could result in a decreased enantioseparation. Enantioseparation of **PEA**, **PPA**, **4F**, and **4FP** at 130 °C and 120°C were compared in Figure 4.21. As seen from Figure 4.21, the enantioseparation of **PEA** was clearly higher than **PPA** on this column.

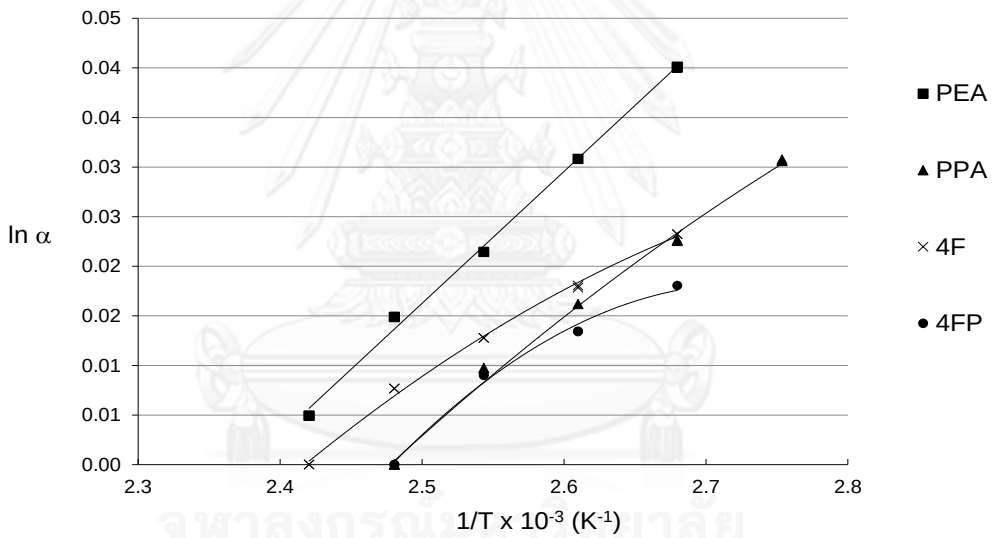

Figure 4.20 Plots of ln α versus 1/T of **PEA**, **PPA**, **4F**, and **4FP** on ASiMe column

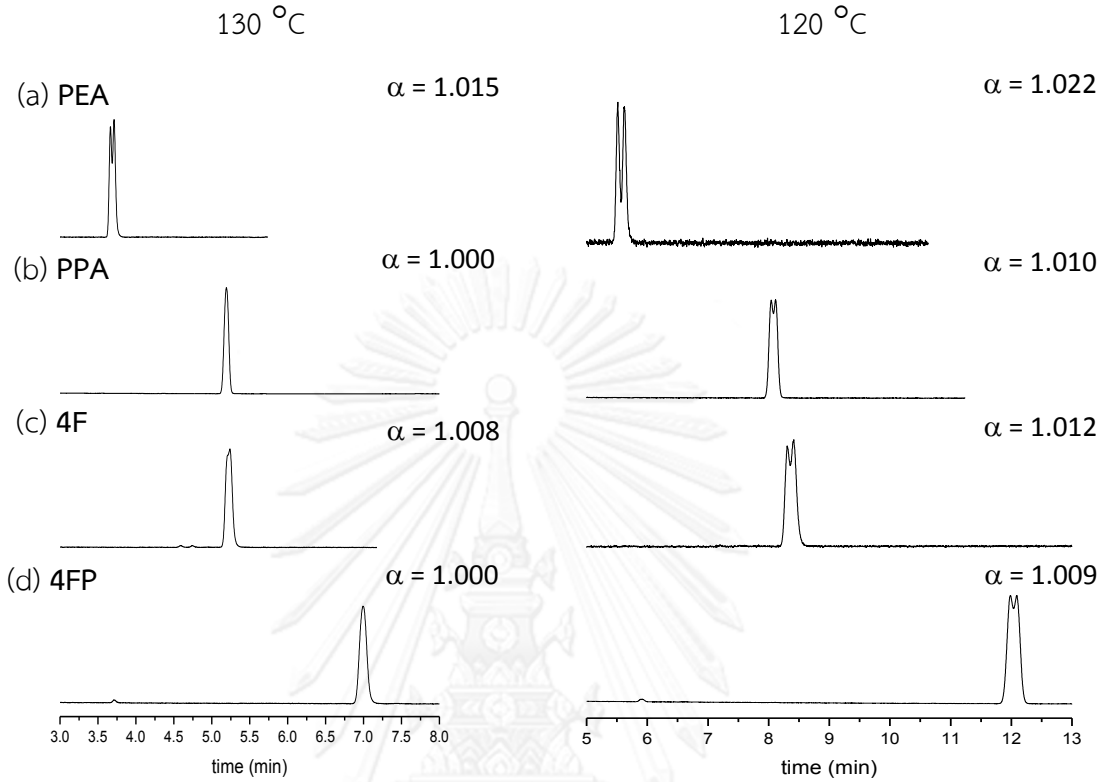

Figure 4.21 Chromatograms of (a) **PEA**, (b) **PPA**, (c) **4F**, and (d) **4FP** at 130 °C (left) and 120 °C (right) on ASiMe column

On BSiMe column, only **4FP** could be enantioseparated with this column (Figure 4.19(b)). These observations did not agree with those obtained from *para*-substituted of PEAs where all *para*-substituted PEAs could be enantioseparated on BSiMe column. The results obtained from BSiMe column were compared to those previously obtained from ASiMe column. The $-\Delta\Delta H$ value of **4FP** on BSiMe column was higher than ASiMe column (Figure 4.19). Chromatograms of enantioseparation of **4FP** at 130 °C and 120°C on both columns were compared in Figure 4.22. As seen from Figure 4.22, the enantioseparation of **4FP on** BSiMe column was clearly better than ASiMe column.

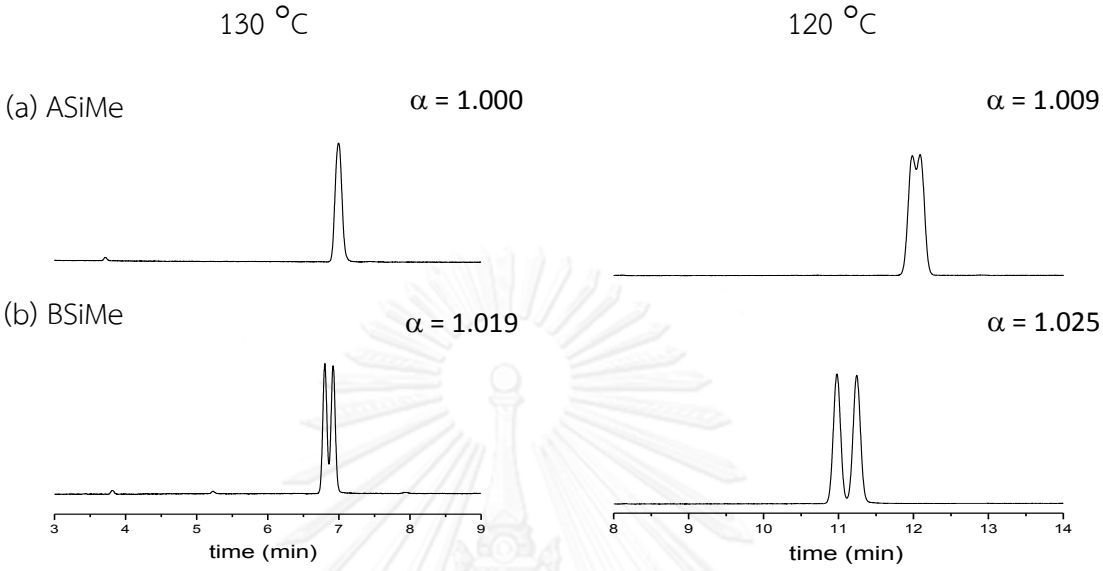

Figure 4.22 Chromatograms of **4FP** at 130 °C (left) and 120 °C (right) on (a) ASiMe and (b) BSiMe columns

On GSiMe column, only two analytes (**4MeP** and **4CFP)** could be enantioseparated on this column (Figure 4.19(c)). These observations also agree with those obtained from *para*-substituted of PEAs where only **4Me** and **4CF** could be enantioseparated on this column. The results obtained from GSiMe column were compared to those previously obtained from both ASiMe and BSiMe columns. Interestingly, **4MeP** and **4CFP** which could not be separated on both ASiMe and BSiMe columns but they could be enantioseparated on GSiMe column.

Nevertheless, the $-\Delta\Delta H$ values of most analytes in group 2 on three chiral columns are rather small or could not be separated. This pointed to aliphatic side chain length on the chiral center, especially for large group at *para*-substituted analytes increased flexibility of analyte molecules and could result in a decreased enantioseparation.

Group 3: 1-Aminoindane with mono-substitution at 5′ position on the aromatic ring

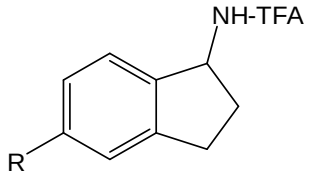

R = H, F, Cl, Br, Me, OMe,

Group 3 analytes contain six TFA derivatives of 1-aminoindane (AI) with mono-substitution on the aromatic ring at 5′ position as shown above. The substituent type includes fluoro, chloro, bromo, methyl, and methoxy. The $-\Delta\Delta H$ values of all analytes in this group on three CSP columns were compared to *para*-substituted of PEAs and PPAs in Figure 4.23. It was quite clear that the enantioseparation of analytes in this group are quite different from *para*-substituted of PEAs and PPAs.

On ASiMe column, four enantiomers from six enantiomers of mono-substituted AIs could be separated. Considering all analytes in group 3, while **AI**, **5ClA, 5BrA,** and **5MeA** show good enantioseparation but **5FA** and **5OMeA** could not be separated. The $-\Delta\Delta H$ values of enantiomer of AIs decreased in descending order of **5BrA** > **5ClA** > **5MeA** > **AI (**Figure 4.23(a)). Plots of ln α versus 1/T of **AI, 5ClA**, **5BrA**, and **5MeA** on ASiMe column were compared in Figure 4.24. Among all analyte, **5BrA** showed the highest slope of ln α versus 1/T indicating that enantioseparation of **5BrA** could be easily improved by slight decrease in temperature. Enantioseparation of **5ClA** and **5BrA** at 190 °C and 180°C were compared in Figure 4.25.

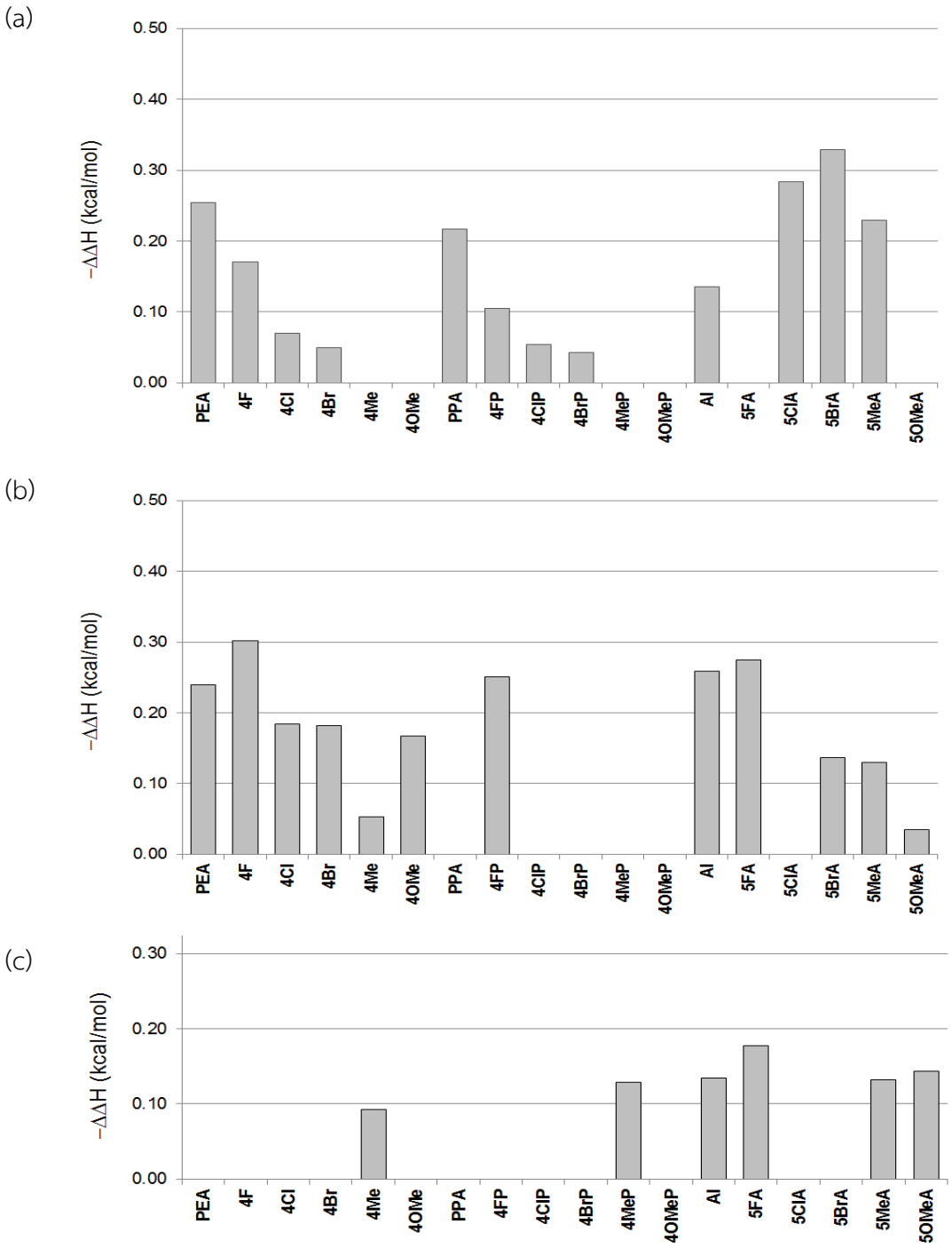

Figure 4.23 Enthalpy difference (−ΔΔH) of the enantiomers of 5′ position substitution of AIs compared to *para*-substituted PEAs and PPAs on (a) ASiMe, (b) BSiMe, and (c) GSiMe columns

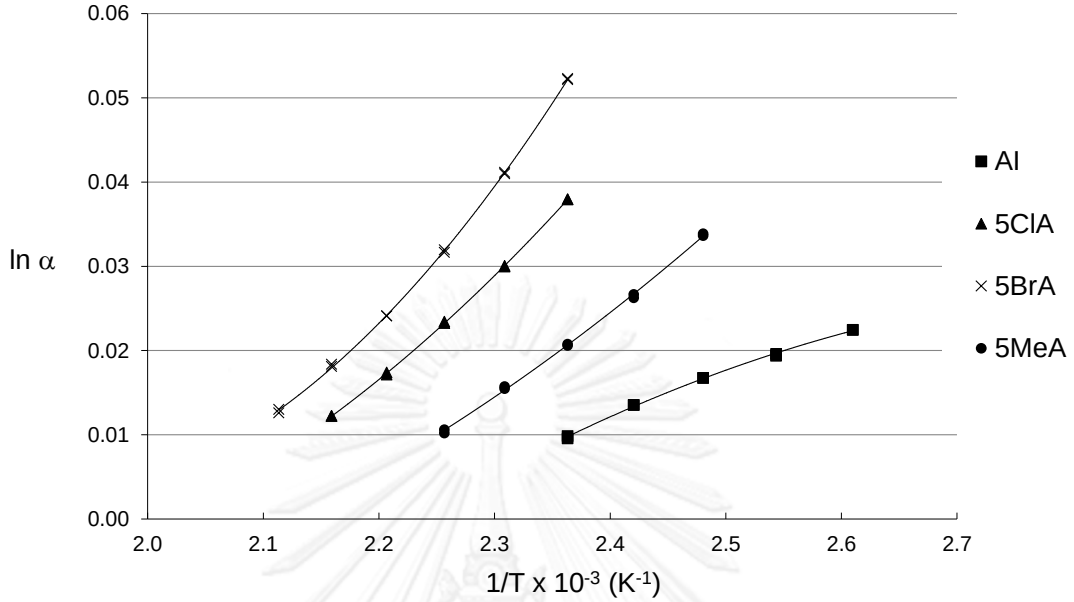

Figure 4.24 Plots of ln α versus 1/T of **AI**, **5ClA**, **5BrA**, and **5MeA** on ASiMe column

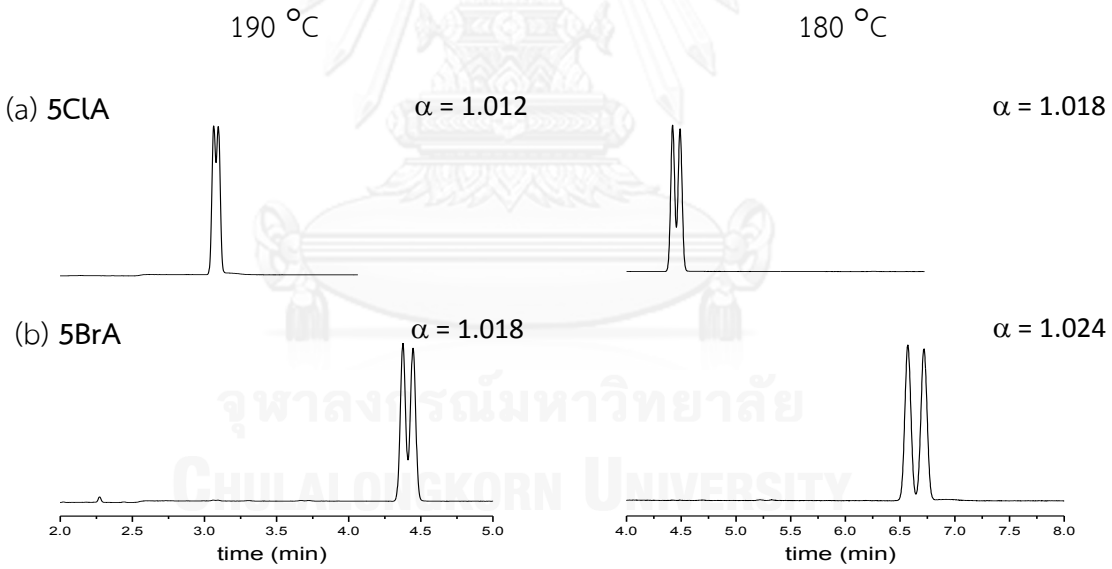

Figure 4.25 Chromatograms of (a) **5ClA** and (b) **5BrA** at 190 °C (left) and 180 °C (right) on ASiMe column

The influence of rigidity of analyte structure on enantioseparation was studied by compare to those results from *para*-substituted of PPAs which have equal carbon atoms in the molecule. It was found that **AI** and **5FA** show poorer enantioseparation than **PPA and 4FP**, respectively (Figure 4.23 (a)). Whereas **5ClA**, **5BrA** and **5MeA** show better enantioseparation than **4ClP, 4BrP** and **4MeP.** Unfortunately, **4OMeP** and **5OMeA** could not be enantioseparated in this column. These observations also agree with those obtained from *para*-substituted of PEAs. These results indicated that the *structural rigidity* of the molecule and the type of substituent were the main influence on enantioseparation. Nevertheless, this effect cannot be generalized from the results obtained in this study due to the limited number of analytes.

On BSiMe column, all analytes in group 3 could be enantioseparated, except for **5ClA**. The $-\Delta\Delta H$ values of enantiomer of *para*-substituted AIs decreased in descending order of **5FA** > **AI > 5BrA** > **5MeA >> 5OMeA** (Figure 4.23(b))**.** Plots of ln α versus 1/T of **AI, 5FA**, **5BrA,** and **5MeA** on BSiMe column were compared in Figure 4.26.

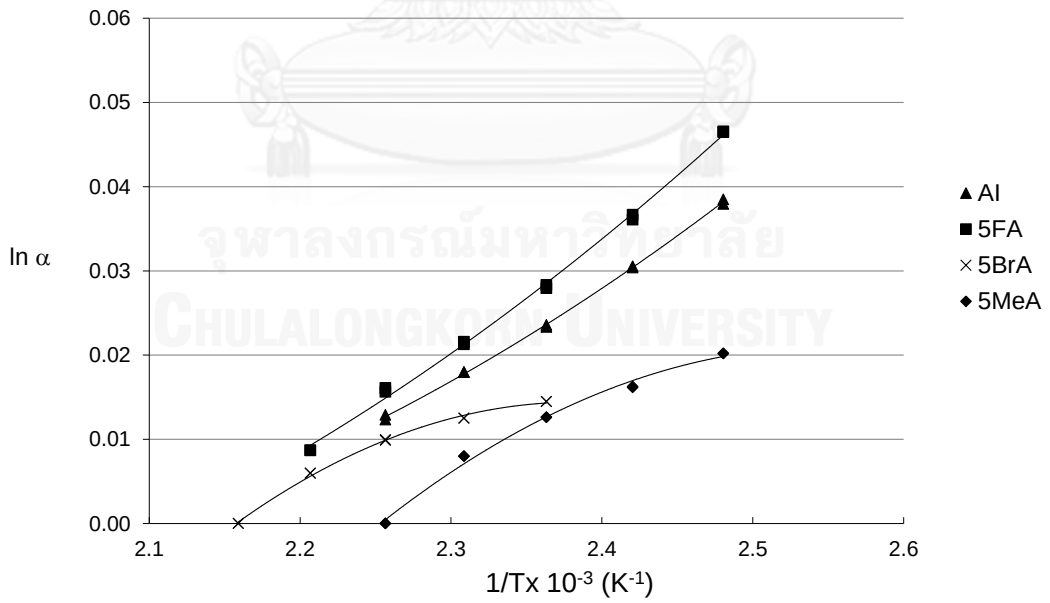

Figure 4.26 Plots of ln α versus 1/T of **AI**, **5FA**, **5BrA**, and **5MeA** on BSiMe column

Compared to *para*-substituted of PPAs, it was found that all analytes in group 3 show better enantioseparation than to their corresponding *para*-substituted of PPAs. Exception was found for chloro-substituted analytes (**4ClP** and **5ClA**) which could not be separated. In general, it was found the increased the *structural rigidity* of the molecule could result in increased the enantioseparation on this column.

The $-\Delta\Delta H$ values obtained from BSiMe column were compared to those previously obtained from ASiMe column. Whereas **AI** showed better enantioseparation on BSiMe than ASiMe column, but **5BrA** and **5MeA** showed better enantioseparation on ASiMe than BSiMe column. These results pointed to type of substituent and size of cavity of cyclodextrin affect the enantioseparation. However, this observation trend could not be generalized due to that many parameters must be considered.

On GSiMe column, four from six enantiomers of analytes in group 3 could be separated. While **AI**, **5FA, 5MeA,** and **5OMeA** could be separated but **5ClA** and **5BrA** show no enantioseparation on this column. The $-\Delta\Delta H$ values of analytes in group 3 decreased in descending order of **5FA** > **5OMeA** > **5MeA** ≈ **AI (**Figure 4.23 (c)). Compared to *para*-substituted of PPAs, it was found that most analytes in group 3 which could be enantioseparated show better enantioseparation than *para*-substituted of PPAs. Exception was found for methyl group analytes (**4MeP** and **5MeA**) which show similarly enantioseparation. Interestingly, **5OMeA** showed higher enantioseparation on GSiMe column than both ASiMe and BSiMe columns.

CHULALONGKORN UNIVERSITY

CHAPTER V

CONCLUSION

Thirty-two trifluoroacetyl (TFA) amine derivatives with different analyte structure were examined to study the effect of type, position and main structure of analytes towards enantioselectivity by gas chromatography using three capillary GC columns containing different size of derivatized CDs as stationary phases: hexakis(2,3-di-*O*-methyl-6-*O*-tert-butyldimethylsilyl)-α-cyclodextrin (ASiMe), heptakis(2,3-di-*O*-methyl-6-*O*-tert-butyldimethylsilyl)-β-cyclodextrin (BSiMe), and octakis(2,3-di-*O*-methyl-6-*O*-*tert*-butyldimethylsilyl)-γ-cyclodextrin (GSiMe). The significance of size of CD to enantioseparation was clearly shown.

On ASiMe column, both type and position of substituent play an important role in the enantioseparation of TFA amine derivatives. Twenty-four from thirty-two enantiomers of TFA amine derivatives could be separated on this column. For PEA derivatives, this column was suitable for *ortho*- and *meta*-substituted PEAs, except for **3CF**. Unfortunately, this column was not suitable for all *para*-substituted PEAs and PPAs. These results showed that the small cavity of α-CD was not suitable for enantioseparation of *para*-substituted amines. For TFA derivatives of 1-aminoindanes, the rigidity of analyte molecule also affects the enantioseparation. ASiMe column could separate four from six enantiomers of TFA 1-aminoindanes, except for **5FA** and **5OMeA**.

BSiMe column could also separate twenty-four from thirty-two enantiomers of TFA amine derivatives. For PEA derivatives, this column was suitable for all positional isomer of halogenated substitution of PEAs including *meta*-substitution of large group substituted (Me, OMe, and CF_3,) PEAs. For other amines, only three analytes (**4FP, AI,** and **5FA)** showed good enantioseparation on this column.

GSiMe column could separate only thirteen from thirty-two enantiomers of TFA amine derivatives. Nevertheless, only **4MeP** and **5OMeA** showed better enantioseparation on GSiMe column than ASiMe and BSiMe columns. These results indicated that GSiMe column was not suitable for enantioseparation of studied analytes.

จุฬาลงกรณ์มหาวิทยาลัย
Chulalongkorn University

REFERENCES

[1] McConathy, J. and Owens, M.J. Stereochemistry in drug action. Journal of Clinical Psychiatry 5 (2003): 70-73.

[2] Fabro, S., Smith, R.L., and Williams, R.T. Toxicity and teratogenicity of optical isomers of thalidomide. Nature 215 (1967): 296-296.

[3] Lin, G.-Q., Zhang, J.-G., and Cheng, J.-F. Overview of chirality and chiral drugs. in Chiral Drugs, pp. 3-28. New York: John Wiley & Sons, 2011.

[4] Schurig, V. Separation of enantiomers by gas chromatography. Journal of Chromatography A 906 (2001): 275-299.

[5] Schneiderman, E. and Stalcup, A.M. Cyclodextrins: a versatile tool in separation science. Journal of Chromatography B: Biomedical Sciences and Applications 745 (2000): 83-102.

[6] Scriba, G.E. Chiral recognition mechanisms in analytical separation sciences. Chromatographia 75 (2012): 815-838.

[7] France, S., Guerin, D.J., Miller, S.J., and Lectka, T. Nucleophilic chiral amines as catalysts in asymmetric synthesis. Chemical Reviews 103 (2003): 2985-3012.

[8] Juaristi, E., León-Romo, J.L., Reyes, A., and Escalante, J. Recent applications of α-phenylethylamine (α-PEA) in the preparation of enantiopure compounds. Part 3: α-PEA as chiral auxiliary. Part 4: α-PEA as chiral reagent in the stereodifferentiation of prochiral substrates. Tetrahedron: Asymmetry 10 (1999): 2441-2495.

[9] Fröstl, W., Mickel, S.J., Schmutz, M., and Bittiger, H. Potent, orally active $GABA_B$ receptor antagonists. Pharmacology Reviews and Communications 8 (1996): 127-133.

[10] Ofner, S., Hauser, K., Schilling, W., Vassout, A., and Veenstra, S.J. SAR of 2-benzyl-4-aminopiperidines: CGP 49823, an orally and centrally active non-peptide NK1 antagonist. Bioorganic & Medicinal Chemistry Letters 6 (1996): 1623-1628.

[11] Heykants, J.J.P., Knaeps, A.G., and Janssen, M.A.C. Synthesis of 3H-etomidate and resolution into its enantiomers. Journal of Labelled Compounds 11 (1975): 401-407.

[12] Arava, V., Gorentla, L., and Dubey, P. A simple and highly efficient enantioselective synthesis of (S)-rivastigmine. International Journal of Organic Chemistry 1 (2011): 26-32.

[13] Warren, S. and Wyatt, P. Organic synthesis: The disconnection approach. 2nd ed. New york: John Wiley & Sons, 2008.

[14] Baxter, E.W. and Reitz, A.B. Reductive aminations of carbonyl compounds with borohydride and borane reducing agents. in Organic Reactions. New York: John Wiley & Sons, 2004.

[15] McNair, H.M. and Miller, J.M. Basic gas chromatography. New York: John Wiley & Sons, 1998.

[16] Blau, K. and Halket, J. Handbook of derivatives for chromatography. 2nd ed. New York: John Wiley & Sons, 1993.

[17] Kataoka, H. Derivatization reactions for the determination of amines by gas chromatography and their applications in environmental analysis. Journal of Chromatography A 733 (1996): 19-34.

[18] Vadim, A.D. Analytical chiral separation methods. Pure and Applied Chemistry 69 (1997): 1469—1474.

[19] Juvancz, Z. and Szejtli, J. The role of cyclodextrins in chiral selective chromatography. TrAC Trends in Analytical Chemistry 21 (2002): 379-388.

[20] Szejtli, J. Introduction and general overview of cyclodextrin chemistry. Chemical Reviews 98 (1998): 1743-1754.

[21] Armstrong, D.W., Li, W., Chang, C.D., and Pitha, J. Polar-liquid, derivatized cyclodextrin stationary phases for the capillary gas chromatography separation of enantiomers. Analytical Chemistry 62 (1990): 914-923.

[22] Li, W.Y., Jin, H.L., and Armstrong, D.W. 2,6-Di-O-pentyl-3-O-trifluoroacetyl cyclodextrin liquid stationary phases for capillary gas chromatographic separation of enantiomers. Journal of Chromatography A 509 (1990): 303-324.

[23] Nie, M.-Y., Zhou, L.-M., Liu, X.-L., Wang, Q.-H., and Zhu, D.-Q. Gas chromatographic enantiomer separation on long-chain alkylated β-cyclodextrin chiral stationary phases. Analytica Chimica Acta 408 (2000): 279-284.

[24] Anderson, J.L., Ding, J., McCulla, R.D., Jenks, W.S., and Armstrong, D.W. Separation of racemic sulfoxides and sulfinate esters on four derivatized cyclodextrin chiral stationary phases using capillary gas chromatography. Journal of Chromatography A 946 (2002): 197-208.

[25] Shi, X., Guo, H., and Wang, M. Enantioseparation of chiral epoxides using four new cyclodextrin derivatives as chiral stationary phases of capillary gas chromatography. Analytica Chimica Acta 553 (2005): 43-49.

[26] Shi, X., Liang, P., and Gao, X. The capillary gas chromatographic properties of four β-cyclodextrin derivatives with allyl groups or propyl groups on 3-position or 6-position of β-cyclodextrin. Analytica Chimica Acta 548 (2005): 86-94.

[27] Kobor, F. and Schomburg, G. 6-tert-Butyldimethylsilyl-2,3-dimethyl-α-, β-, and γ-cyclodextrins, dissolved in polysiloxanes, as chiral selectors for gas chromatography. Influence of selector concentration and polysiloxane matrix polarity on enantioselectivity. Journal of High Resolution Chromatography 16 (1993): 693-699.

[28] Shitangkoon, A. and Vigh, G. Systematic modification of the separation selectivity of cyclodextrin-based gas chromatographic stationary phases by varying the size of the 6-O-substituents. Journal of Chromatography A 738 (1996): 31-42.

[29] Takahisa, E. and Engel, K.-H. 2,3-Di-O-methoxymethyl-6-O-tert-butyldimethylsilyl-γ-cyclodextrin: a new class of cyclodextrin derivatives for gas chromatographic separation of enantiomers. Journal of Chromatography A 1063 (2005): 181-192.

[30] Takahisa, E. and Engel, K.-H. 2,3-Di-O-methoxymethyl-6-O-tert-butyldimethylsilyl-β-cyclodextrin, a useful stationary phase for gas chromatographic separation of enantiomers. Journal of Chromatography A 1076 (2005): 148-154.

[31] Špánik, I., Krupčik, J., and Schurig, V. Comparison of two methods for the gas chromatographic determination of thermodynamic parameters of enantioselectivity. Journal of Chromatography A 843 (1999): 123-128.

[32] Miriyala, B., Bhattacharyya, S., and Williamson, J.S. Chemoselective reductive alkylation of ammonia with carbonyl compounds: synthesis of primary and symmetrical secondary amines. Tetrahedron 60 (2004): 1463-1471.

[33] A. Neidigh, K., A. Avery, M., S. Williamson, J., and Bhattacharyya, S. Facile preparation of N-methyl secondary amines by titanium(IV) isopropoxide-mediated reductive amination of carbonyl compounds. Journal of the Chemical Society, Perkin Transactions 1 (1998): 2527-2532.

[34] Jungclaus, G.A. Formation of amine-N-trifluoroacetyl derivatives from the amine hydrochloride salts. Journal of Chromatography A 139 (1977): 174-176.

[35] Chaytor, J.P., Crathorne, B., and Saxby, M.J. Gas chromatography and mass spectrometry of some isomeric cyclic amines as their trifluoroacetyl derivatives. Journal of Chromatography A 70 (1972): 141-145.

[36] Knapp, D.R. Handbook of analytical derivatization reactions. New York: John Wiley & Sons, 1979.

APPENDICES

จุฬาลงกรณ์มหาวิทยาลัย
Chulalongkorn University

Appendix A

Thermodynamic parameters

Table A1 Slope and y-intercept from ln k′ versus 1/T plots and thermodynamic parameters of 32 TFA amines derivatives on OV-1701 column

analytes	temperature range (°C)	retained enantiomer			−ΔH (kcal/mol)	−ΔS (cal/mol·K)
		ln k′ = m(1/T) + c		R^2		
		m	c			
PEA	110-170	6858.5	-15.302	0.9996	13.63	19.43
2F	110-160	6652.4	-15.054	0.9996	13.22	18.94
3F	110-160	7264.2	-16.032	0.9995	14.43	20.88
4F	110-160	7221.5	-15.938	0.9995	14.35	20.70
2Cl	120-180	7309.9	-15.624	0.9997	14.52	20.07
3Cl	120-180	7790.7	-16.335	0.9996	15.48	21.49
4Cl	120-180	7773.8	-16.253	0.9997	15.45	21.32
2Br	130-190	7480.5	-15.577	0.9996	14.86	19.98
3Br	130-190	7879.4	-16.075	0.9993	15.66	20.97
4Br	130-190	7899.6	-16.078	0.9995	15.70	20.98
2Me	110-170	7123.8	-15.631	0.9995	14.15	20.09
3Me	110-170	7207.6	-15.784	0.9995	14.32	20.39
4Me	110-170	7203.6	-15.726	0.9995	14.31	20.28
2OMe	120-180	7020.3	-15.030	0.9996	13.95	18.89
3OMe	120-180	7041.7	-15.387	0.9996	13.99	19.60
4OMe	120-180	7844.8	-16.392	0.9987	15.59	21.60
2CF	110-170	7340.6	-16.302	0.9995	14.59	21.42
3CF	110-170	7636.3	-16.785	0.9995	15.17	22.38

Table A1 (continued)

analytes	temperature range (°C)	retained enantiomer			−ΔH (kcal/mol)	−ΔS (cal/mol·K)
		ln k′ = m(1/T) + c		R^2		
		m	c			
4CF	110-170	7662.9	-16.748	0.9995	15.23	22.31
PPA	110-180	7103.5	-15.548	0.9996	14.11	19.92
4FP	120-180	7327.0	-15.861	0.9996	14.56	20.54
4ClP	140-210	7625.5	-15.640	0.9993	15.15	20.11
4BrP	150-220	7727.1	-15.455	0.9992	15.35	19.74
4MeP	120-180	7765.8	-16.709	0.9995	15.43	22.23
4OMeP	140-210	7672.0	-15.700	0.9992	15.24	20.22
4CFP	120-180	7337.6	-15.722	0.9994	14.58	20.27
AI	130-190	7144.5	-15.124	0.9992	14.20	19.08
5FA	130-190	7428.6	-15.573	0.9992	14.76	19.97
5ClA	150-210	7829.0	-15.561	0.9997	15.56	19.95
5BrA	160-220	8049.5	-15.623	0.9994	15.99	20.07
5MeA	140-200	7332.6	-15.190	0.9994	14.57	19.21
5OMeA	150-210	7857.8	-15.609	0.9997	15.61	20.04

CHULALONGKORN UNIVERSITY

Table A2 Slope and y-intercept from ln k′ versus 1/T plots of 32 TFA amines derivatives on ASiMe column

analytes	temperature range (°C)	less retained enantiomer			more retained enantiomer		
		ln k′ = m(1/T) + c		R^2	ln k′ = m(1/T) + c		R^2
		m	c		m	c	
PEA	100-150	7421.2	-16.616	0.9997	7549.3	-16.920	0.9997
2F	90-140	7285.9	-16.550	0.9998	7412.6	-16.854	0.9998
3F	110-160	7726.3	-17.113	0.9997	7919.5	-17.552	0.9996
4F	100-140	8221.0	-18.209	0.9998	8306.7	-18.415	0.9998
2Cl	120-170	7724.6	-16.559	0.9998	7856.2	-16.853	0.9998
3Cl	120-170	8640.0	-18.238	0.9997	9055.7	-19.160	0.9994
4Cl	110-170	9538.4	-20.037	0.9996	9573.8	-20.119	0.9995
2Br	130-180	7929.0	-16.578	0.9997	8047.7	-16.839	0.9998
3Br	130-190	8726.2	-17.946	0.9994	9090.8	-18.732	0.9989
4Br	120-180	9792.3	-20.098	0.9995	9832.8	-20.190	0.9994
2Me	110-160	7585.7	-16.684	0.9996	7730.6	-17.017	0.9996
3Me	110-160	7901.5	-17.326	0.9996	8051.7	-17.674	0.9995
4Me	110-160	8189.2	-17.850	0.9996	8189.2	-17.850	0.9996
2OMe	100-140	7929.2	-17.135	0.9998	8001.4	-17.310	0.9998
3OMe	110-150	7981.7	-17.529	0.9995	8154.0	-17.933	0.9995
4OMe	130-180	8263.0	-17.246	0.9998	8263.0	-17.246	0.9998
2CF	110-170	7447.5	-16.542	0.9990	7556.5	-16.786	0.9991
3CF	110-170	7805.8	-17.267	0.9996	7805.8	-17.267	0.9996
4CF	100-170	8014.1	-17.622	0.9995	8034.0	-17.669	0.9994
PPA	90-130	7786.9	-17.258	0.9998	7896.0	-17.528	0.9999
4FP	100-160	8339.3	-18.152	0.9997	8391.9	-18.277	0.9996
4ClP	120-210	9099.4	-18.698	0.9984	9126.6	-18.758	0.9983

Table A2 (continued)

analytes	temperature range (°C)	less retained enantiomer			more retained enantiomer		
		ln k′ = m(1/T) + c		R^2	ln k′ = m(1/T) + c		R^2
		m	c		m	c	
4BrP	130-220	9172.4	-18.348	0.9989	9194.1	-18.394	0.9987
4MeP	110-190	8082.7	-17.477	0.9982	8082.7	-17.477	0.9982
4OMeP	140-210	8222.8	-16.837	0.9994	8222.8	-16.837	0.9994
4CFP	110-190	8233.9	-17.591	0.9990	8233.9	-17.591	0.9990
AI	110-160	7613.0	-16.205	0.9998	7681.1	-16.358	0.9999
5FA	130-190	8067.8	-16.870	0.9992	8067.8	-16.870	0.9992
5ClA	150-200	9217.9	-18.372	0.9995	9360.9	-18.672	0.9995
5BrA	150-210	9532.2	-18.617	0.9994	9698.0	-18.957	0.9994
5MeA	130-180	8021.9	-16.622	0.9992	8137.5	-16.875	0.9993
5OMeA	150-210	8180.9	-16.272	0.9998	8180.9	-16.272	0.9998

จุฬาลงกรณ์มหาวิทยาลัย
CHULALONGKORN UNIVERSITY

Table A3 Slope and y-intercept from ln k′ versus 1/T plots of 32 TFA amines derivatives on BSiMe column

analytes	temperature range (°C)	less retained enantiomer			more retained enantiomer		
		ln k′ = m(1/T) + c		R^2	ln k′ = m(1/T) + c		R^2
		m	c		m	c	
PEA	100-160	7154.4	-15.931	0.9993	7275.0	-16.202	0.9993
2F	110-160	6680.9	-15.083	0.9997	6865.3	-15.493	0.9997
3F	110-170	7455.6	-16.429	0.9992	7635.5	-16.822	0.9992
4F	110-170	7360.3	-16.168	0.9994	7512.4	-16.501	0.9994
2Cl	120-180	7375.5	-15.775	0.9994	7621.1	-16.311	0.9994
3Cl	120-180	8103.1	-17.030	0.9993	8274.7	-17.402	0.9993
4Cl	120-160	8316.0	-17.412	0.9994	8408.6	-17.624	0.9994
2Br	120-180	7786.4	-16.287	0.9993	7991.9	-16.551	0.9992
3Br	120-180	8409.8	-17.294	0.9995	8554.6	-17.605	0.9997
4Br	120-160	8950.5	-18.397	0.9996	9042.3	-18.614	0.9997
2Me	90-160	7508.3	-16.517	0.9991	7529.8	-16.569	0.9999
3Me	100-150	7677.4	-16.866	0.9994	7763.1	-17.067	0.9994
4Me	100-170	7399.0	-16.088	0.9993	7425.8	-16.151	0.9992
2OMe	120-180	7337.2	-15.696	0.9994	7337.2	-15.696	0.9994
3OMe	100-150	7678.8	-16.869	0.9994	7763.4	-17.067	0.9994
4OMe	110-150	8359.5	-17.561	0.9997	8447.3	-17.766	0.9997
2CF	90-140	7775.0	-17.539	0.9998	7855.1	-17.729	0.9990
3CF	110-160	7857.4	-17.327	0.9990	7963.3	-17.568	0.9990
4CF	100-140	8563.7	-18.828	1.0000	8648.0	-19.034	1.0000
PPA	100-180	7285.4	-15.940	0.9995	7285.4	-15.940	0.9995
4FP	110-150	7871.1	-17.114	0.9997	7997.3	-17.410	0.9998
4ClP	130-210	8036.9	-16.472	0.9997	8036.9	-16.472	0.9997

Table A3 (continued)

analytes	temperature range (°C)	less retained enantiomer			more retained enantiomer		
		ln k′ = m(1/T) + c		R^2	ln k′ = m(1/T) + c		R^2
		m	c		m	c	
4BrP	130-220	8422.5	-16.865	0.9994	8422.5	-16.865	0.9994
4MeP	110-190	8149.5	-17.509	0.9997	8149.5	-17.509	0.9997
4OMeP	130-210	7899.6	-16.152	0.9997	7899.6	-16.152	0.9997
4CFP	110-190	7430.7	-15.865	0.9997	7430.7	-15.865	0.9997
AI	130-180	7782.5	-16.389	0.9994	7912.6	-16.673	0.9995
5FA	130-190	8088.8	-16.868	0.9994	8227.1	-17.165	0.9994
5ClA	140-210	8652.3	-17.183	0.9995	8652.3	-17.183	0.9995
5BrA	150-190	9284.8	-18.150	0.9998	9353.8	-18.297	0.9999
5MeA	130-170	8068.2	-16.721	0.9996	8133.5	-16.865	0.9997
5OMeA	130-210	8689.4	-17.317	0.9981	8706.8	-17.355	0.9980

จุฬาลงกรณ์มหาวิทยาลัย
CHULALONGKORN UNIVERSITY

Table A4 Slope and y-intercept from ln k′ versus 1/T plots of 32 TFA amines derivatives on GSiMe column

analytes	temperature range (°C)	less retained enantiomer			more retained enantiomer		
		ln k′ = m(1/T) + c		R^2	ln k′ = m(1/T) + c		R^2
		m	c		m	c	
PEA	110-170	7012.8	-15.578	0.9996	7012.8	-15.578	0.9996
2F	90-130	7220.7	-16.390	0.9997	7280.3	-16.540	0.9997
3F	110-170	7383.2	-16.251	0.9995	7383.2	-16.251	0.9995
4F	110-170	7354.7	-16.174	0.9995	7354.7	-16.174	0.9995
2Cl	90-130	8152.1	-17.626	0.9998	8232.2	-17.824	0.9998
3Cl	120-170	8015.9	-16.800	0.9997	8015.9	-16.800	0.9997
4Cl	120-180	7933.4	-16.537	0.9995	7933.4	-16.537	0.9995
2Br	130-180	7693.2	-15.979	0.9996	7693.2	-15.979	0.9996
3Br	130-190	8111.7	-16.555	0.9997	8111.7	-16.555	0.9997
4Br	130-190	9010.1	-18.545	0.9998	9086.8	-18.724	0.9998
2Me	100-140	7578.9	-16.681	0.9998	7633.4	-16.812	0.9998
3Me	100-140	7721.3	-16.957	0.9998	7790.7	-17.125	0.9998
4Me	90-130	7897.2	-17.360	0.9996	7943.8	-17.477	0.9998
2OMe	120-180	7181.8	-15.287	0.9997	7181.8	-15.287	0.9997
3OMe	100-140	7686.2	-16.869	0.9997	7763.6	-17.058	0.9997
4OMe	120-180	7951.0	-16.520	0.9996	7951.0	-16.520	0.9996
2CF	110-150	7482.1	-16.616	0.9996	7482.1	-16.616	0.9996
3CF	110-160	7844.7	-17.277	0.9997	7844.7	-17.277	0.9997
4CF	110-150	7963.6	-17.444	0.9996	8046.8	-17.638	0.9996
PPA	110-180	7257.2	-15.833	0.9993	7257.2	-15.833	0.9993
4FP	120-180	7490.4	-16.186	0.9995	7490.4	-16.186	0.9995
4ClP	140-210	7822.8	-16.009	0.9996	7822.8	-16.009	0.9996

Table A4 (continued)

analytes	temperature range (°C)	less retained enantiomer			more retained enantiomer		
		ln k′ = m(1/T) + c		R^2	ln k′ = m(1/T) + c		R^2
		m	c		m	c	
4BrP	150-220	7962.9	-15.886	0.9993	7962.9	-15.886	0.9993
4MeP	110-150	8319.2	-18.024	0.9997	8383.9	-18.176	0.9997
4OMeP	140-210	7865.2	-16.037	0.9996	7865.2	-16.037	0.9996
4CFP	100-190	7588.9	-16.205	0.9991	7602.2	-16.235	0.9990
AI	110-150	7735.8	-16.423	0.9997	7803.5	-16.581	0.9998
5FA	110-150	8061.1	-16.984	0.9997	8150.5	-17.194	0.9998
5ClA	150-210	8037.2	-15.911	0.9997	8037.2	-15.911	0.9997
5BrA	160-220	8194.4	-15.822	0.9995	8194.4	-15.822	0.9995
5MeA	110-150	8075.4	-17.123	0.9999	8141.8	-17.289	0.9999
5OMeA	130-190	8574.7	-16.816	0.9997	8647.1	-16.971	0.9998

จุฬาลงกรณ์มหาวิทยาลัย
CHULALONGKORN UNIVERSITY

Table A5 Thermodynamic parameters of 32 TFA amines derivatives on ASiMe column

analytes	enthalpy term (kcal/mol)			entropy term (cal/mol·K)		
	$-\Delta H_1$	$-\Delta H_2$	$-\Delta\Delta H$	$-\Delta S_1$	$-\Delta S_2$	$-\Delta\Delta S$
PEA	14.75	15.00	0.25	22.04	22.65	0.60
2F	14.48	14.73	0.25	21.91	22.52	0.60
3F	15.35	15.74	0.38	23.03	23.90	0.87
4F	16.34	16.51	0.17	25.21	25.62	0.41
2Cl	15.35	15.61	0.26	21.93	22.52	0.58
3Cl	17.17	17.99	0.83	25.27	27.10	1.83
4Cl	18.95	19.02	0.07	28.84	29.01	0.16
2Br	15.75	15.99	0.24	21.97	22.49	0.52
3Br	17.34	18.06	0.72	24.69	26.25	1.56
4Br	19.46	19.54	0.08	28.96	29.15	0.18
2Me	15.07	15.36	0.29	22.18	22.84	0.66
3Me	15.70	16.00	0.30	23.46	24.15	0.69
4Me	16.27	16.27	0.00	24.50	24.50	0.00
2OMe	15.76	15.90	0.14	23.08	23.42	0.35
3OMe	15.86	16.20	0.34	23.86	24.66	0.80
4OMe	16.42	16.42	0.00	23.30	23.30	0.00
2CF	14.80	15.01	0.22	21.90	22.38	0.48
3CF	15.51	15.51	0.00	23.34	23.34	0.00
4CF	15.92	15.96	0.04	24.04	24.14	0.09
PPA	15.47	15.69	0.22	23.32	23.86	0.54
4FP	16.57	16.67	0.10	25.10	25.35	0.25
4ClP	18.08	18.13	0.05	26.18	26.30	0.12

Table A5 (continued)

analytes	enthalpy term (kcal/mol)			entropy term (cal/mol·K)		
	$-\Delta H_1$	$-\Delta H_2$	$-\Delta\Delta H$	$-\Delta S_1$	$-\Delta S_2$	$-\Delta\Delta S$
4BrP	18.23	18.27	0.04	25.49	25.58	0.09
4MeP	16.06	16.06	0.00	23.76	23.76	0.00
4OMeP	16.34	16.34	0.00	22.48	22.48	0.00
4CFP	16.36	16.36	0.00	23.98	23.98	0.00
AI	15.13	15.26	0.14	21.23	21.53	0.30
5FA	16.03	16.03	0.00	22.55	22.55	0.00
5ClA	18.32	18.60	0.28	25.53	26.13	0.60
5BrA	18.94	19.27	0.33	26.02	26.70	0.68
5MeA	15.94	16.17	0.23	22.06	22.56	0.50
5OMeA	16.26	16.26	0.00	21.36	21.36	0.00

จุฬาลงกรณ์มหาวิทยาลัย
CHULALONGKORN UNIVERSITY

Table A6 Thermodynamic parameters of 32 TFA amines derivatives on BSiMe column

analytes	enthalpy term (kcal/mol)			entropy term (cal/mol·K)		
	$-\Delta H_1$	$-\Delta H_2$	$-\Delta\Delta H$	$-\Delta S_1$	$-\Delta S_2$	$-\Delta\Delta S$
PEA	14.22	14.46	0.24	20.68	21.22	0.54
2F	13.27	13.64	0.37	19.00	19.81	0.81
3F	14.81	15.17	0.36	21.67	22.45	0.78
4F	14.62	14.93	0.30	21.15	21.82	0.66
2Cl	14.66	15.14	0.49	20.37	21.44	1.07
3Cl	16.10	16.44	0.34	22.87	23.61	0.74
4Cl	16.52	16.71	0.18	23.63	24.05	0.42
2Br	15.47	15.88	0.41	21.39	21.92	0.52
3Br	16.71	17.00	0.29	23.39	24.01	0.62
4Br	17.90	18.06	0.15	25.88	26.23	0.36
2Me	14.92	14.96	0.04	21.85	21.95	0.10
3Me	15.25	15.43	0.17	22.54	22.94	0.40
4Me	14.70	14.76	0.05	21.00	21.12	0.13
2OMe	14.58	14.58	0.00	20.22	20.22	0.00
3OMe	15.26	15.43	0.17	22.55	22.94	0.39
4OMe	16.61	16.78	0.17	23.92	24.33	0.41
2CF	15.45	15.61	0.16	23.88	24.26	0.38
3CF	15.61	15.82	0.21	23.46	23.94	0.48
4CF	17.02	17.18	0.17	26.44	26.85	0.41
PPA	14.48	14.48	0.00	20.70	20.70	0.00
4FP	15.64	15.89	0.25	23.03	23.62	0.59
4ClP	15.97	15.97	0.00	21.76	21.76	0.00

Table A6 (continued)

analytes	enthalpy term (kcal/mol)			entropy term (cal/mol·K)		
	$-\Delta H_1$	$-\Delta H_2$	$-\Delta\Delta H$	$-\Delta S_1$	$-\Delta S_2$	$-\Delta\Delta S$
4BrP	16.74	16.74	0.00	22.54	22.54	0.00
4MeP	16.19	16.19	0.00	23.82	23.82	0.00
4OMeP	15.70	15.70	0.00	21.12	21.12	0.00
4CFP	14.76	14.76	0.00	20.55	20.55	0.00
AI	15.46	15.72	0.26	21.59	22.16	0.56
5FA	16.07	16.35	0.27	22.55	23.14	0.59
5ClA	17.19	17.19	0.00	23.17	23.17	0.00
5BrA	18.45	18.59	0.14	25.09	25.38	0.29
5MeA	16.03	16.16	0.13	22.25	22.54	0.29
5OMeA	17.27	17.30	0.03	23.44	23.51	0.08

จุฬาลงกรณ์มหาวิทยาลัย
CHULALONGKORN UNIVERSITY

Table A7 Thermodynamic parameters of 32 TFA amines derivatives on GSiMe column

analytes	enthalpy term (kcal/mol)			entropy term (cal/mol·K)		
	$-\Delta H_1$	$-\Delta H_2$	$-\Delta\Delta H$	$-\Delta S_1$	$-\Delta S_2$	$-\Delta\Delta S$
PEA	13.93	13.93	0.00	19.98	19.98	0.00
2F	14.35	14.47	0.12	21.60	21.89	0.30
3F	14.67	14.67	0.00	21.32	21.32	0.00
4F	14.61	14.61	0.00	21.17	21.17	0.00
2Cl	16.20	16.36	0.16	24.05	24.45	0.39
3Cl	15.93	15.93	0.00	22.41	22.41	0.00
4Cl	15.76	15.76	0.00	21.89	21.89	0.00
2Br	15.29	15.29	0.00	20.78	20.78	0.00
3Br	16.12	16.12	0.00	21.92	21.92	0.00
4Br	16.14	16.14	0.00	21.81	21.81	0.00
2Me	15.06	15.17	0.11	22.17	22.43	0.26
3Me	15.34	15.48	0.14	22.72	23.06	0.33
4Me	15.69	15.78	0.09	23.52	23.76	0.23
2OMe	14.27	14.27	0.00	19.40	19.40	0.00
3OMe	15.27	15.43	0.15	22.55	22.92	0.38
4OMe	15.80	15.80	0.00	21.85	21.85	0.00
2CF	14.87	14.87	0.00	22.04	22.04	0.00
3CF	15.59	15.59	0.00	23.36	23.36	0.00
4CF	15.82	15.99	0.17	23.69	24.08	0.39
PPA	14.42	14.42	0.00	20.49	20.49	0.00
4FP	14.88	14.88	0.00	21.19	21.19	0.00
4ClP	15.54	15.54	0.00	20.84	20.84	0.00

Table A7 (continued)

analytes	enthalpy term (kcal/mol)			entropy term (cal/mol·K)		
	$-\Delta H_1$	$-\Delta H_2$	$-\Delta\Delta H$	$-\Delta S_1$	$-\Delta S_2$	$-\Delta\Delta S$
4BrP	15.82	15.82	0.00	20.59	20.59	0.00
4MeP	16.53	16.66	0.13	24.84	25.14	0.30
4OMeP	15.63	15.63	0.00	20.89	20.89	0.00
4CFP	15.08	15.11	0.03	21.23	21.29	0.06
AI	15.37	15.51	0.13	21.66	21.98	0.31
5FA	16.02	16.20	0.18	22.78	23.19	0.42
5ClA	15.97	15.97	0.00	20.64	20.64	0.00
5BrA	16.28	16.28	0.00	20.47	20.47	0.00
5MeA	16.05	16.18	0.13	23.05	23.38	0.33
5OMeA	17.04	17.18	0.14	22.44	22.75	0.31

จุฬาลงกรณ์มหาวิทยาลัย
CHULALONGKORN UNIVERSITY

Appendix B

Retention factor, selectivity, and resolution

Table B1 Retention factor (k'_2), selectivity (α), and resolution (R_s) of 32 TFA amines derivatives on ASiMe column

analytes	temperature (°C)	k'_2	α	R_s
PEA	110	16.11	1.031	1.81
2F	110	11.94	1.027	1.50
3F	130	7.95	1.038	1.79
4F	100	47.34	1.024	1.83
2Cl	130	13.87	1.032	1.57
3Cl	160	5.72	1.037	1.86
4Cl	110	134.94	1.013	0.74
2Br	140	13.95	1.026	1.53
3Br	170	5.79	1.032	1.61
4Br	120	128.60	1.012	1.00
2Me	120	14.01	1.035	1.96
3Me	120	16.43	1.033	1.88
4Me	110	34.62	1.000	-
2OMe	100	62.80	1.017	1.39
3OMe	120	16.42	1.034	2.07
4OMe	130	26.11	1.000	-
2CF	120	11.40	1.033	1.82
3CF	110	23.02	1.000	-
4CF	100	49.58	1.010	0.84
PPA	90	68.37	1.031	2.49

Table B1 (continued)

analytes	temperature (°C)	k'_2	α	R_s
4FP	100	68.70	1.018	1.37
4ClP	120	94.64	1.014	1.18
4BrP	130	90.11	1.013	0.74
4MeP	110	40.26	1.000	-
4OMeP	140	22.21	1.000	-
4CFP	110	52.22	1.000	-
AI	110	40.36	1.023	1.81
5FA	130	26.50	1.000	-
5ClA	160	18.70	1.031	1.89
5BrA	170	18.10	1.032	1.92
5MeA	140	16.75	1.027	1.62
5OMeA	150	21.71	1.000	-

จุฬาลงกรณ์มหาวิทยาลัย
CHULALONGKORN UNIVERSITY

Table B2 Retention factor (k'_2), selectivity (α), and resolution (R_s) of 32 TFA amines derivatives on BSiMe column

analytes	temperature (°C)	k'_2	α	R_s
PEA	120	9.85	1.036	1.88
2F	140	3.02	1.034	1.54
3F	140	5.03	1.041	2.09
4F	140	5.16	1.034	1.66
2Cl	150	5.35	1.040	2.04
3Cl	150	8.39	1.032	1.73
4Cl	120	43.86	1.023	1.72
2Br	150	8.40	1.036	1.95
3Br	150	13.44	1.030	1.64
4Br	120	81.01	1.017	1.34
2Me	90	67.43	1.012	0.94
3Me	100	42.83	1.029	2.25
4Me	100	44.21	1.012	0.96
2OMe	120	19.97	1.000	-
3OMe	110	24.32	1.023	1.61
4OMe	110	72.91	1.024	1.21
2CF	100	27.46	1.025	1.80
3CF	120	14.68	1.029	1.60
4CF	100	63.35	1.020	1.10
PPA	100	37.78	**1.000**	**-**
4FP	110	32.14	1.033	2.51
4ClP	130	33.07	1.000	-
4BrP	130	59.03	1.000	-

Table B2 (continued)

analytes	temperature (°C)	k'_2	α	R_s
4MeP	110	44.71	1.000	-
4OMeP	130	32.30	1.000	-
4CFP	110	35.25	1.000	-
AI	140	11.83	1.031	1.72
5FA	150	9.53	1.028	1.59
5ClA	140	43.93	1.000	-
5BrA	150	45.48	1.015	1.13
5MeA	130	27.76	1.020	1.44
5OMeA	130	75.06	1.008	0.50

จุฬาลงกรณ์มหาวิทยาลัย
CHULALONGKORN UNIVERSITY

Table B3 Retention factor (k'_2), selectivity (α), and resolution (R_s) of 32 TFA amines derivatives on GSiMe column

analytes	temperature (°C)	k'_2	α	R_s
PEA	110	15.64	1.000	-
2F	90	33.80	1.015	1.01
3F	110	21.02	1.000	-
4F	110	21.06	1.000	-
2Cl	90	128.78	1.022	1.65
3Cl	120	36.86	1.000	-
4Cl	120	39.19	1.000	-
2Br	130	22.61	1.000	-
3Br	130	36.12	1.000	-
4Br	130	39.14	1.000	-
2Me	100	38.90	1.015	1.10
3Me	100	43.39	1.018	1.32
4Me	90	82.75	1.012	0.92
2OMe	120	20.08	1.000	-
3OMe	100	42.96	1.018	1.31
4OMe	120	41.01	1.000	-
2CF	110	18.66	1.000	-
3CF	110	24.94	1.000	-
4CF	110	29.24	1.022	1.44
PPA	110	23.30	1.000	-
4FP	120	18.06	1.000	-
4ClP	140	19.17	1.000	-
4BrP	150	19.31	1.000	-

Table B3 (continued)

analytes	temperature (°C)	k'_2	α	R_s
4MeP	110	41.24	1.016	1.14
4OMeP	140	20.61	1.000	-
4CFP	100	66.92	1.008	0.58
AI	110	44.63	1.018	1.29
5FA	110	59.79	1.023	1.66
5ClA	150	22.15	1.000	-
5BrA	160	22.52	1.000	-
5MeA	110	72.98	1.017	1.29
5OMeA	130	64.46	1.013	0.96

จุฬาลงกรณ์มหาวิทยาลัย
CHULALONGKORN UNIVERSITY

Appendix C

NMR Spectra

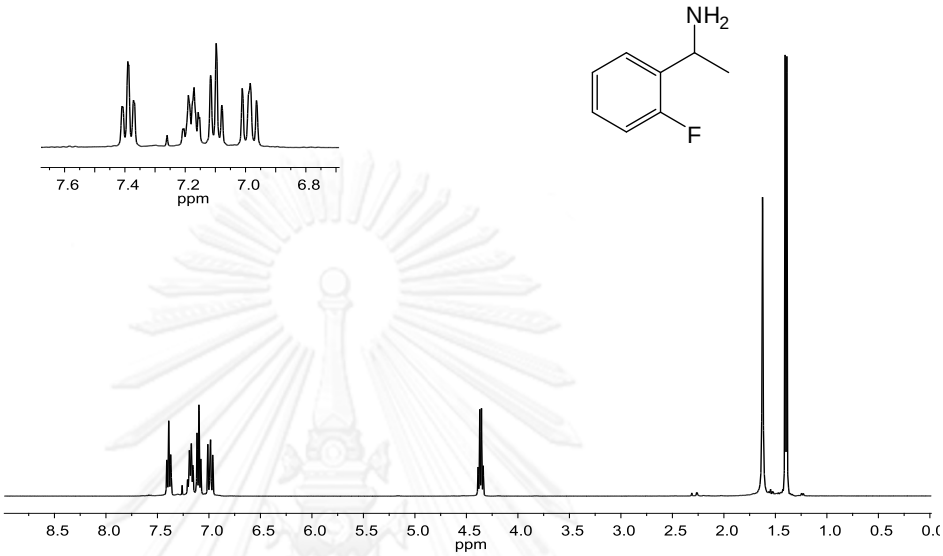

Figure C1 NMR spectrum of **2F;** ^{1}H NMR (400 MHz, $CDCl_3$) δ (ppm): 7.39 (t, *J* = 7.5 Hz, 1H, Ar<u>H</u>), 7.18 (dd, *J* = 15.5, 7.5 Hz, 1H, Ar<u>H</u>), 7.10 (t, *J* = 7.5 Hz, 1H, Ar<u>H</u>), 6.99 (dd, *J* = 11.2, 7.5 Hz, 1H, Ar<u>H</u>), 4.36 (q, *J* = 6.7 Hz, 1H, C<u>H</u>CH_3), 1.62 (br s, 2H, N<u>H</u>$_2$), 1.40 (d, *J* = 6.7 Hz, 3H, CHC<u>H</u>$_3$).

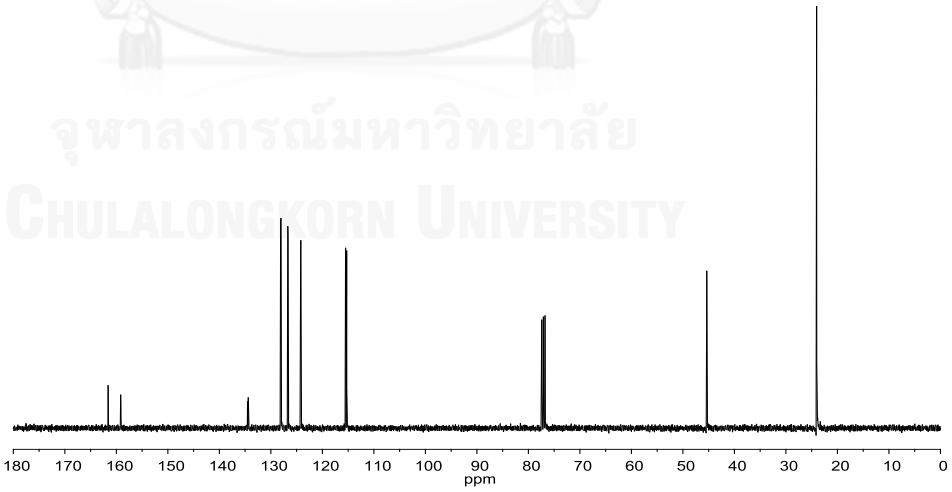

Figure C2 NMR spectrum of **2F**; ^{13}C NMR (100 MHz, $CDCl_3$) δ (ppm): 160.4 (d, J_{CF} = 245.1 Hz), 134.5 (d, J_{CF} = 13.3 Hz), 128.1 (d, J_{CF} = 8.3 Hz), 126.7 (d, J_{CF} = 5.0 Hz), 124.2 (d, J_{CF} = 3.5 Hz), 115.4 (d, J_{CF} = 22.2 Hz), 45.4 (d, J_{CF} = 2.8 Hz), 24.0.

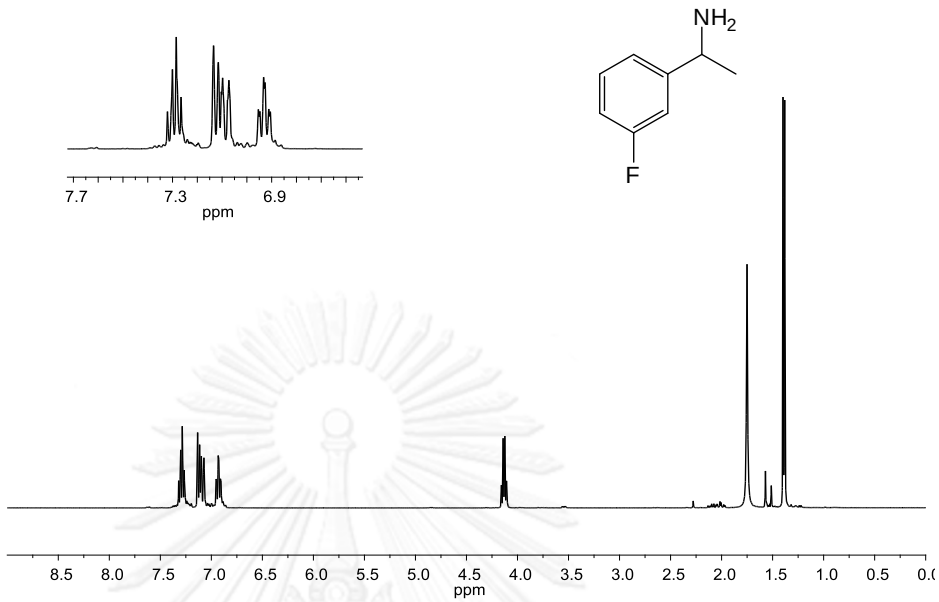

Figure C3 NMR spectrum of **3F**; ^{1}H NMR (400 MHz, $CDCl_3$) δ (ppm): 7.29 (dd, *J* = 14.0, 7.8 Hz, 1H, Ar<u>H</u>), 7.16–7.05 (m, 2H, Ar<u>H</u>), 6.93 (dd, *J* = 7.8, 7.8 Hz, 1H, Ar<u>H</u>), 4.13 (q, *J* = 6.6 Hz, 1H, C<u>H</u>CH_3), 1.75 (br s, 2H, N$\underline{H}_2$), 1.39 (d, *J* = 6.6 Hz, 3H, CHC$\underline{H}_3$).

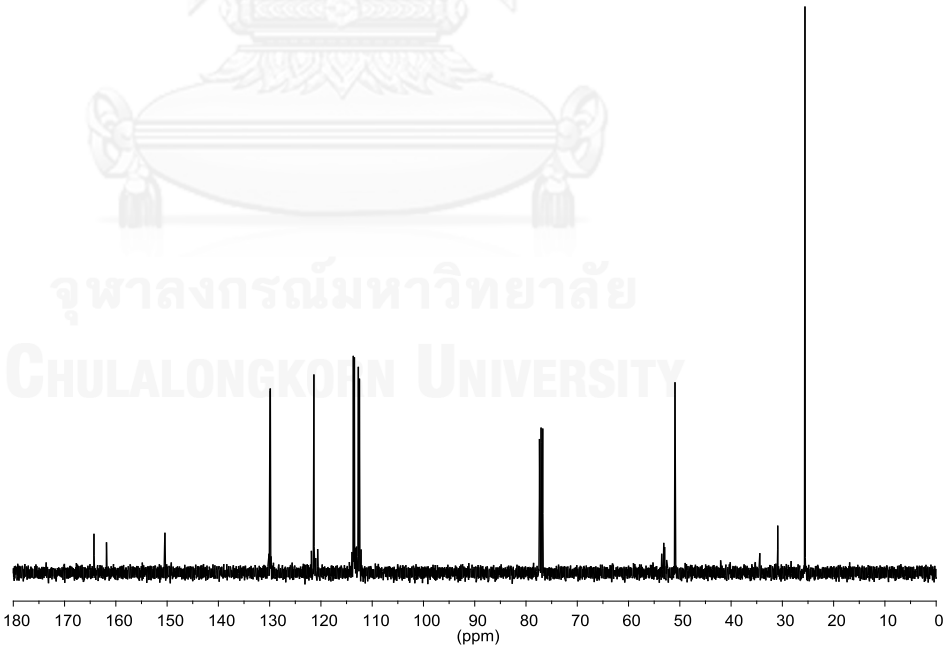

Figure C4 NMR spectrum of **3F;** ^{13}C NMR (100 MHz, $CDCl_3$) δ (ppm): 163.0 (d, J_{CF} = 245.5 Hz), 150.5 (d, J_{CF} = 6.4 Hz), 130.0 (d, J_{CF} = 8.1 Hz), 121.4 (d, J_{CF} = 2.7 Hz), 113.6 (d, J_{CF} = 21.2 Hz), 112.6 (d, J_{CF} = 21.4 Hz), 50.9, 25.6.

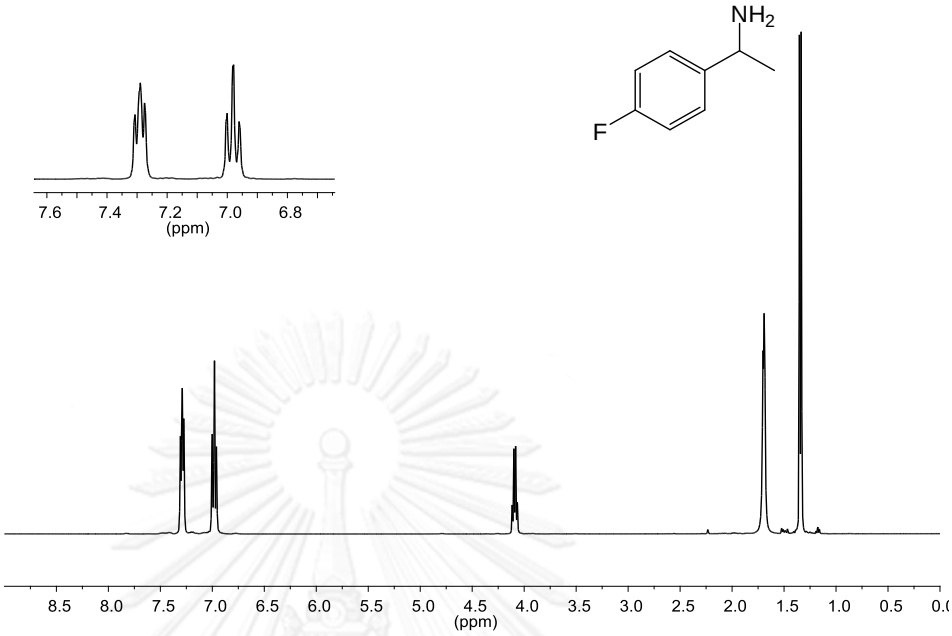

Figure C5 NMR spectrum of **4F;** ^{1}H NMR (400 MHz, $CDCl_3$) δ (ppm): 7.29 (dd, *J* = 7.8, 5.0 Hz, 2H, Ar<u>H</u>), 6.99 (dd, *J* = 7.8, 5.0 Hz, 2H, Ar<u>H</u>), 4.09 (q, *J* = 6.6 Hz, 1H, C<u>H</u>CH_3), 1.69 (br s, 2H, N<u>H</u>$_2$), 1.34 (d, *J* = 6.6 Hz, 3H, CHC<u>H</u>$_3$).

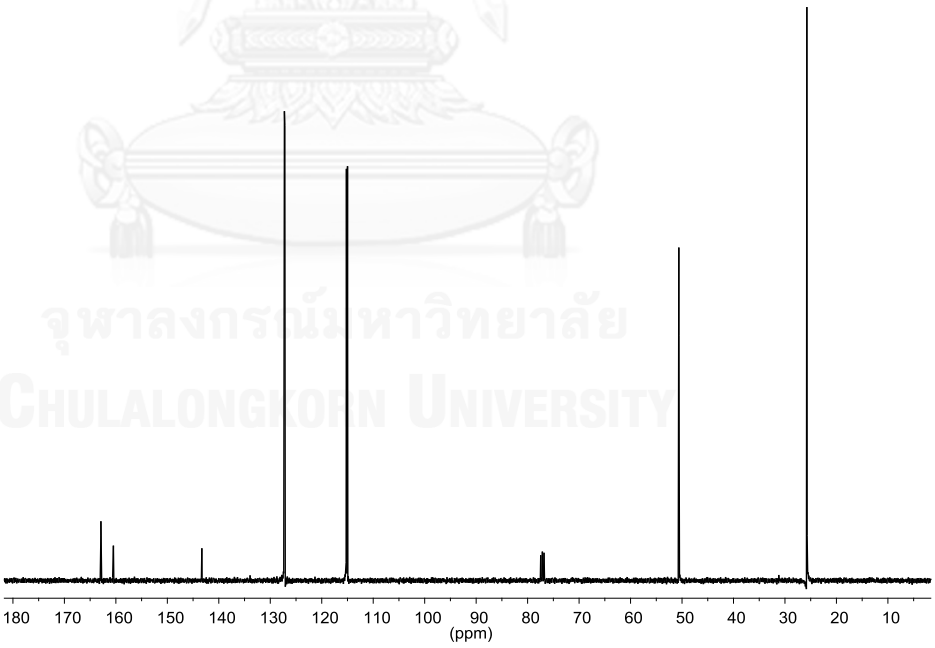

Figure C6 NMR spectrum of **4F;** ^{13}C NMR (100 MHz, $CDCl_3$) δ (ppm): 161.7 (d, J_{CF} = 244.3 Hz), 143.3 (d, J_{CF} = 2.0 Hz), 127.2 (d, J_{CF} = 7.9 Hz), 115.1 (d, J_{CF} = 21.2 Hz), 50.6, 25.8.

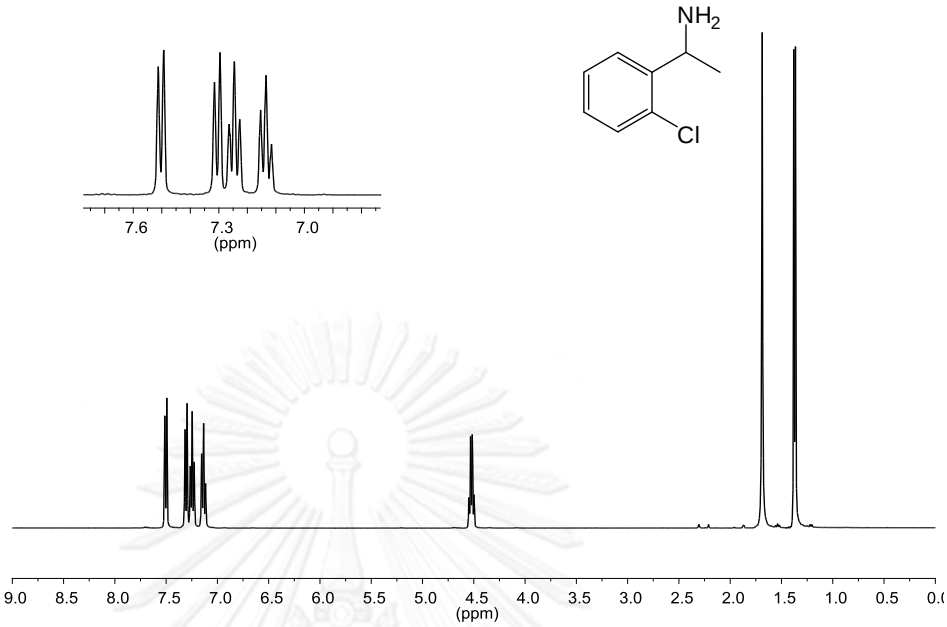

Figure C7 NMR spectrum of **2Cl;** ^{1}H NMR (400 MHz, $CDCl_3$) δ (ppm): 7.50 (d, *J* = 7.8 Hz, 1H, Ar<u>H</u>), 7.31 (d, *J* = 7.8 Hz, 1H, Ar<u>H</u>), 7.25 (t, *J* = 7.8 Hz, 1H, Ar<u>H</u>), 7.13 (t, *J* = 7.8 Hz, 1H, Ar<u>H</u>), 4.52 (q, *J* = 6.6 Hz, 1H, C<u>H</u>CH_3), 1.69 (br s, 2H, N<u>H</u>$_2$), 1.37 (d, *J* = 6.6 Hz, 3H, CHC<u>H</u>$_3$).

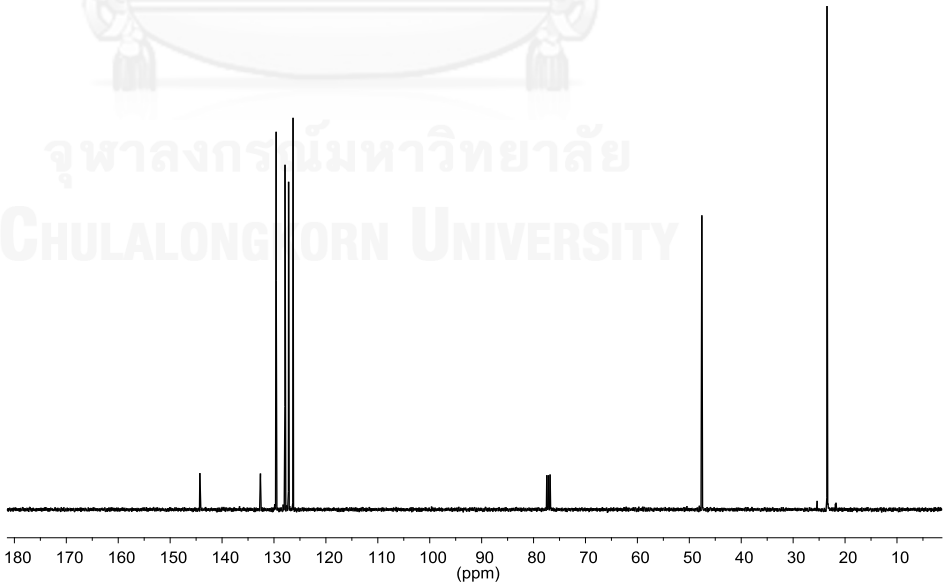

Figure C8 NMR spectrum of **2Cl;** ^{13}C NMR (100 MHz, $CDCl_3$) δ (ppm): 144.3, 132.6, 129.6, 127.9, 127.2, 126.3, 47.6, 23.5.

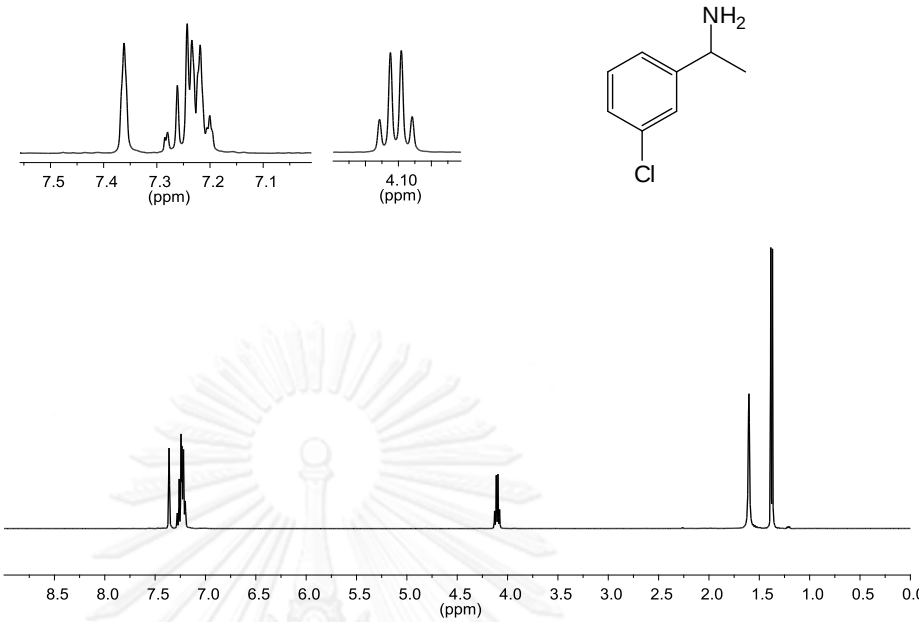

Figure C9 NMR spectrum of **3Cl;** ^{1}H NMR (400 MHz, $CDCl_3$) δ (ppm): 7.36 (s, 1H, Ar<u>H</u>), 7.30–7.17 (m, 3H, Ar<u>H</u>), 4.10 (q, *J* = 6.6 Hz, 1H, C<u>H</u>CH_3), 1.60 (br s, 2H, N<u>H</u>$_2$), 1.38 (d, *J* = 6.6 Hz, 3H, CHC<u>H</u>$_3$).

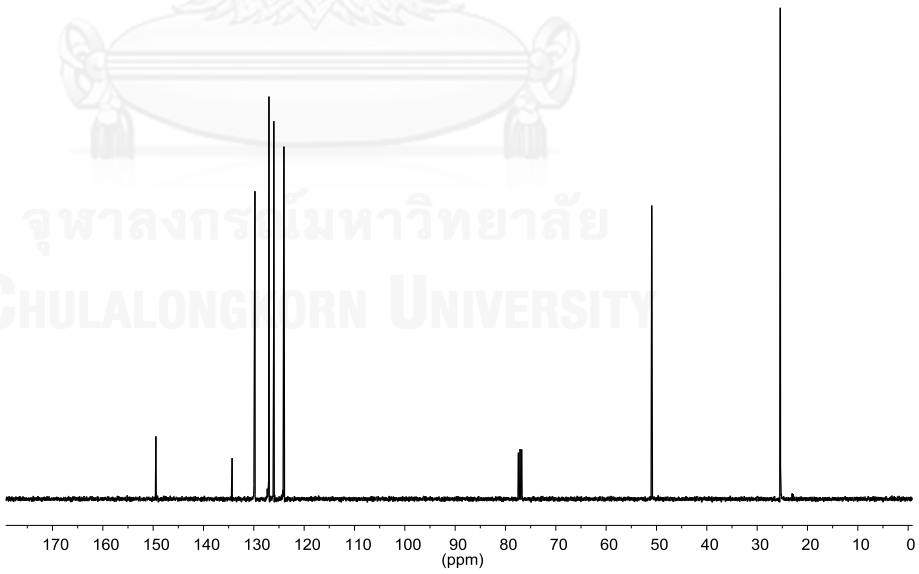

Figure C10 NMR spectrum of **3Cl;** ^{13}C NMR (100 MHz, $CDCl_3$) δ (ppm): 149.5, 134.3, 129.8, 127.0, 126.0, 124.0, 51.0, 25.4.

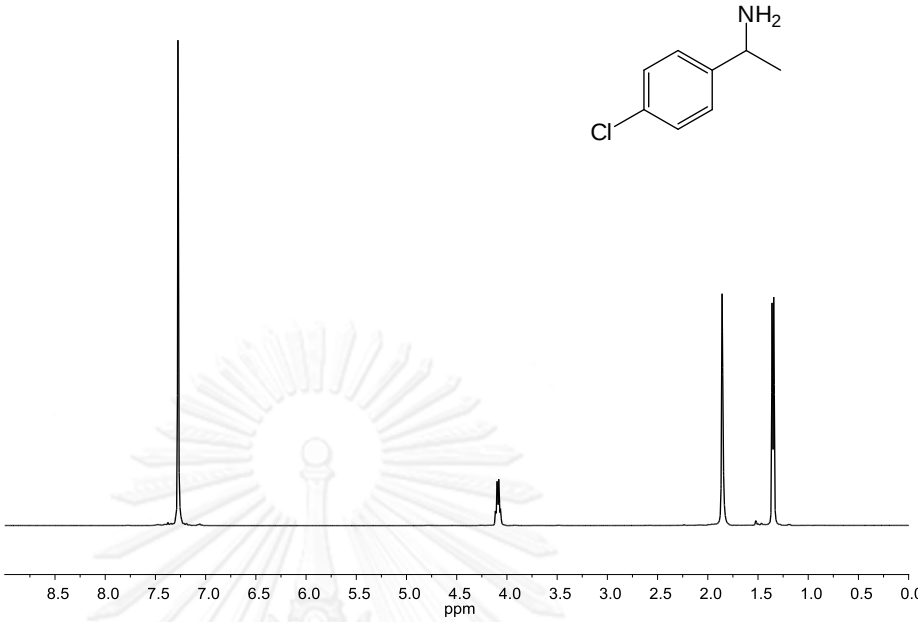

Figure C11 NMR spectrum of **4Cl;** ^{1}H NMR (400 MHz, $CDCl_3$) δ (ppm): 7.28 (s, 4H, Ar<u>H</u>), 4.09 (q, *J* = 6.6 Hz, 1H, C<u>H</u>CH_3), 1.86 (br s, 2H, N<u>H</u>$_2$), 1.35 (d, *J* = 6.6 Hz, 3H, CHC<u>H</u>$_3$).

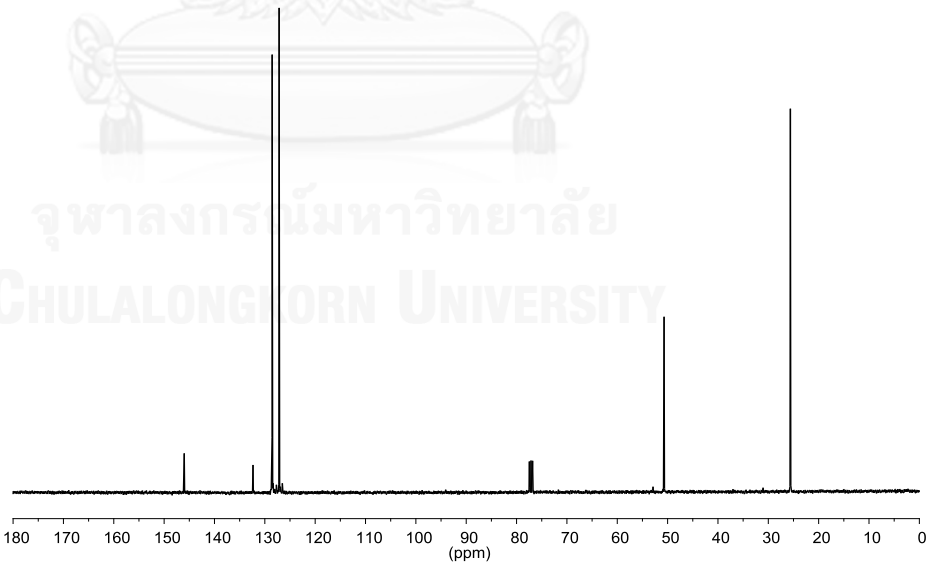

Figure C12 NMR spectrum of **4Cl;** ^{13}C NMR (100 MHz, $CDCl_3$) δ (ppm): 146.0, 132.4, 128.5, 127.2, 50.7, 25.6.

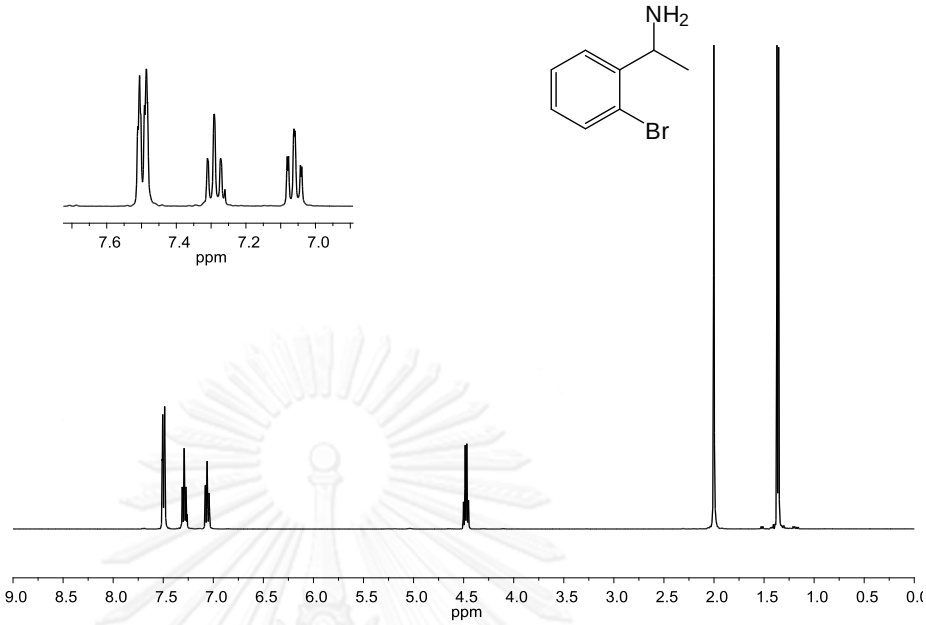

Figure C13 NMR spectrum of **2Br;** ^{1}H NMR (400 MHz, $CDCl_3$) δ (ppm): 7.50 (dd, *J* = 7.8, 2.0 Hz, 2H, Ar<u>H</u>), 7.29 (t, *J* = 7.8 Hz, 1H, Ar<u>H</u>), 7.06 (t, *J* = 7.8 Hz, 1H, Ar<u>H</u>), 4.48 (q, *J* = 6.6 Hz, 1H, C<u>H</u>CH_3), 2.00 (br s, 2H, N$\underline{H}_2$), 1.36 (d, *J* = 6.6 Hz, 3H, CHC$\underline{H}_3$).

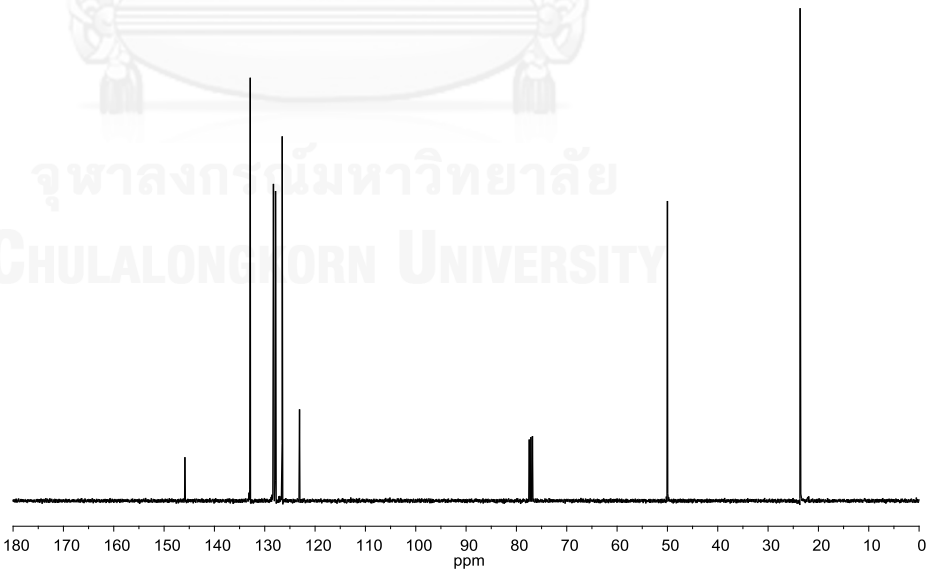

Figure C14 NMR spectrum of **2Br;** ^{13}C NMR (100 MHz, $CDCl_3$) δ (ppm): 145.9, 132.9, 128.3, 127.9, 126.5, 123.1, 50.0, 23.6.

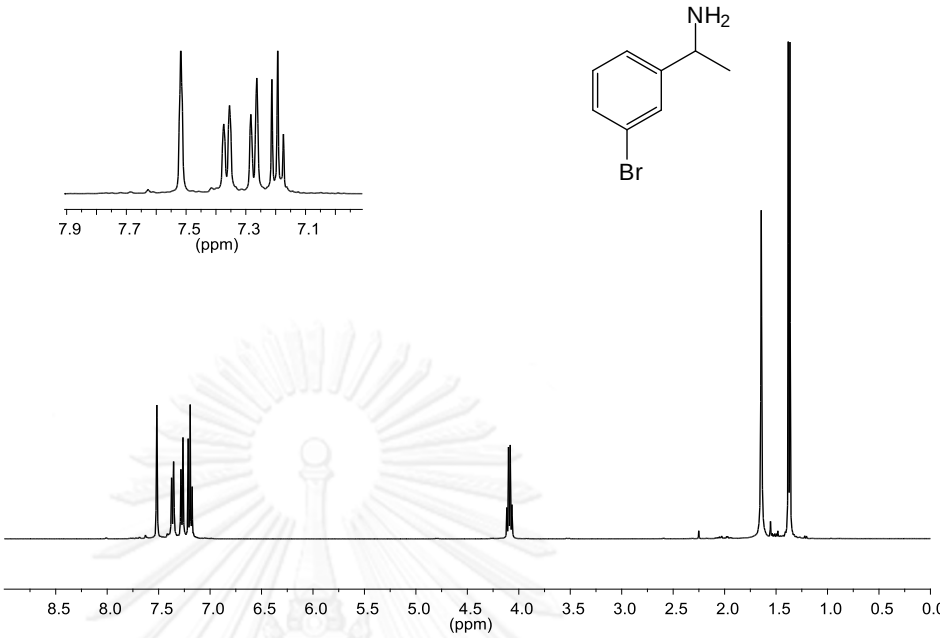

Figure C15 NMR spectrum of **3Br;** ^{1}H NMR (400 MHz, $CDCl_3$) δ (ppm): 7.52 (s, 1H, Ar<u>H</u>), 7.36 (d, *J* = 7.8 Hz, 1H, Ar<u>H</u>), 7.27 (d, *J* = 7.8 Hz, 1H, Ar<u>H</u>), 7.19 (t, *J* = 7.8 Hz, 1H, Ar<u>H</u>), 4.09 (q, *J* = 6.6 Hz, 1H, C<u>H</u>CH_3), 1.64 (br s, 2H, N$\underline{H}_2$), 1.37 (d, *J* = 6.6 Hz, 3H, CHC$\underline{H}_3$).

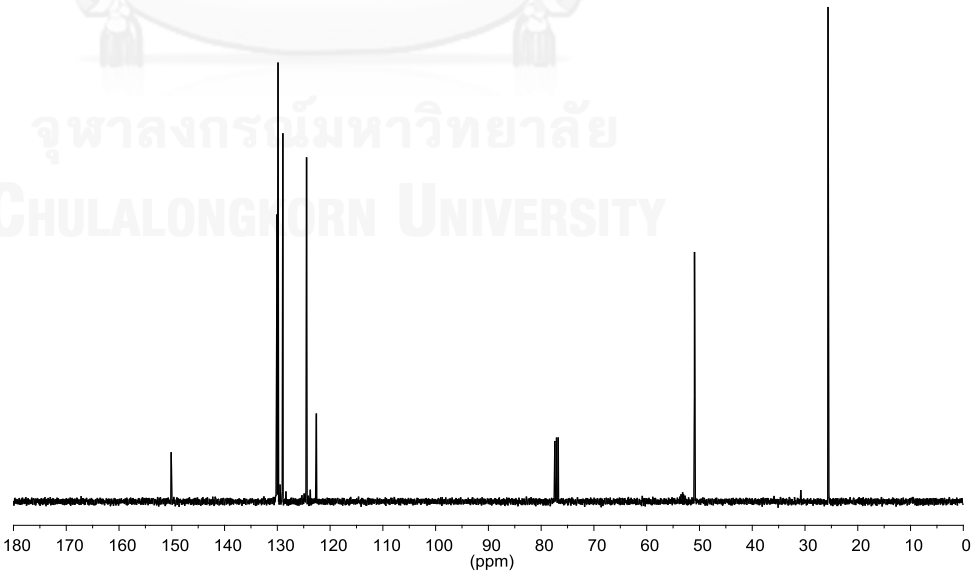

Figure C16 NMR spectrum of **3Br;** ^{13}C NMR (100 MHz, $CDCl_3$) δ (ppm): 150.1, 130.1, 129.9, 129.0, 124.5, 122.6, 50.9, 25.6.

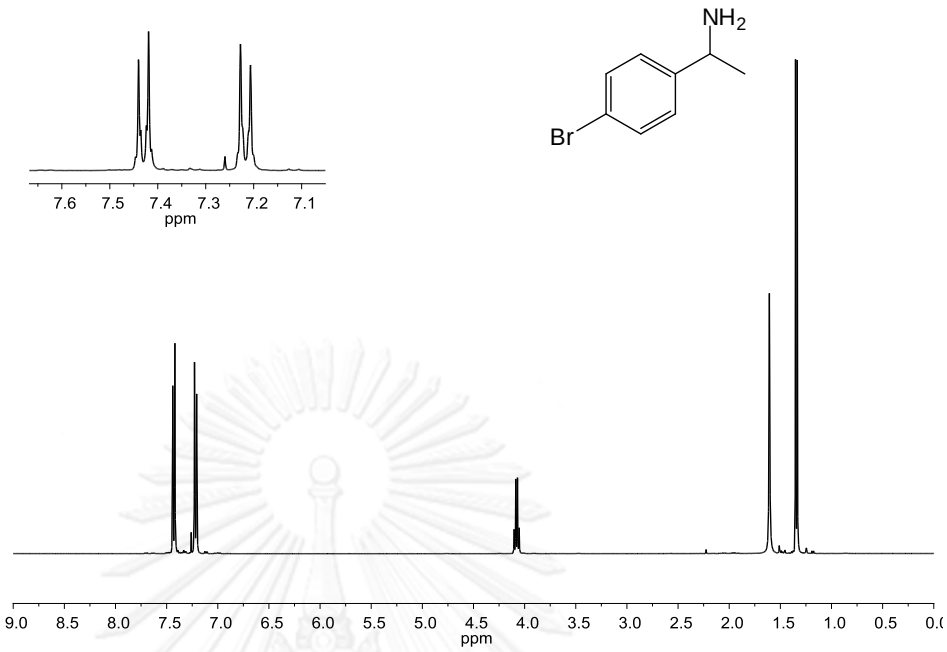

Figure C17 NMR spectrum of **4Br;** ^{1}H NMR (400 MHz, $CDCl_3$) δ (ppm): 7.43 (d, *J* = 8.2 Hz, 2H, Ar<u>H</u>), 7.22 (d, *J* = 8.2 Hz, 2H, Ar<u>H</u>), 4.08 (q, *J* = 6.6 Hz, 1H, C<u>H</u>CH_3), 1.61 (br s, 2H, N<u>H</u>$_2$), 1.34 (d, *J* = 6.6 Hz, 3H, CHC<u>H</u>$_3$).

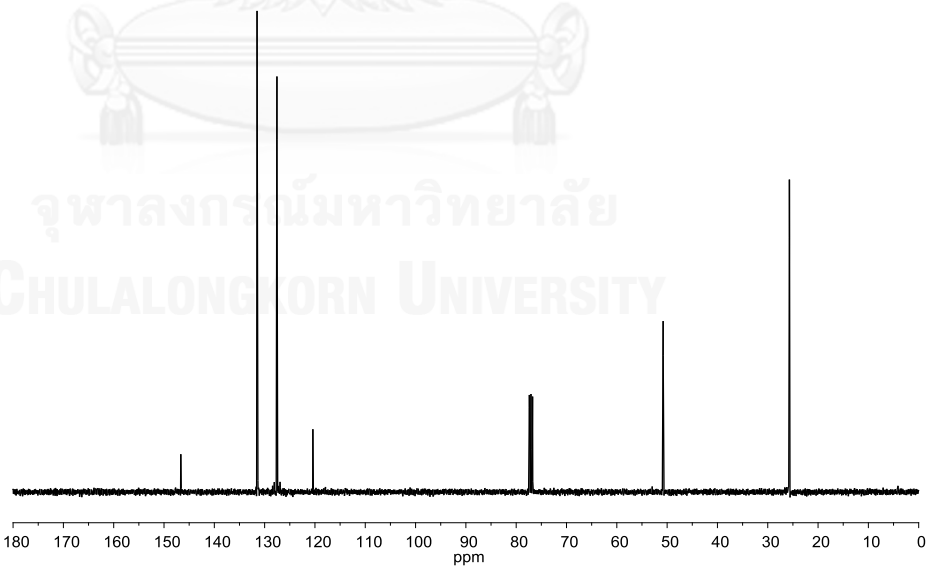

Figure C18 NMR spectrum of **4Br;** ^{13}C NMR (100 MHz, $CDCl_3$) δ (ppm): 146.3, 131.5, 127.6, 127.6, 120.4, 50.8, 25.7.

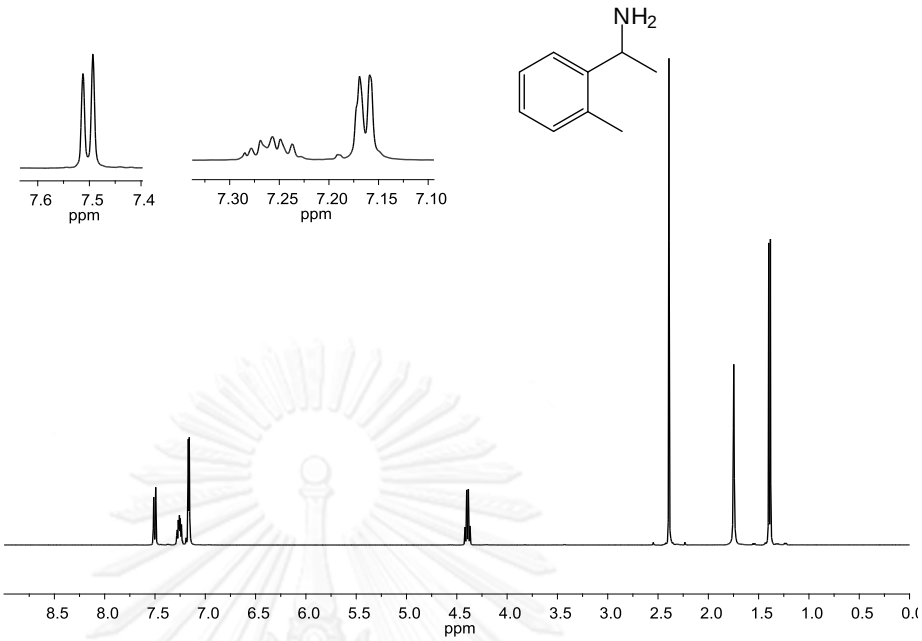

Figure C19 NMR spectrum of **2Me;** ^{1}H NMR (400 MHz, $CDCl_3$) δ (ppm): 7.50 (d, *J* = 7.6 Hz, 1H, Ar<u>H</u>), 7.30–7.22 (m, 1H, Ar<u>H</u>), 7.17 (br s, 1H, Ar<u>H</u>), 7.16 (br s, 1H, Ar<u>H</u>), 4.39 (q, *J* = 6.6 Hz, 1H, C<u>H</u>CH_3), 2.39 (s, 3H, CC<u>H</u>$_3$), 1.75 (br s, 2H, N<u>H</u>$_2$), 1.39 (d, *J* = 6.6 Hz, 3H, CHC<u>H</u>$_3$).

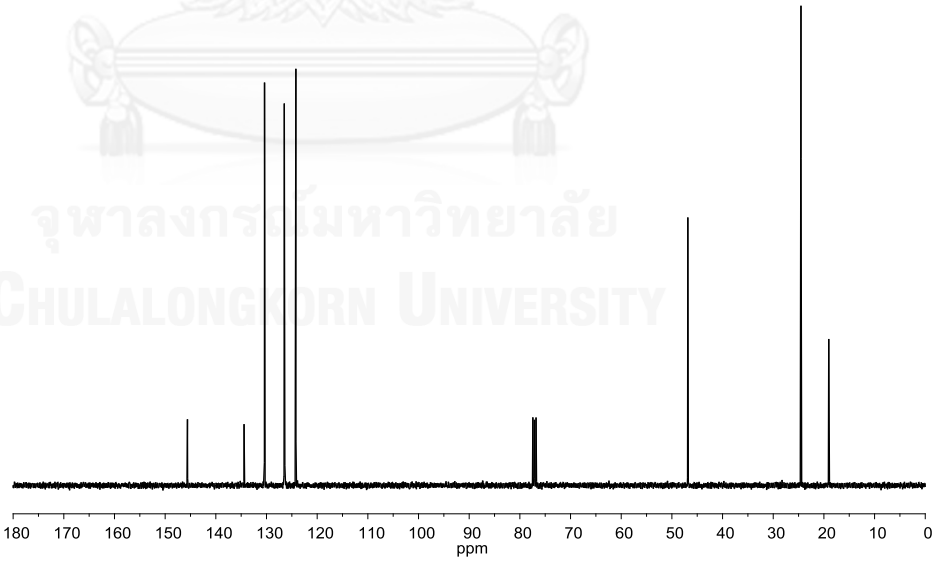

Figure C20 NMR spectrum of **2Me;** ^{13}C NMR (100 MHz, $CDCl_3$) δ (ppm): 145.6, 134.4, 130.4, 126.5, 126.4, 124.2, 46.9, 24.5, 19.0.

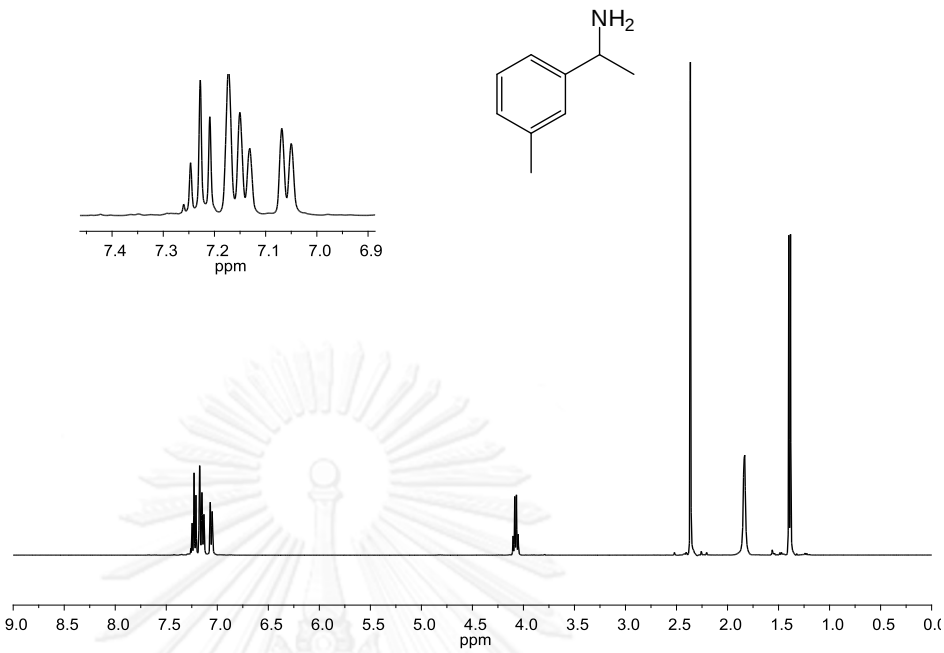

Figure C21 NMR spectrum of **3Me;** ^{1}H NMR (400 MHz, $CDCl_3$) δ (ppm): 7.23 (t, *J* = 7.5 Hz, 1H, Ar<u>H</u>), 7.17 (s, 1H, Ar<u>H</u>), 7.14 (d, *J* = 7.5 Hz, 1H, Ar<u>H</u>), 7.06 (d, *J* = 7.5 Hz, 1H, Ar<u>H</u>), 4.08 (q, *J* = 6.6 Hz, 1H, C<u>H</u>CH_3), 2.36 (s, 3H, CC<u>H</u>$_3$), 1.83 (br s, 2H, N<u>H</u>$_2$), 1.39 (d, *J* = 6.6 Hz, 3H, CHC<u>H</u>$_3$).

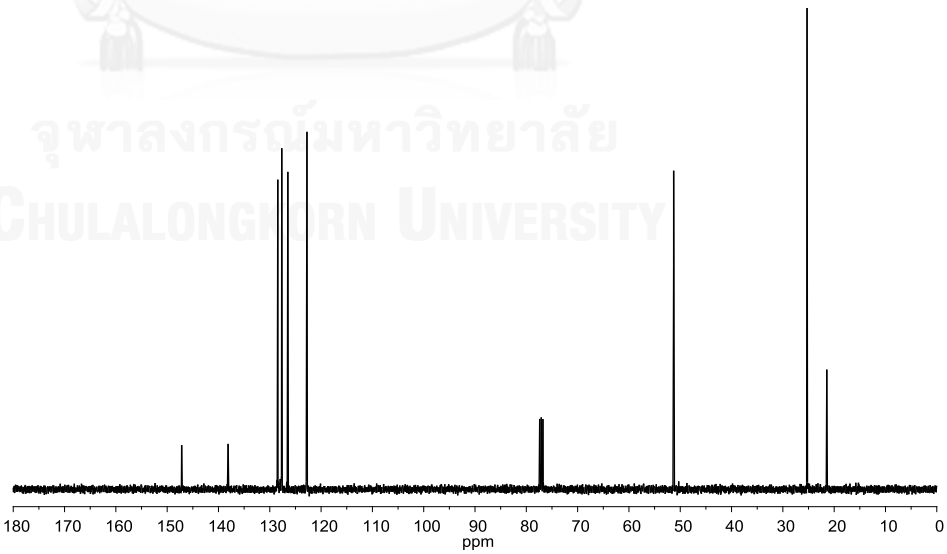

Figure C22 NMR spectrum of **3Me;** ^{13}C NMR (100 MHz, $CDCl_3$) δ (ppm): 147.2, 138.1, 128.4, 127.7, 126.5, 122.8, 51.2, 25.3, 21.4.

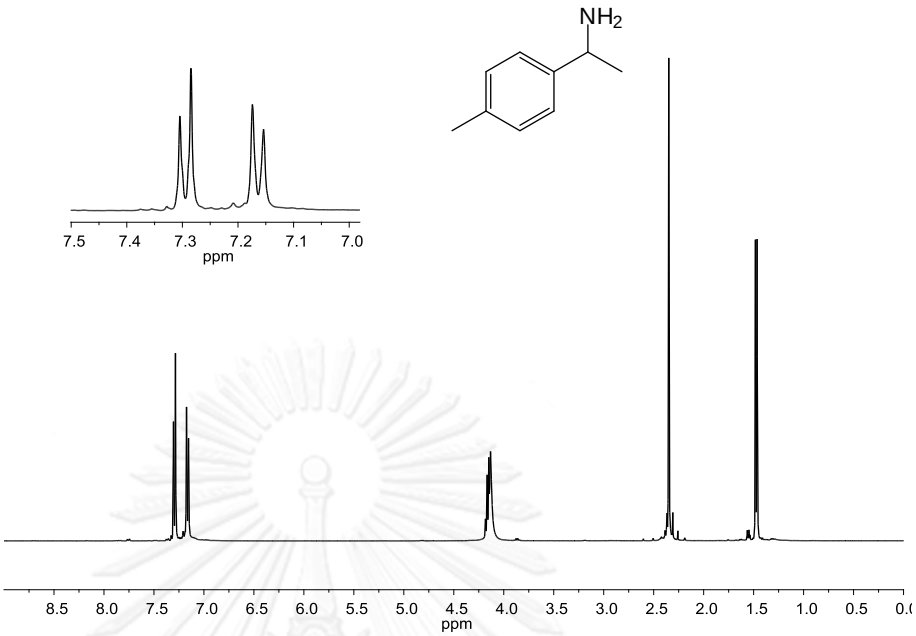

Figure C23 NMR spectrum of **4Me;** ^{1}H NMR (400 MHz, $CDCl_3$) δ (ppm): 7.29 (d, *J* = 8.0 Hz, 2H, Ar<u>H</u>), 7.16 (d, *J* = 8.0 Hz, 2H, Ar<u>H</u>), 4.17 (q, *J* = 6.5 Hz, 1H, C<u>H</u>CH_3), 4.13 (br s, 2H, N<u>H</u>$_2$), 2.35 (s, 3H, CC<u>H</u>$_3$), 1.47 (d, *J* = 6.5 Hz, 3H, CHC<u>H</u>$_3$).

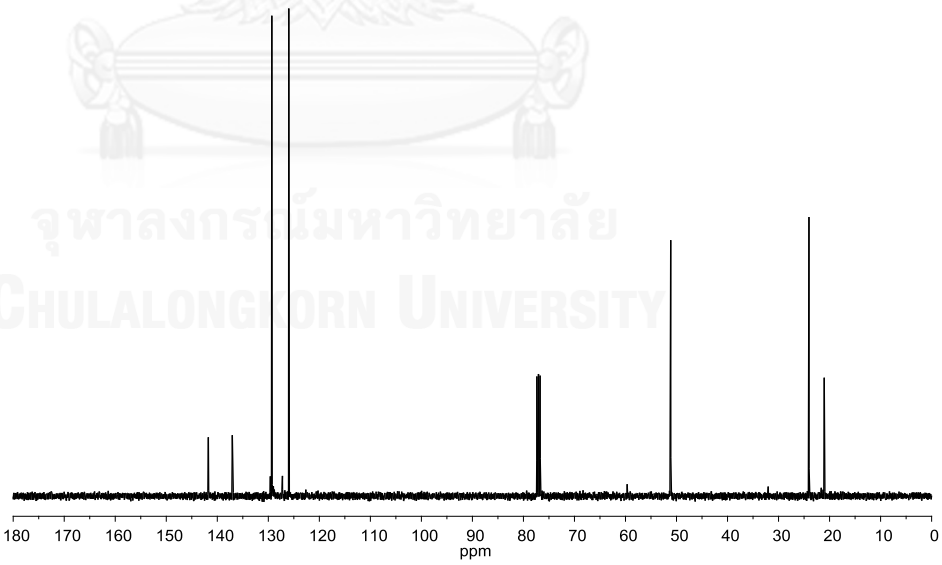

Figure C24 NMR spectrum of **4Me;** ^{13}C NMR (100 MHz, $CDCl_3$) δ (ppm): 141.8, 137.1, 129.3, 126.0, 51.2, 24.0, 21.0.

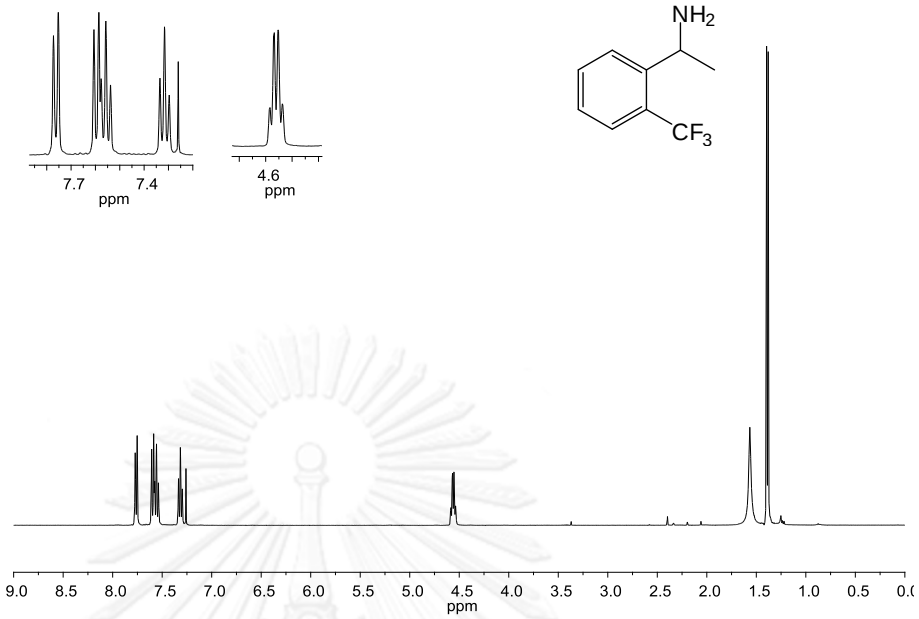

Figure C25 NMR spectrum of **2CF;** ^{1}H NMR (400 MHz, $CDCl_3$) δ (ppm): 7.76 (d, *J* = 7.8 Hz, 1H, Ar<u>H</u>), 7.62 (d, *J* = 7.8 Hz, 1H, Ar<u>H</u>), 7.58 (t, *J* = 7.8 Hz, 1H, Ar<u>H</u>), 7.32 (t, *J* = 7.8 Hz, 1H, Ar<u>H</u>), 4.56 (q, *J* = 6.5 Hz, 1H, C<u>H</u>CH_3), 1.61 (br s, 2H, N$\underline{H}_2$), 1.39 (d, *J* = 6.5 Hz, 3H, CHC$\underline{H}_3$).

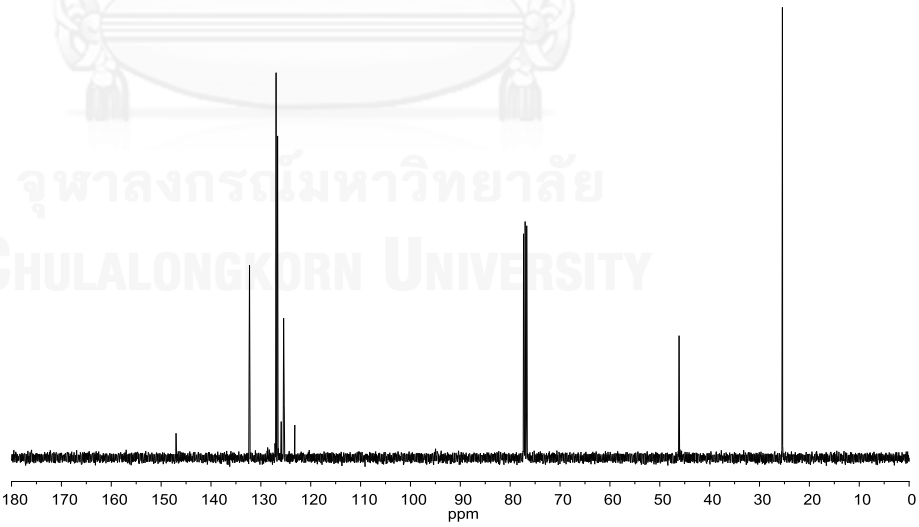

Figure C26 NMR spectrum of **2CF;** ^{13}C NMR (100 MHz, $CDCl_3$) δ (ppm): 147.0, 132.3, 127.0, 126.6, 125.9, 125.4 (q, J_{CF} = 6.0 Hz), 123.2, 46.1 (d, *J* = 2.4 Hz), 25.4.

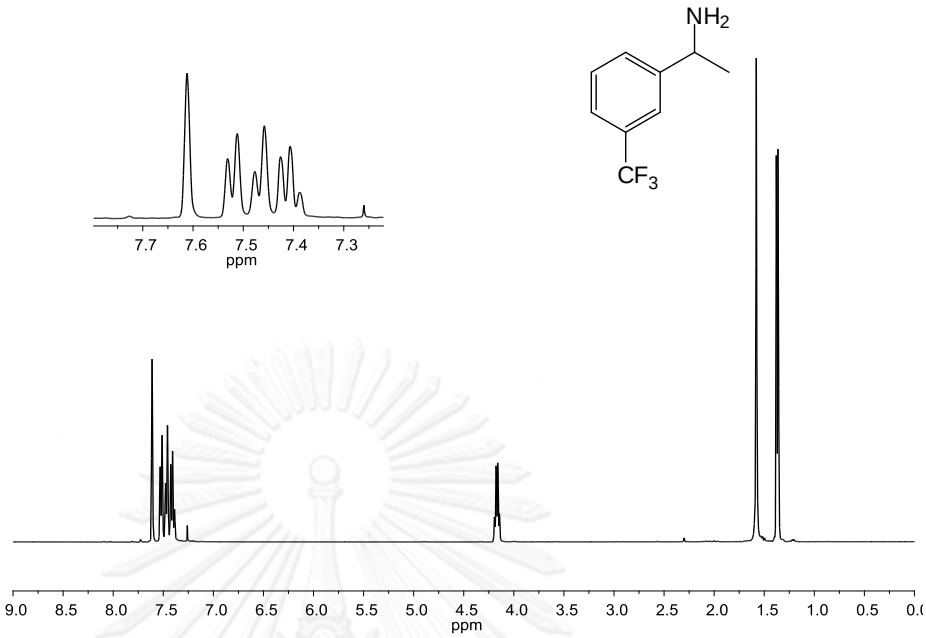

Figure C27 NMR spectrum of **3CF;** ^{1}H NMR (400 MHz, $CDCl_3$) δ (ppm): 7.61 (s, 1H, Ar<u>H</u>), 7.52 (d, *J* = 7.6 Hz, 1H, Ar<u>H</u>), 7.47 (d, *J* = 7.6 Hz, 1H, Ar<u>H</u>), 7.41 (t, *J* = 7.6 Hz, 1H, Ar<u>H</u>), 4.17 (q, *J* = 6.6 Hz, 1H, C<u>H</u>CH_3), 1.58 (br s, 2H, N$\underline{H}_2$), 1.37 (d, *J* = 6.6 Hz, 3H, CHC$\underline{H}_3$).

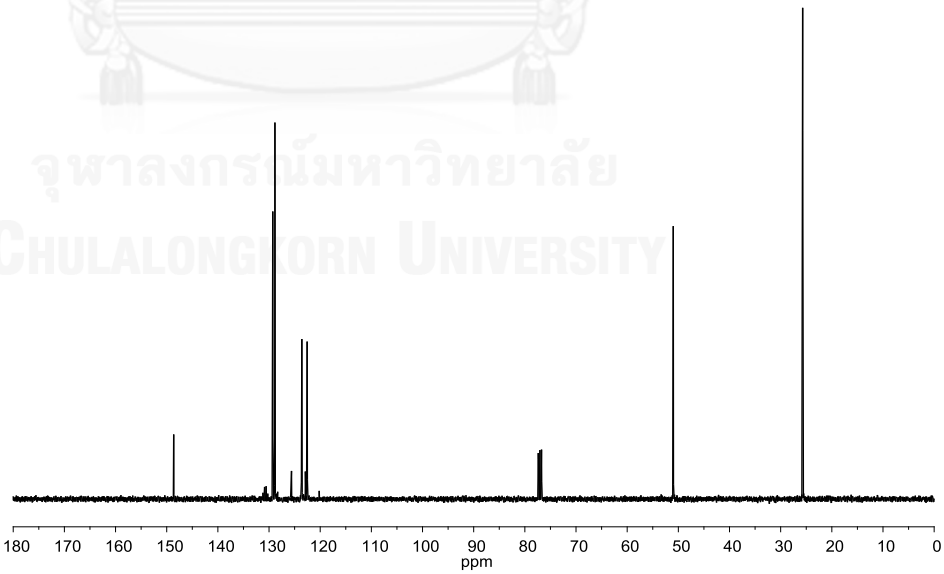

Figure C28 NMR spectrum of **3CF;** ^{13}C NMR (100 MHz, $CDCl_3$) δ (ppm): 148.6, 130.7 (q, J_{CF} = 34.0 Hz), 129.3, 128.8, 123.6 (q, J_{CF} = 3.6 Hz), 123.5 (q, J_{CF} = 272.0 Hz), 122.6 (q, J_{CF} = 3.8 Hz), 51.0, 25.7.

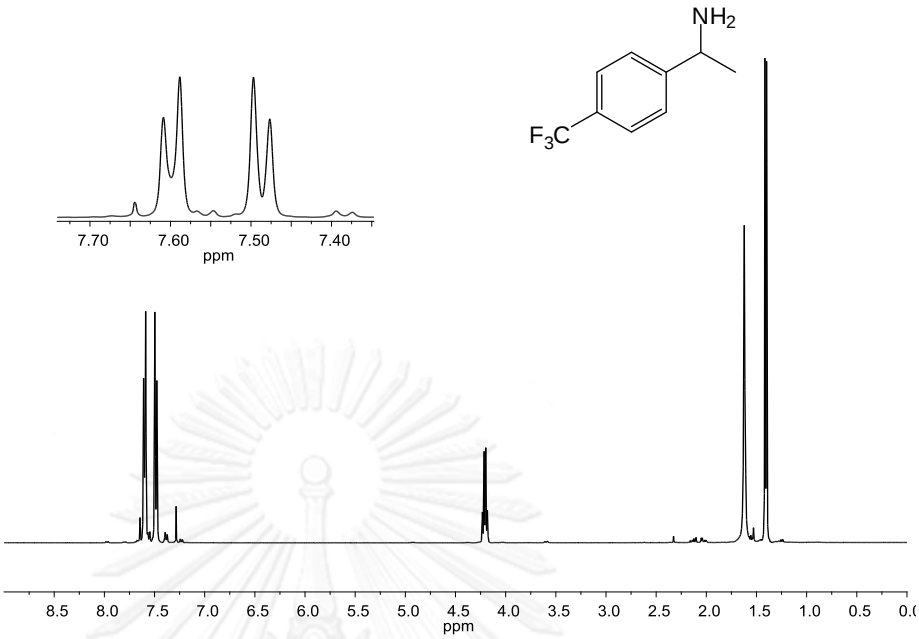

Figure C29 NMR spectrum of **4CF;** ^{1}H NMR (400 MHz, $CDCl_3$) δ (ppm): 7.60 (d, *J* = 8.1 Hz, 2H, Ar<u>H</u>), 7.49 (d, *J* = 8.1 Hz, 2H, Ar<u>H</u>), 4.21 (q, *J* = 6.6 Hz, 1H , C<u>H</u>CH_3), 1.62 (br s, 2H, N<u>H</u>$_2$), 1.41 (d, *J* = 6.6 Hz, 3H, CHC<u>H</u>$_3$).

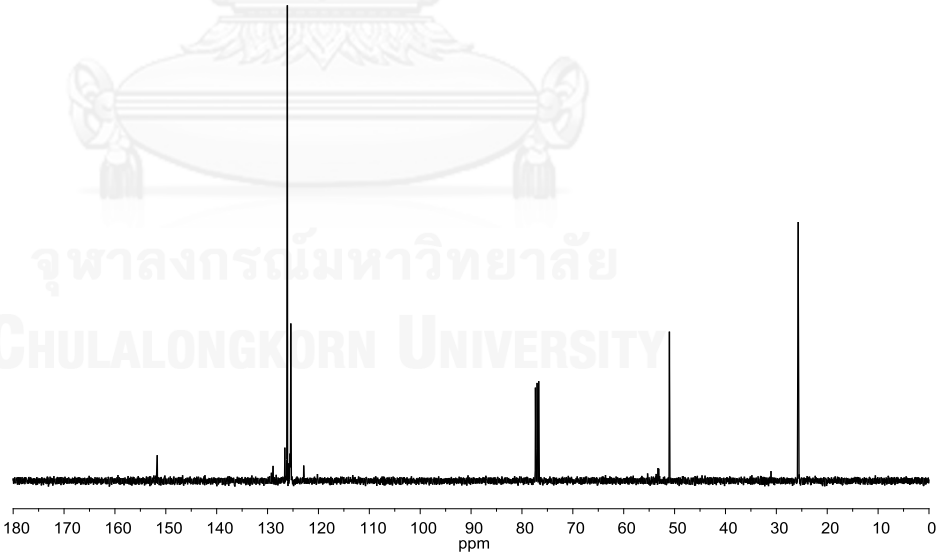

Figure C30 NMR spectrum of **4CF;** ^{13}C NMR (100 MHz, $CDCl_3$) δ (ppm): 151.7, 126.1, 126.0 (q, J_{CF} = 25.7 Hz), 125.7 (q, J_{CF} = 278.1 Hz), 125.4 (q, J_{CF} = 3.6 Hz), 51.0, 25.7.

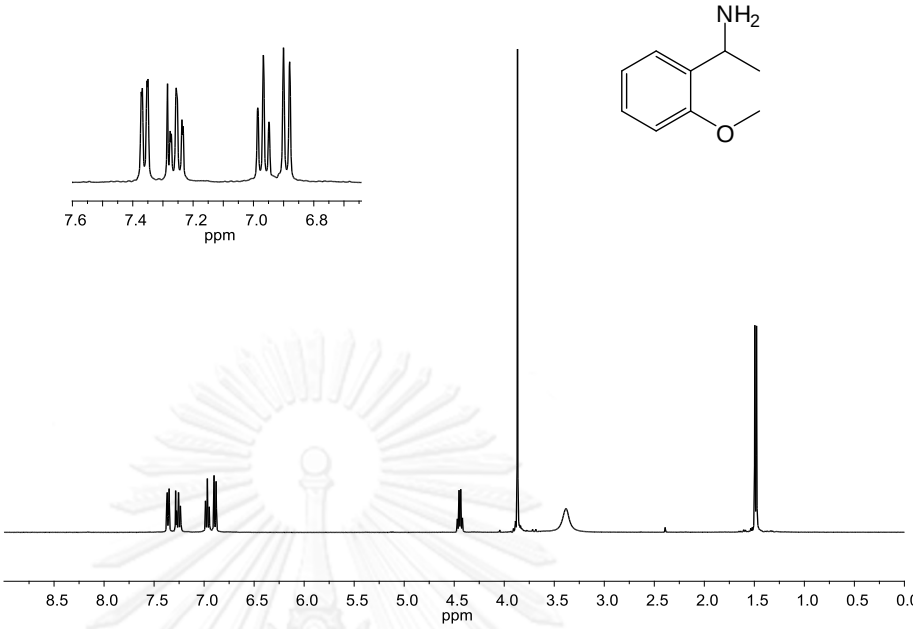

Figure C31 NMR spectrum of **2OMe;** ^{1}H NMR (400 MHz, $CDCl_3$) δ (ppm): 7.36 (d, *J* = 7.7 Hz, 1H, Ar<u>H</u>), 7.25 (t, *J* = 7.7 Hz, 1H, Ar<u>H</u>), 6.97 (t, *J* = 7.7 Hz, 1H, Ar<u>H</u>), 6.89 (d, *J* = 7.7 Hz, 1H, Ar<u>H</u>), 4.44 (q, *J* = 6.8 Hz, 1H, C<u>H</u>CH_3), 3.87 (s, 3H, COC<u>H</u>$_3$), 3.38 (br s, 2H, N<u>H</u>$_2$), 1.49 (d, *J* = 6.8 Hz, 3H, CHC<u>H</u>$_3$).

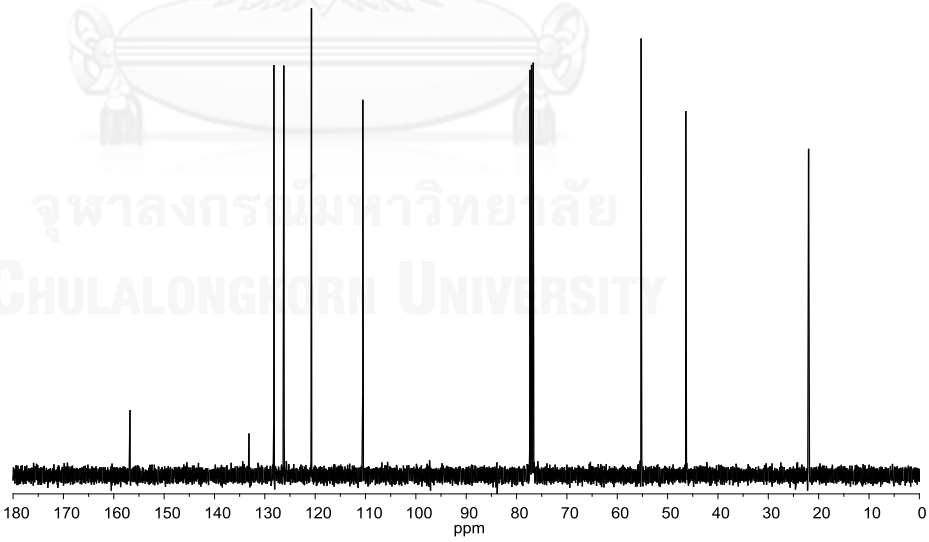

Figure C32 NMR spectrum of **2OMe;** ^{13}C NMR (100 MHz, $CDCl_3$) δ (ppm): 156.8, 133.1, 128.2, 126.2, 120.7, 110.5, 55.3, 46.4, 22.0.

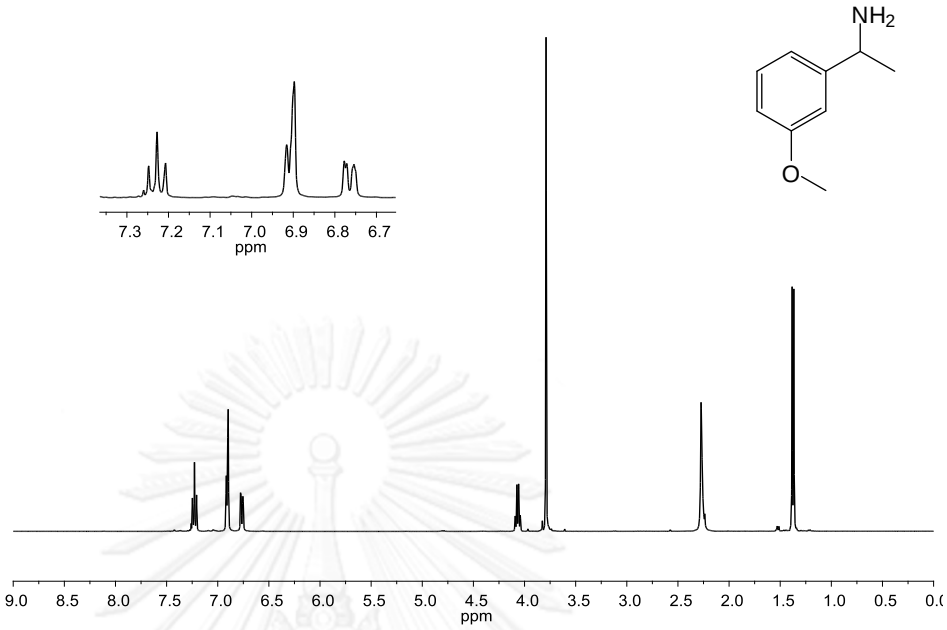

Figure C33 NMR spectrum of **3OMe;** ^{1}H NMR (400 MHz, $CDCl_3$) δ (ppm): 7.23 (t, *J* = 8.1 Hz, 1H, Ar<u>H</u>), 6.91 (d, *J* = 8.1 Hz, 1H, Ar<u>H</u>), 6.90 (s, 1H, Ar<u>H</u>), 6.76 (d, *J* = 8.1 Hz, 1H, Ar<u>H</u>), 4.07 (q, *J* = 6.6 Hz, 1H, C<u>H</u>CH_3), 3.79 (s, 3H, COC<u>H</u>$_3$), 2.27 (br, s, 2H, N<u>H</u>$_2$), 1.38 (d, *J* = 6.6 Hz, 3H, CHC<u>H</u>$_3$).

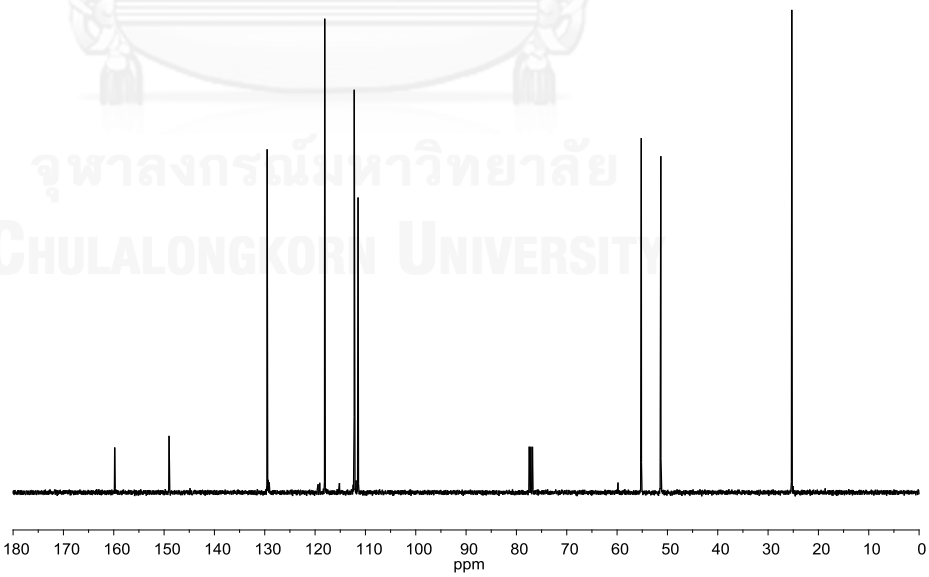

Figure C34 NMR spectrum of **3OMe;** ^{13}C NMR (100 MHz, $CDCl_3$) δ (ppm): 159.8, 149.0, 129.5, 118.1, 112.2, 111.5, 55.2, 51.3, 25.3.

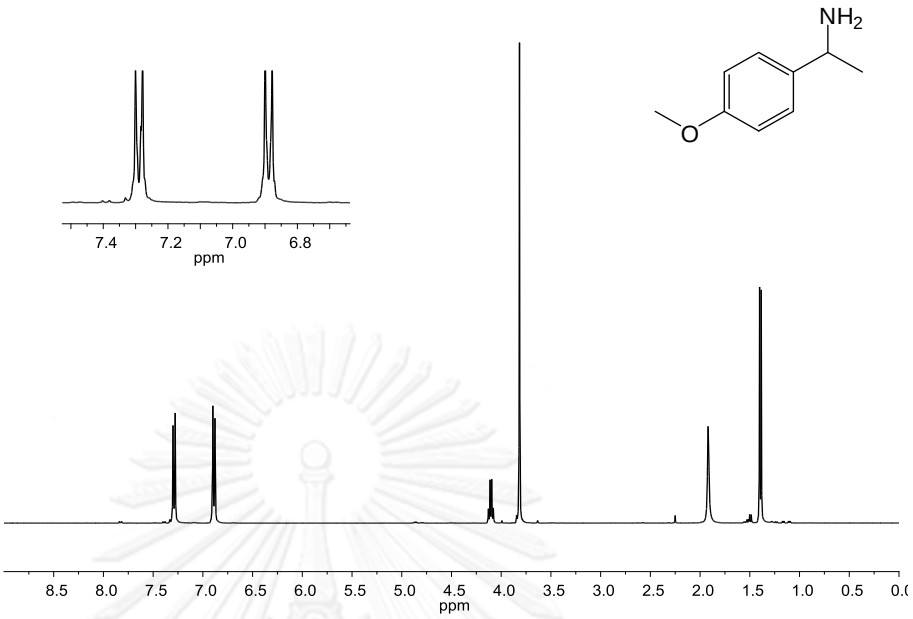

Figure C35 NMR spectrum of **4OMe;** ^{1}H NMR (400 MHz, $CDCl_3$) δ (ppm): 7.29 (d, *J* = 8.6 Hz, 2H, Ar<u>H</u>), 6.89 (d, *J* = 8.6 Hz, 2H, Ar<u>H</u>), 4.10 (q, *J* = 6.6 Hz, 1H , C<u>H</u>CH_3), 3.82 (s, 3H, COC<u>H</u>$_3$), 1.92 (br s, 2H, N<u>H</u>$_2$), 1.39 (d, *J* = 6.6 Hz, 3H, CHC<u>H</u>$_3$).

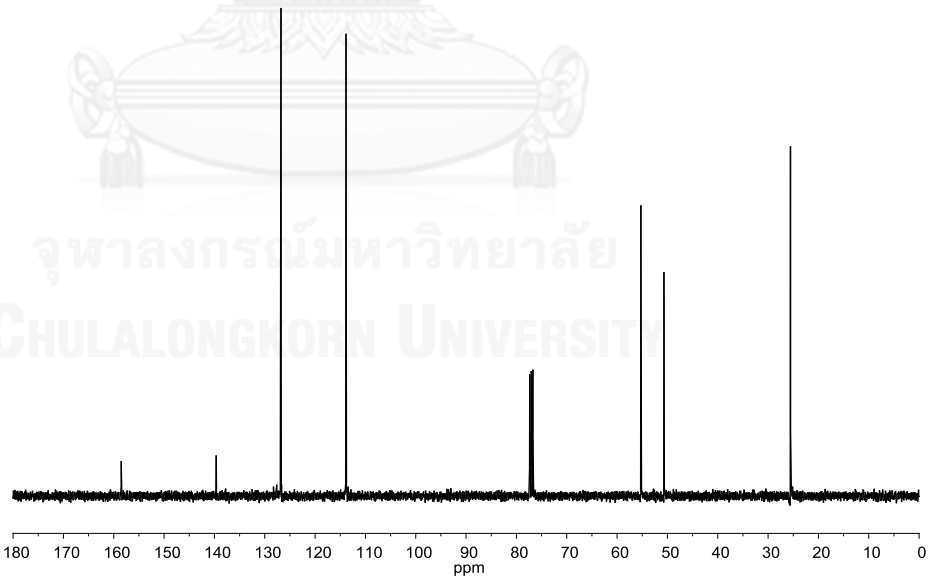

Figure C36 NMR spectrum of **4OMe;** ^{13}C NMR (100 MHz, $CDCl_3$) δ (ppm): 158.5, 139.7, 126.8, 113.9, 55.3, 50.7, 25.6.

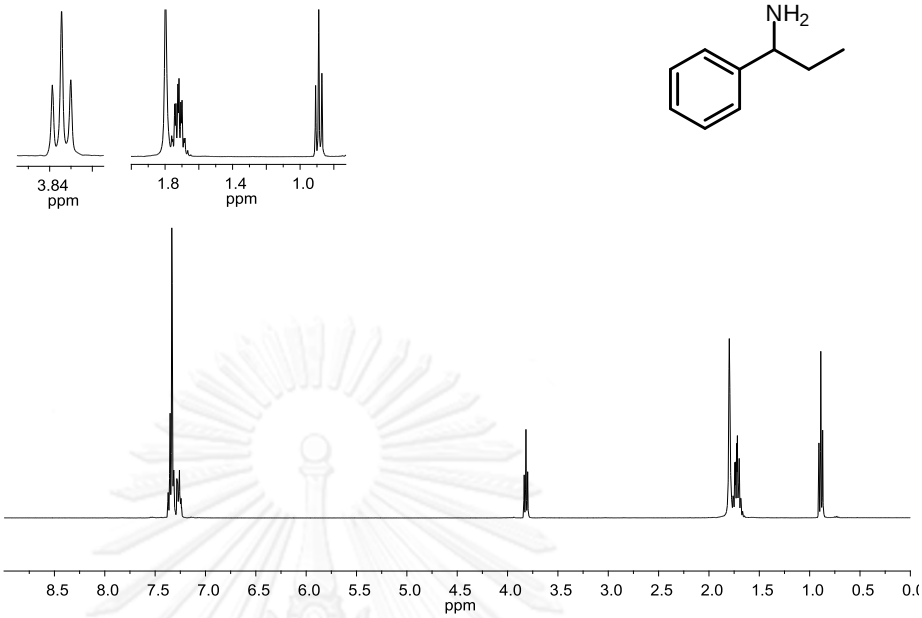

Figure C37 NMR spectrum of **PPA;** ^{1}H NMR (400 MHz, $CDCl_3$) δ (ppm): 7.39 – 7.21 (m, 5H, Ar<u>H</u>), 3.82 (t, *J* = 6.9 Hz, 1H, C<u>H</u>CH_3), 1.80 (br s, 2H, N<u>H</u>$_2$), 1.77 – 1.65 (m, 2H, C<u>H</u>$_2$$CH_3$), 0.89 (t, *J* = 7.4 Hz, 3H, CHC<u>H</u>$_3$).

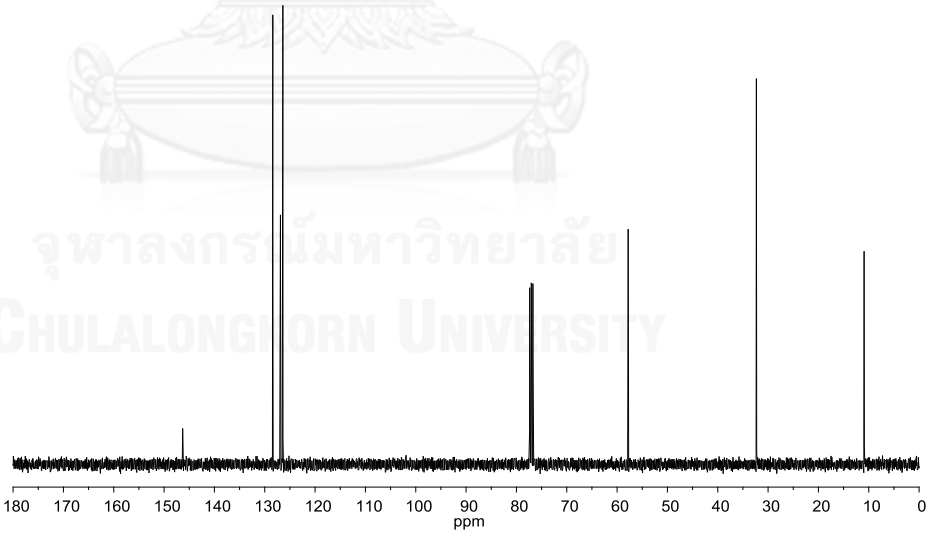

Figure C38 NMR spectrum of **PPA;** ^{13}C NMR (100 MHz, $CDCl_3$) δ (ppm): 146.3, 128.4, 126.9, 126.4, 57.8, 32.3, 10.9.

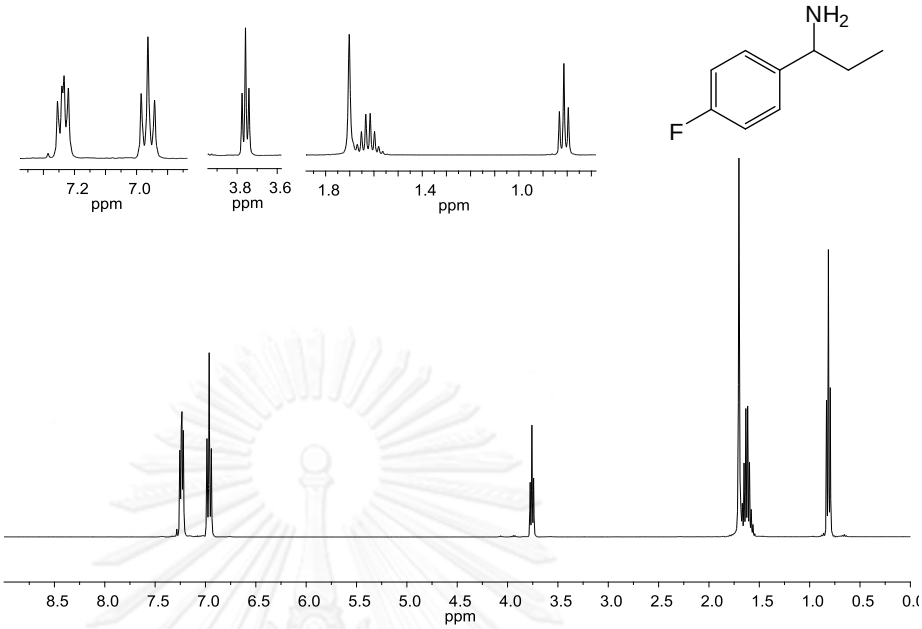

Figure C39 NMR spectrum of **4FP;** ^{1}H NMR (400 MHz, $CDCl_3$) δ (ppm): 7.24 (dd, *J* = 8.3, 5.6 Hz, 2H, Ar<u>H</u>), 6.96 (dd, *J* = 8.3, 8.3 Hz, 2H, Ar<u>H</u>), 3.76 (t, *J* = 6.8 Hz, 1H, C<u>H</u>CH_3), 1.70 (br s, 2H, N<u>H</u>$_2$), 1.69 – 1.55 (m, 2H, C<u>H</u>$_2$$CH_3$), 0.81 (t, *J* = 7.4 Hz, 3H, CHC<u>H</u>$_3$).

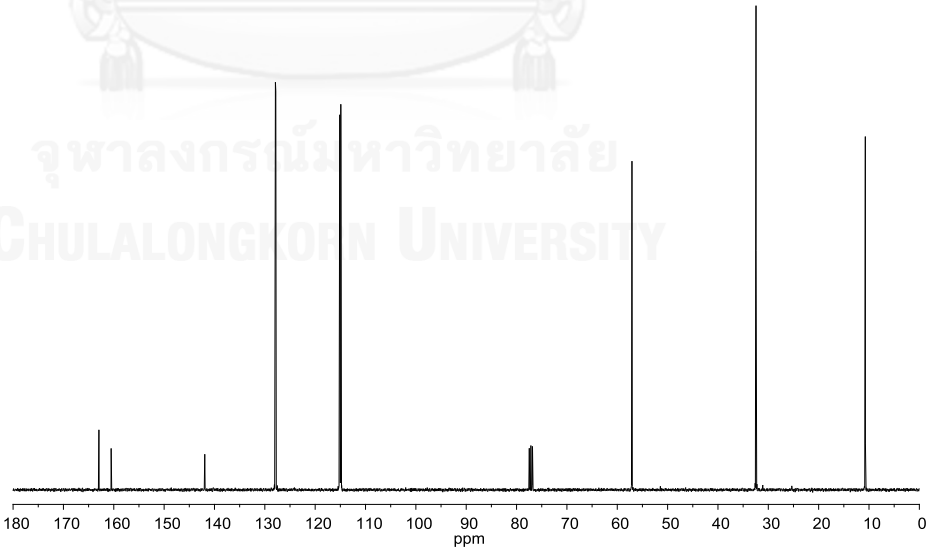

Figure C40 NMR spectrum of **4FP;** ^{13}C NMR (100 MHz, $CDCl_3$) δ (ppm): 161.7 (d, *J* = 244.3 Hz), 142.0 (d, *J* = 2.9 Hz), 127.9 (d, *J* = 7.9 Hz), 115.0 (d, *J* = 21.1 Hz), 57.1, 32.4, 10.7.

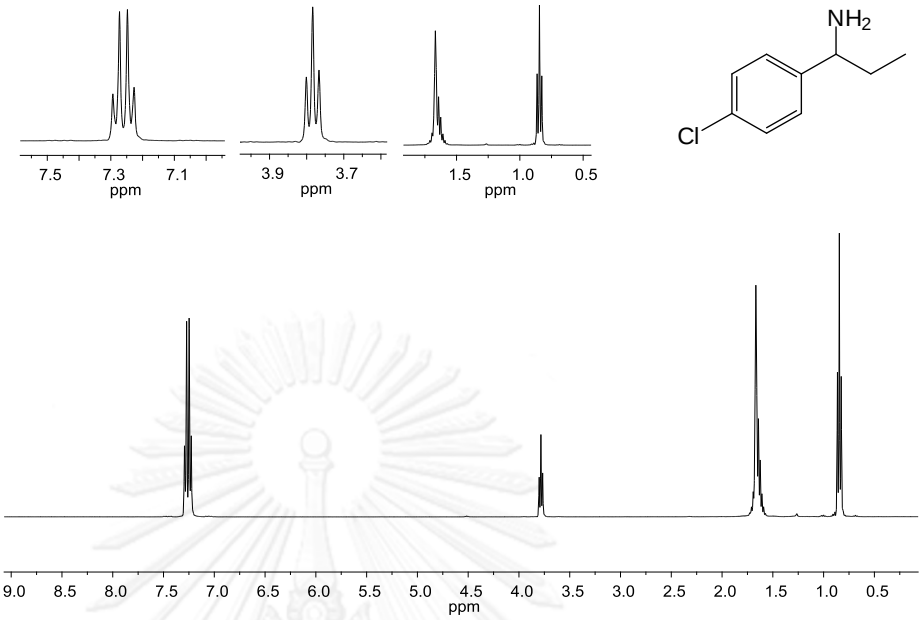

Figure C41 NMR spectrum of **4ClP;** ^{1}H NMR (400 MHz, $CDCl_3$) δ (ppm): 7.28 (d, *J* = 8.4 Hz, 2H, Ar<u>H</u>), 7.24 (d, *J* = 8.4 Hz, 2H, Ar<u>H</u>), 3.78 (t, *J* = 6.8 Hz, 1H, C<u>H</u>CH_3), 1.67 (br s, 2H, N<u>H</u>$_2$), 1.73 – 1.54 (m, 2H, C<u>H</u>$_2$$CH_3$), 0.85 (t, *J* = 7.4 Hz, 3H, CHC<u>H</u>$_3$).

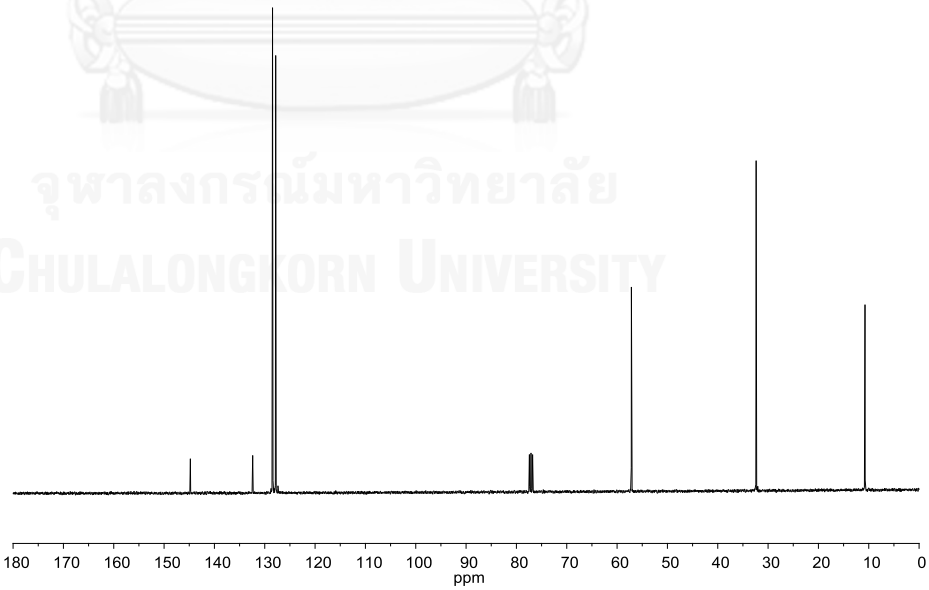

Figure C42 NMR spectrum of **4ClP;** ^{13}C NMR (100 MHz, $CDCl_3$) δ (ppm): 144.8, 132.4, 128.5, 127.8, 57.2, 32.4, 10.8.

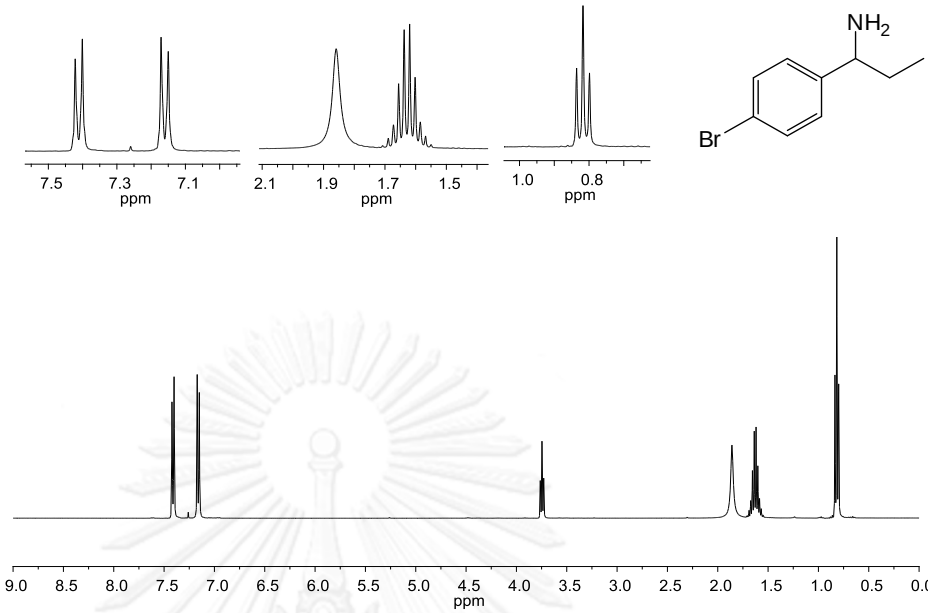

Figure C43 NMR spectrum of **4BrP;** ^{1}H NMR (400 MHz, $CDCl_3$) δ (ppm): 7.44 (d, *J* = 8.3 Hz, 2H, Ar<u>H</u>), 7.19 (d, *J* = 8.3 Hz, 2H, Ar<u>H</u>), 3.77 (t, *J* = 6.8 Hz, 1H, C<u>H</u>CH_3), 1.88 (br s, 2H, N<u>H</u>$_2$), 1.73 – 1.58 (m, 2H, C<u>H</u>$_2$$CH_3$), 0.84 (t, *J* = 7.4 Hz, 3H, C<u>H</u>$_2$$CH_3$).

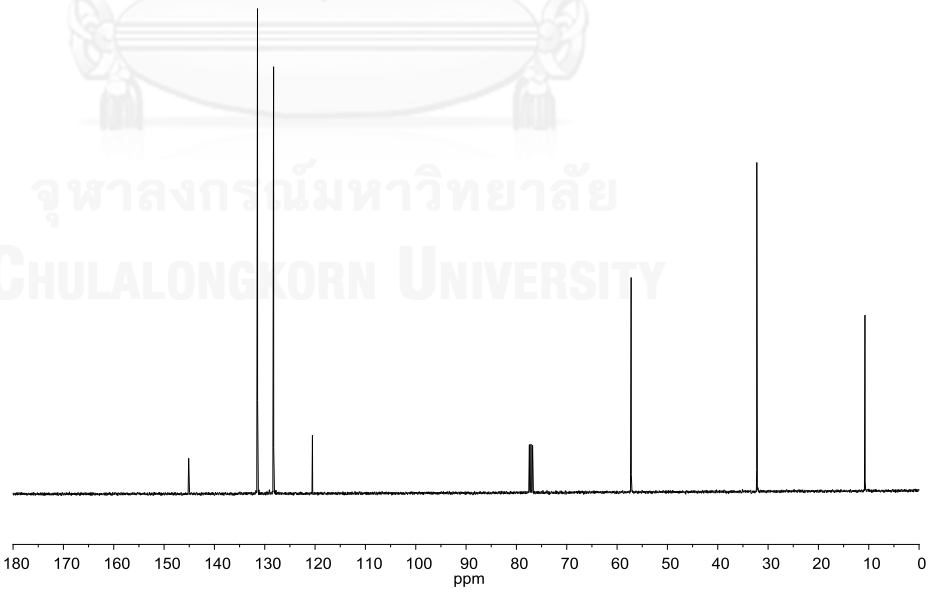

Figure C44 NMR spectrum of **4BrP;** ^{13}C NMR (100 MHz, $CDCl_3$) δ (ppm): 145.1, 131.4, 128.2, 120.5, 57.2, 32.2, 10.7.

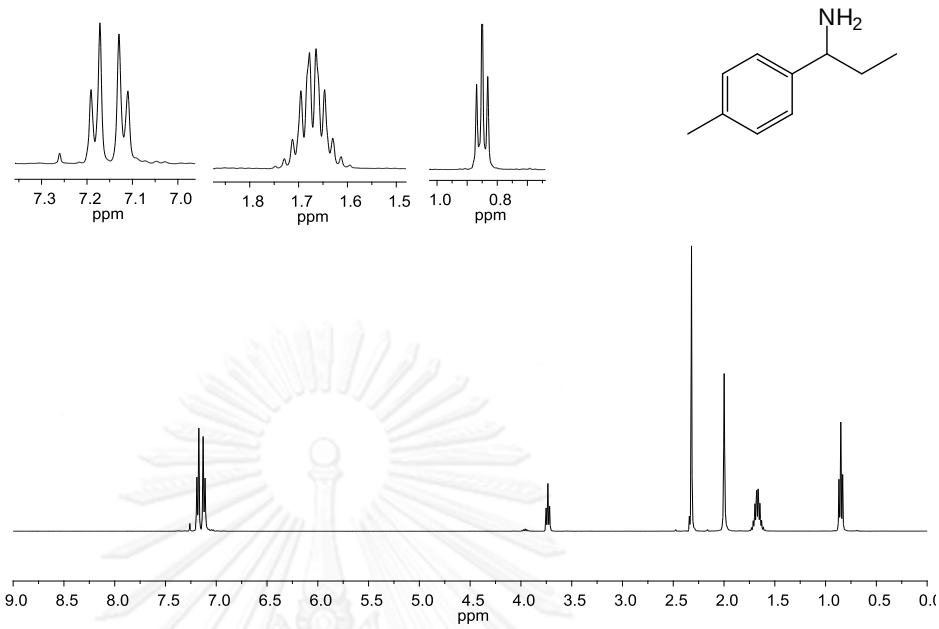

Figure C45 NMR spectrum of **4MeP;** ^{1}H NMR (400 MHz, $CDCl_3$) δ (ppm): 7.21 (d, *J* = 7.8 Hz, 2H, Ar<u>H</u>), 7.14 (d, *J* = 7.8 Hz, 2H, Ar<u>H</u>), 3.76 (t, *J* = 6.9 Hz, 1H, C<u>H</u>CH_3), 2.35 (s, 3H, CC<u>H</u>$_3$), 2.02 (br s, 2H, N<u>H</u>$_2$), 1.77 – 1.54 (m, 2H, C<u>H</u>$_2$$CH_3$), 0.88 (t, *J* = 7.4 Hz, 3H, CHC<u>H</u>$_3$).

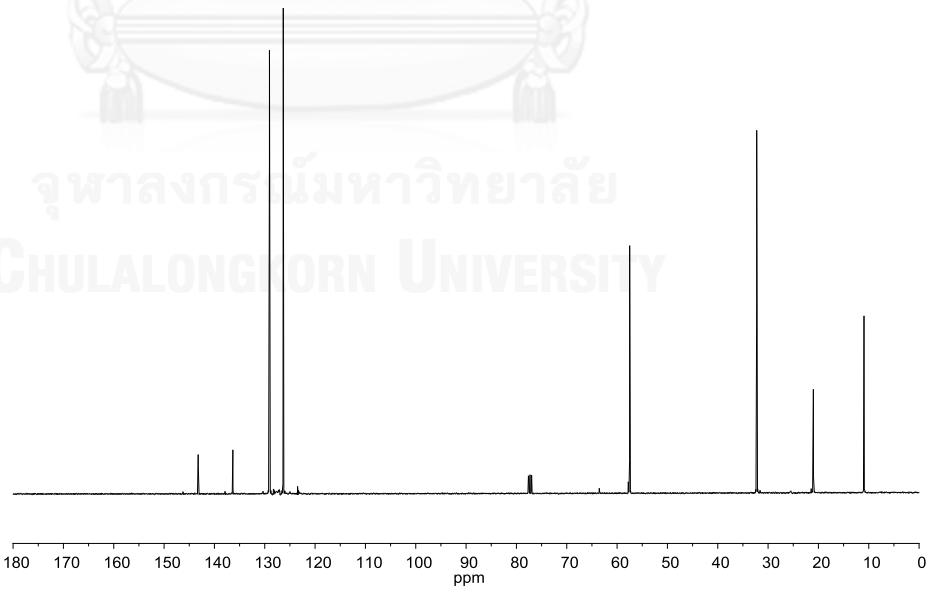

Figure C46 NMR spectrum of **4MeP;** ^{13}C NMR (100 MHz, $CDCl_3$) δ (ppm): 143.2, 136.3, 128.3, 126.3, 57.5, 32.3, 21.0, 10.9.

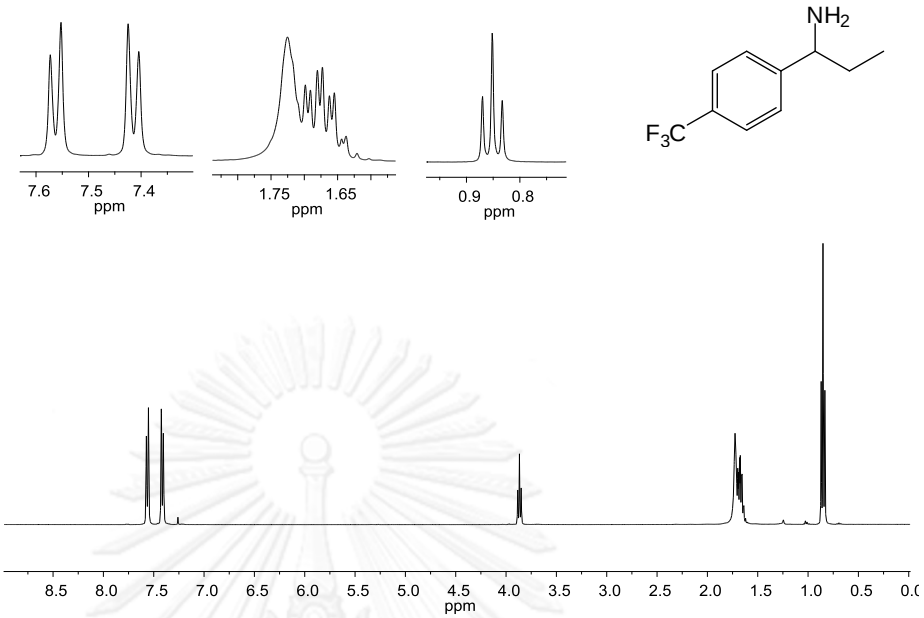

Figure C47 NMR spectrum of **4CFP;** ^{1}H NMR (400 MHz, $CDCl_3$) δ (ppm): 7.59 (d, *J* = 8.1 Hz, 2H, Ar<u>H</u>), 7.44 (d, *J* = 8.1 Hz, 2H, Ar<u>H</u>), 3.89 (t, *J* = 6.8 Hz, 1H, C<u>H</u>CH_3), 1.75 (br s, 2H, N<u>H</u>$_2$), 1.73 – 1.63 (m, 2H, C<u>H</u>$_2$$CH_3$), 0.88 (t, *J* = 7.4 Hz, 3H, CHC<u>H</u>$_3$).

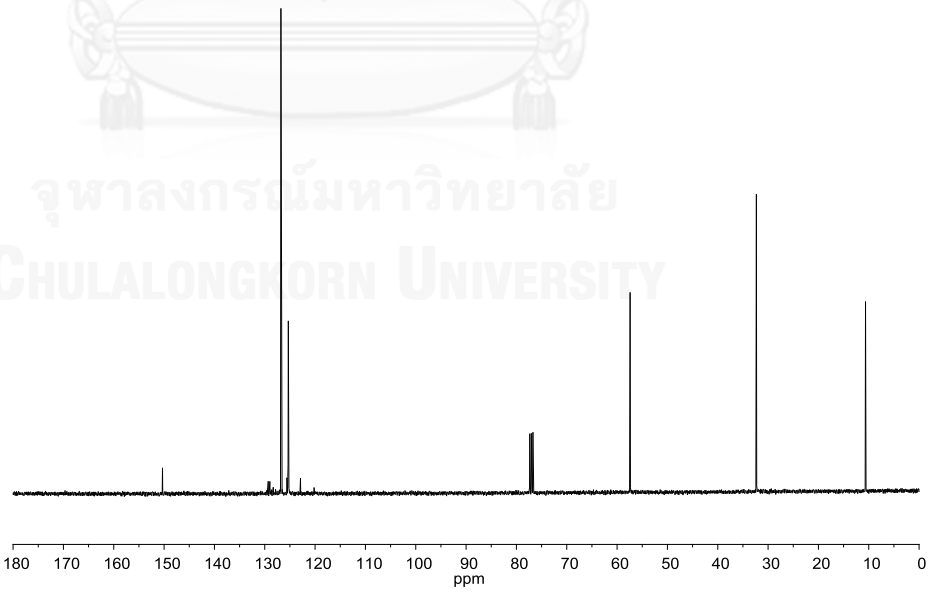

Figure C48 NMR spectrum of **4CFP;** ^{13}C NMR (100 MHz, $CDCl_3$) δ (ppm): 150.2 (d, J_{CF} = 22.4 Hz), 129.2 (d, J_{CF} = 32.2 Hz), 126.8, 125.3 (q, J_{CF} = 3.8 Hz), 122.9, 57.4, 32.3, 10.6.

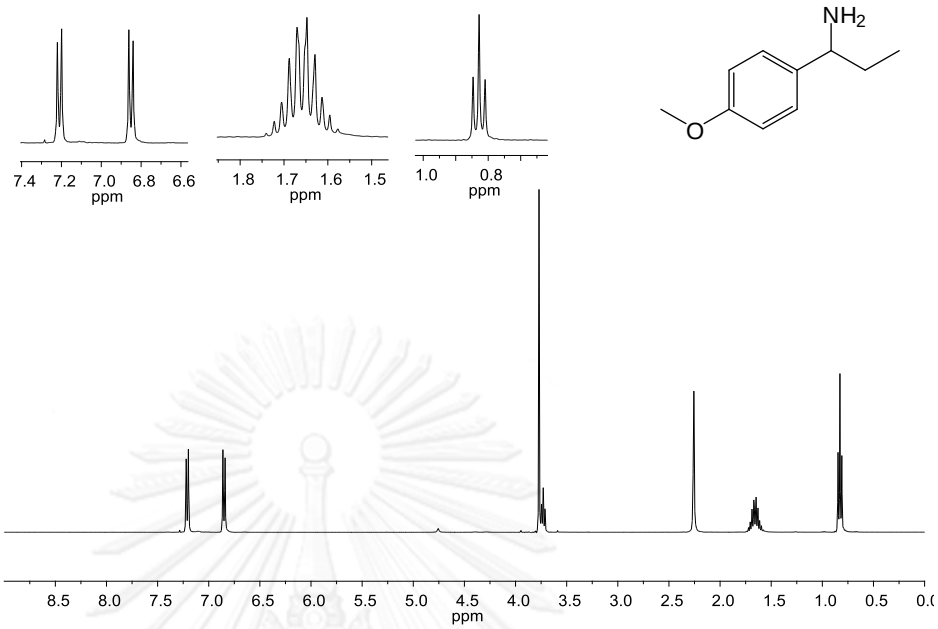

Figure C49 NMR spectrum of **4OMeP;** ^{1}H NMR (400 MHz, $CDCl_3$) δ (ppm): 7.21 (d, *J* = 8.6 Hz, 2H, Ar<u>H</u>), 6.85 (d, *J* = 8.6 Hz, 2H, Ar<u>H</u>), 3.77 (s, 3H, CC<u>H</u>$_3$), 3.73 (t, *J* = 6.9 Hz, 1H, C<u>H</u>CH$_3$), 2.26 (br s, 2H, N<u>H</u>$_2$), 1.76 – 1.56 (m, 2H, C<u>H</u>$_2$CH$_3$), 0.83 (t, *J* = 7.4 Hz, 3H, CHC<u>H</u>$_3$).

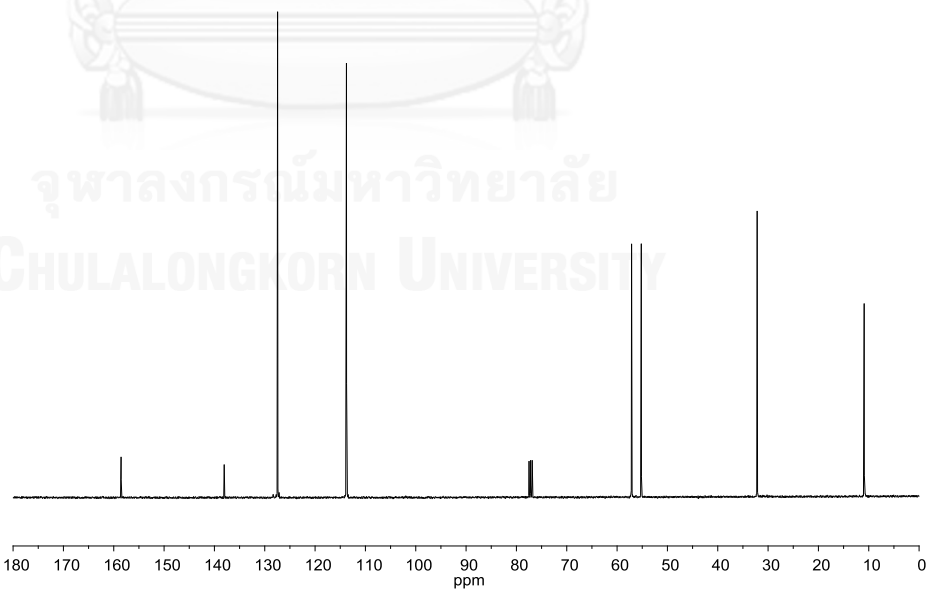

Figure C50 NMR spectrum of **4OMeP;** ^{13}C NMR (100 MHz, $CDCl_3$) δ (ppm): 158.5, 138.1, 127.5, 113.8, 57.1, 55.2, 32.2, 10.9.

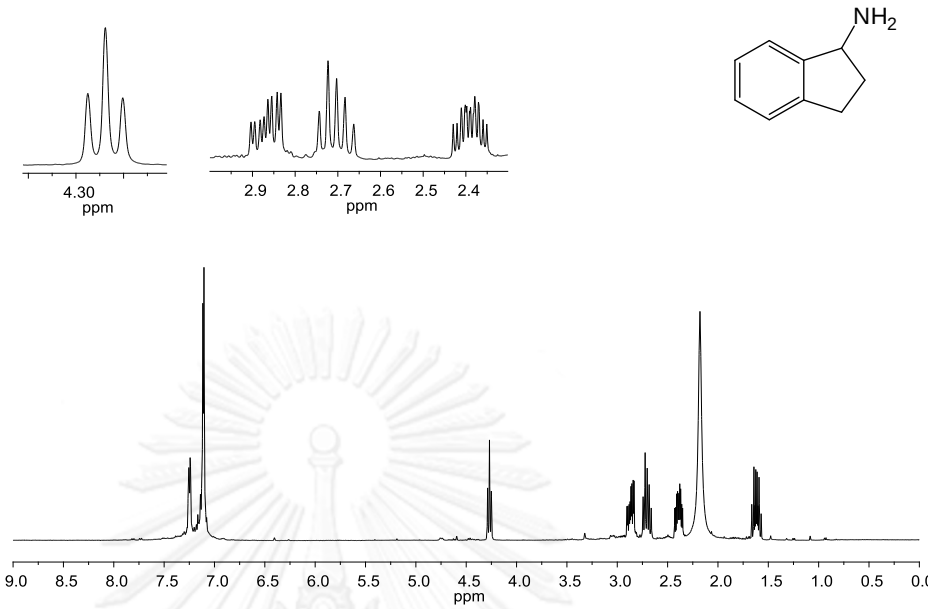

Figure C51 NMR spectrum of **AI;** ^{1}H NMR (400 MHz, $CDCl_3$) δ (ppm): 7.29 – 7.18 (m, 1H, Ar<u>H</u>), 7.21 – 7.05 (m, 3H, Ar<u>H</u>), 4.27 (t, *J* = 7.3 Hz, 1H, C<u>H</u>NH_2), 2.92 – 2.79 (m, 1H, CHC<u>H</u>$_2$), 2.79 – 2.63 (m, 1H, CHC<u>H</u>$_2$), 2.45 – 2.32 (m, 1H, C<u>H</u>$_2$CH_2), 2.18 (br s, 2H, N<u>H</u>$_2$), 1.69 – 1.52 (m, 1H, C<u>H</u>$_2$CH_2).

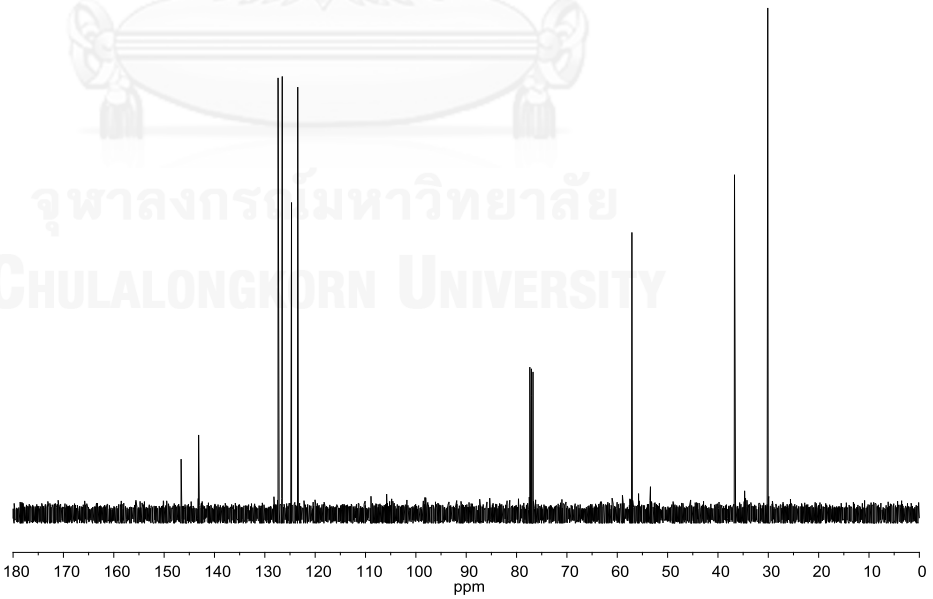

Figure C52 NMR spectrum of **AI;** ^{13}C NMR (100 MHz, $CDCl_3$) δ (ppm): 146.6, 143.2, 127.4, 126.5, 124.7, 123.5, 57.1, 36.7, 30.1.

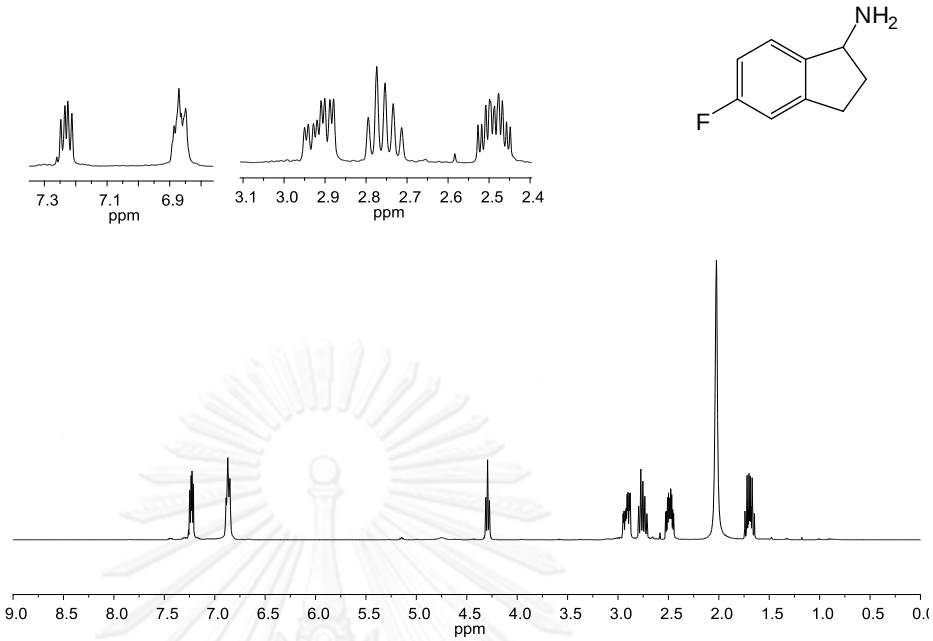

Figure C53 NMR spectrum of **5FA;** ^{1}H NMR (400 MHz, $CDCl_3$) δ (ppm): 7.33 – 7.10 (m, 1H, Ar<u>H</u>), 6.94 – 6.76 (m, 2H, Ar<u>H</u>), 4.29 (t, J = 7.3 Hz, 1H, C<u>H</u>NH_2), 3.03 – 2.85 (m, 1H, CHC<u>H</u>$_2$), 2.82 – 2.64 (m, 1H, CHC<u>H</u>$_2$), 2.52 – 2.42 (m, 1H, CH_2C<u>H</u>$_2$), 2.02 (br s, 2H, N<u>H</u>$_2$), 1.85 – 1.52 (m, 1H, CH_2C<u>H</u>$_2$).

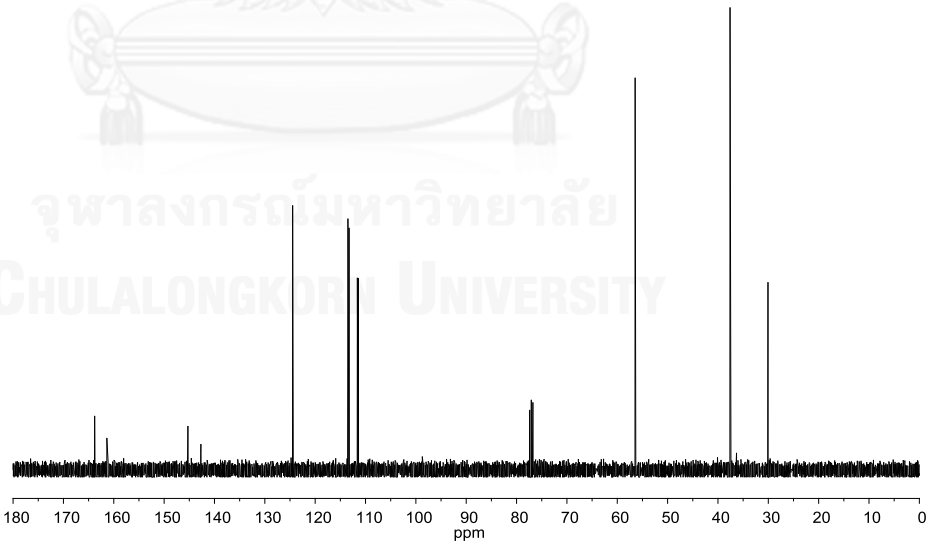

Figure C54 NMR spectrum of **5FA;** ^{13}C NMR (100 MHz, $CDCl_3$) δ (ppm): 162.6 (d, J_{CF} = 246.8 Hz), 145.3 (d, J_{CF} = 8.1 Hz), 142.7 (d, J_{CF} = 2.8 Hz), 124.4 (d, J_{CF} = 9.1 Hz), 113.4 (d, J_{CF} = 22.6 Hz), 111.5 (d, J_{CF} = 21.9 Hz), 56.5, 37.6, 30.1 (d, J_{CF} = 2.6 Hz).

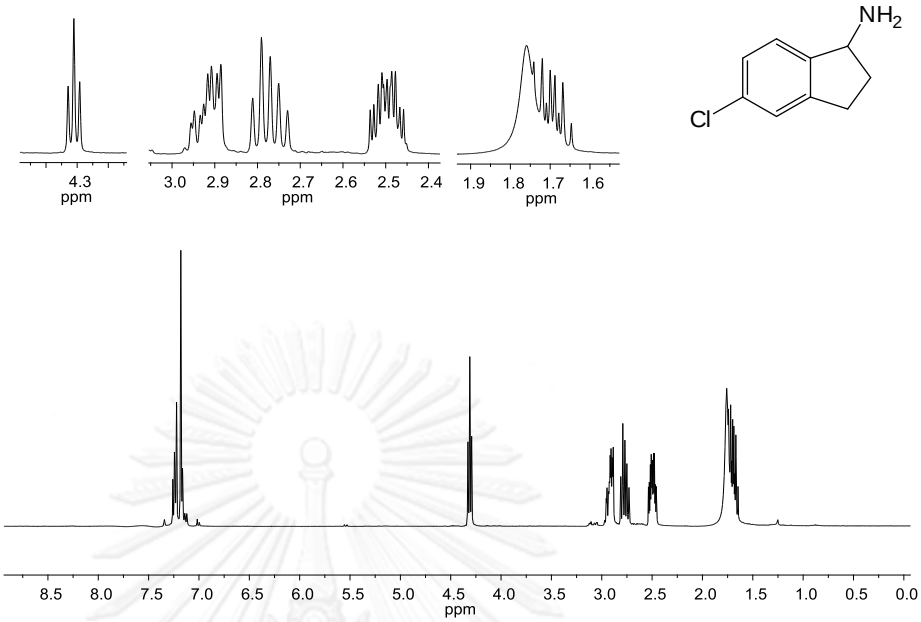

Figure C55 NMR spectrum of **5ClA;** ^{1}H NMR (400 MHz, $CDCl_3$) δ (ppm): 7.32 – 7.06 (m, 3H, Ar<u>H</u>), 4.31 (t, *J* = 7.4 Hz, 1H, C<u>H</u>NH_2), 2.97 – 2.84 (m, 1H, CHC<u>H_2</u>), 2.84 – 2.63 (m, 1H, CHC<u>H_2</u>), 2.56 – 2.37 (m, 1H, CH_2C<u>H_2</u>), 1.76 (br s, 2H, N<u>H_2</u>), 1.75 – 1.59 (m, 1H, CH_2C<u>H_2</u>).

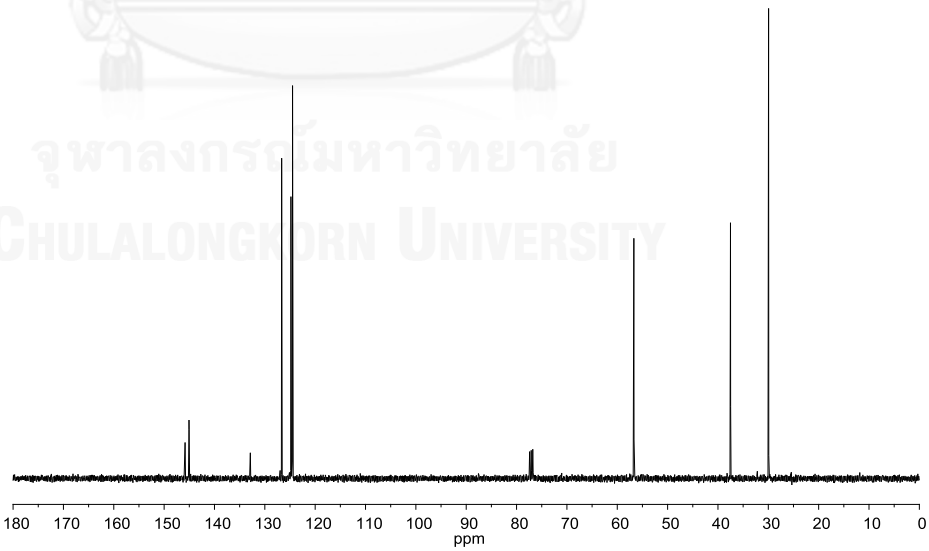

Figure C56 NMR spectrum of **5ClA;** ^{13}C NMR (100 MHz, $CDCl_3$) δ (ppm): 145.8, 145.1, 132.9, 126.7, 124.8, 124.5, 56.7, 37.5, 29.9.

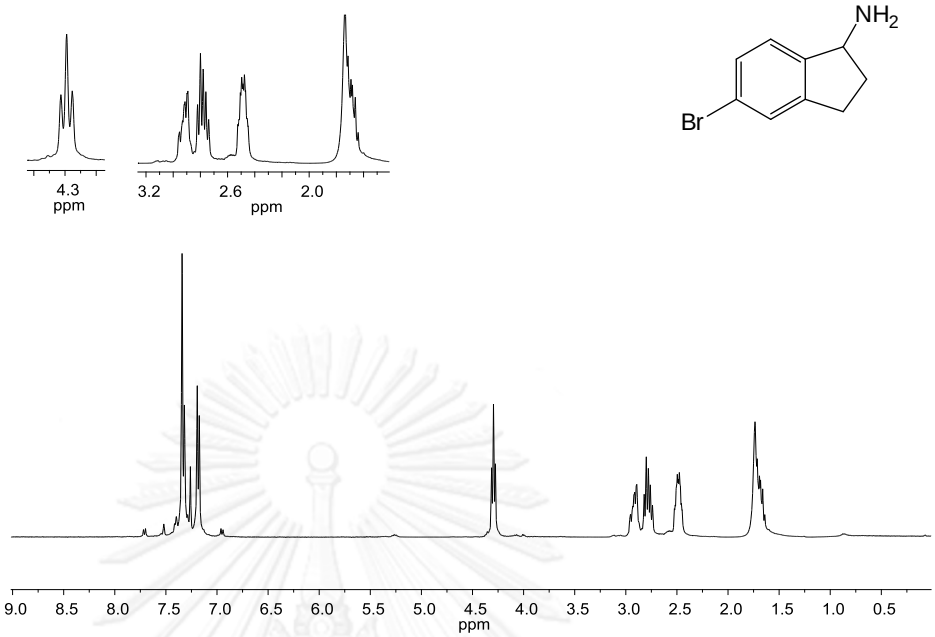

Figure C57 NMR spectrum of **5BrA;** ^{1}H NMR (400 MHz, $CDCl_3$) δ (ppm): 7.41 – 7.29 (m, 2H, Ar<u>H</u>), 7.18 (d, *J* = 7.8 Hz, 1H, Ar<u>H</u>), 4.47 – 4.20 (m, 1H, C<u>H</u>NH_2), 3.07 – 2.86 (m, 1H, CHC<u>H</u>$_2$), 2.86 – 2.70 (m, 1H, CHC<u>H</u>$_2$), 2.63 – 2.31 (m, 1H, CH_2C<u>H</u>$_2$), 1.74 (br s, 2H, N<u>H</u>$_2$), 1.72 – 1.61 (m, 1H, CH_2C<u>H</u>$_2$).

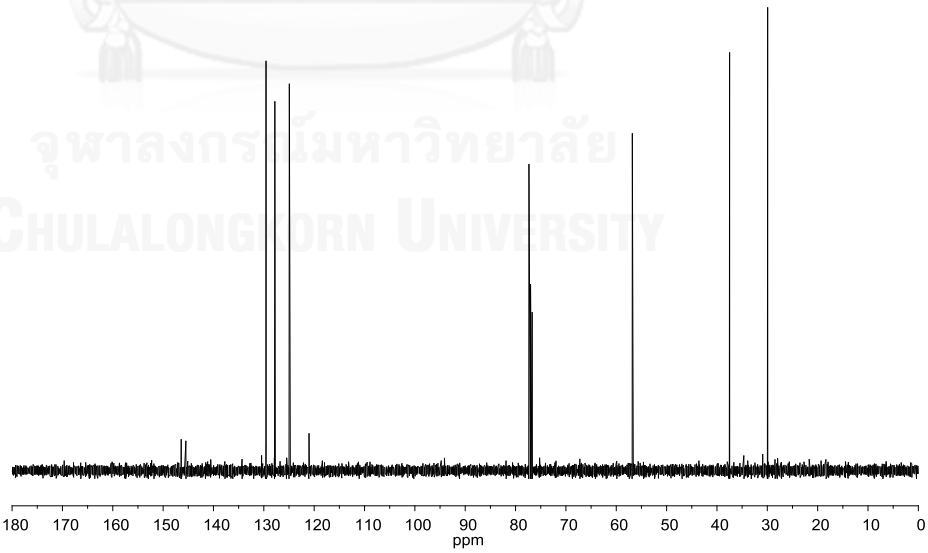

Figure C58 NMR spectrum of **5BrA;** ^{13}C NMR (100 MHz, $CDCl_3$) δ (ppm): 146.4, 145.5, 129.6, 127.8, 124.9, 121.0, 56.8, 37.5, 29.9.

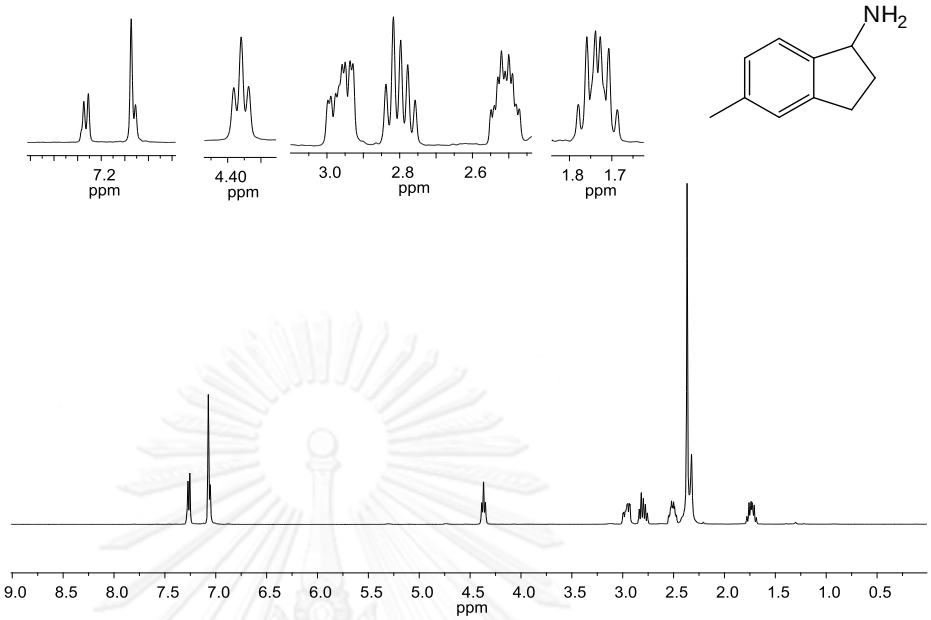

Figure C59 NMR spectrum of **5MeA;** ^{1}H NMR (400 MHz, $CDCl_3$) δ (ppm): 7.26 (d, *J* = 7.4 Hz, 1H, Ar<u>H</u>), 7.06 (d, *J* = 7.4 Hz, 2H, Ar<u>H</u>), 4.37 (t, *J* = 7.1 Hz, 1H, C<u>H</u>NH_2), 3.04 – 2.89 (m, 1H, CHC<u>H</u>$_2$), 2.87 – 2.72 (m, 1H, CHC<u>H</u>$_2$), 2.58 – 2.45 (m, 1H, CH_2C<u>H</u>$_2$), 2.37 (s, 3H, CC<u>H</u>$_3$), 2.32 (br s, 2H, N<u>H</u>$_2$), 1.85 – 1.55 (m, 1H, CH_2C<u>H</u>$_2$).

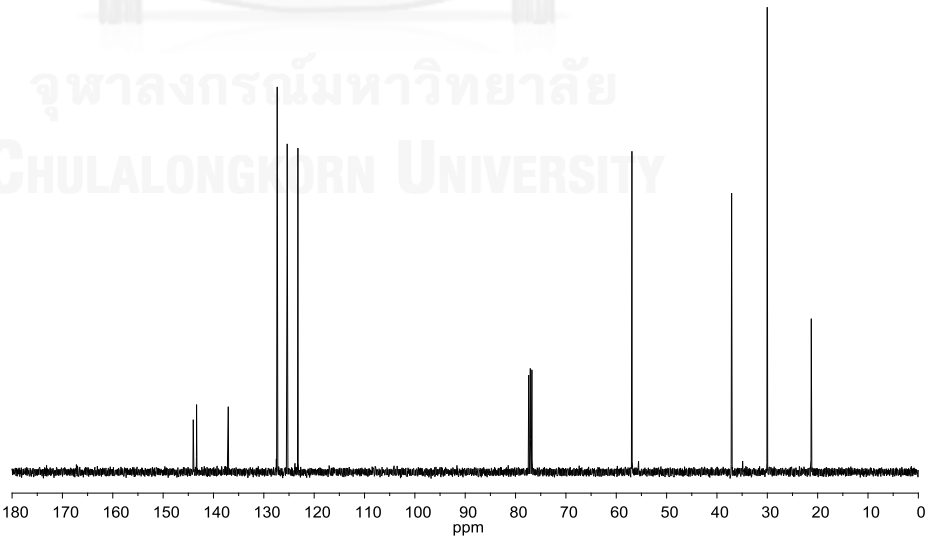

Figure C60 NMR spectrum of **5MeA;** ^{13}C NMR (100 MHz, $CDCl_3$) δ (ppm): 144.0, 143.4, 137.1, 127.4, 125.4, 123.3, 56.9, 37.1, 30.0, 21.3.

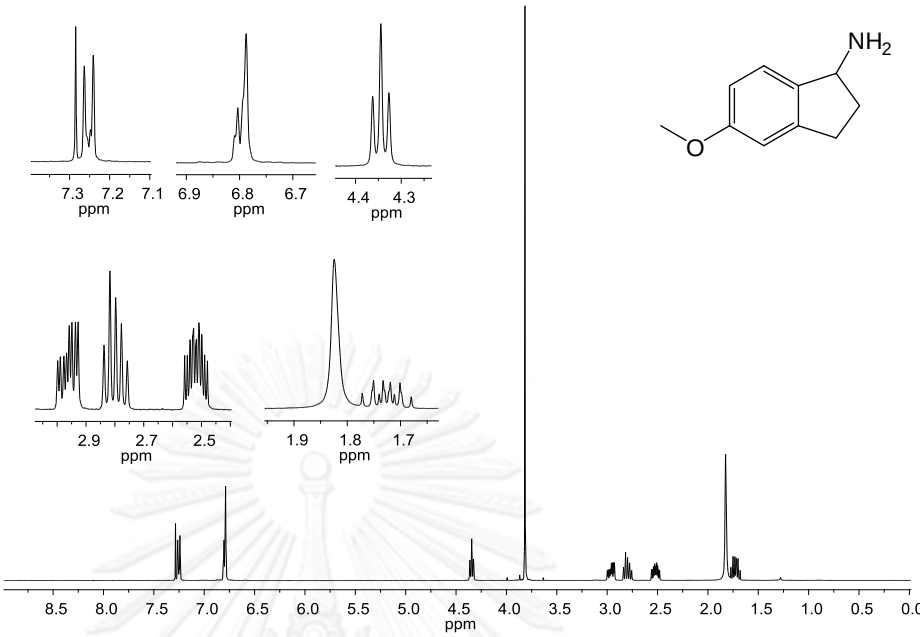

Figure C61 NMR spectrum of **5OMeA;** ^{1}H NMR (400 MHz, $CDCl_3$) δ (ppm): 7.31 – 7.23 (m, 1H, Ar<u>H</u>), 6.87 – 6.70 (m, 2H, Ar<u>H</u>), 4.34 (t, *J* = 7.1 Hz, 1H, C<u>H</u>NH_2), 3.82 (s, 3H, COC<u>H</u>$_3$), 3.04 – 2.88 (m, 1H, CHC<u>H</u>$_2$), 2.87 – 2.71 (m, 1H, CHC<u>H</u>$_2$), 2.57 – 2.44 (m, 1H, CH_2C<u>H</u>$_2$), 1.82 (br s, 2H, N<u>H</u>$_2$), 1.79 – 1.65 (m, 1H, CH_2C<u>H</u>$_2$).

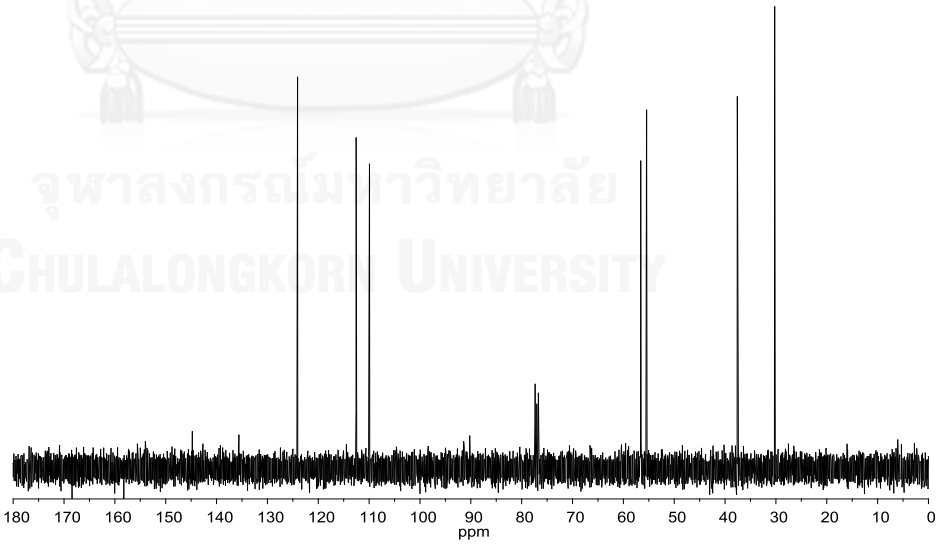

Figure C62 NMR spectrum of **5OMeA;** ^{13}C NMR (100 MHz, $CDCl_3$) δ (ppm): 144.8, 133.9, 124.1, 112.5, 109.9, 56.6, 55.4, 37.6, 30.2.

VITA

Mr. Natthapol Issaraseriruk was born on May 30, 1983 in Bangkok, Thailand. After completing his secondary school from Suankularb Wittayalai School, he entered the Department of Chemistry, Faculty of Science, Chulalongkorn University in 2001. He completed his Bachelor of Science Degree in March 2005. After graduation, He continued his graduate study in analytical chemistry, focusing on the chromatographic separation at the same university. He completed his Master of Science Degree in March 2008. He then continued his Ph.D. study at the same university and will complete his Doctor of Philosophy in 2014. His current address is 43/90 Soi Phetkasem 5/2 Phetkasem Road, Wat Thaphra, Bangkok Yai, Bangkok, 10600 Thailand.

จุฬาลงกรณ์มหาวิทยาลัย
CHULALONGKORN UNIVERSITY